

University of South bohemia, Faculty of Science
Department of Molecular biology



Regulation of cellular metabolism by
the Notch receptor signalling pathway

Master thesis

Author: Bc. Věra Slaninová

Supervisor: RNDr. Alena Krejčí, Ph.D.

České Budějovice, 2012

Master thesis

Slaninová, V., 2012: Regulation of cell metabolism by Notch signalling pathway.
Mgr. Thesis, in English – 80 p., Faculty of Science, University of South bohemia, Czech republic.

Annotation

Seven genes involved in metabolism were tested as direct targets of the Notch signalling pathway. For each gene the occupancy of its enhancers by Su(H), its transcriptional response to Notch pathway and its biological functionality was verified *in vitro* and *in vivo*.

Prohlašuji, že v souladu s § 47b zákona č. 111/1998 Sb. v platném znění souhlasím se zveřejněním své diplomové práce, a to v nezkrácené podobě elektronickou cestou ve veřejně přístupné části databáze STAG provozované Jihočeskou univerzitou v Českých Budějovicích na jejích internetových stránkách, a to se zachováním mého autorského práva k odevzdanému textu této kvalifikační práce. Souhlasím dále s tím, aby toutéž elektronickou cestou byly v souladu s uvedeným ustanovením zákona č. 111/1998 Sb. zveřejněny posudky školitele a oponentů práce i záznam o průběhu a výsledku obhajoby kvalifikační práce. Rovněž souhlasím s porovnáním textu mé kvalifikační práce s databází kvalifikačních prací Theses.cz provozovanou Národním registrem vysokoškolských kvalifikačních prací a systémem na odhalování plagiátů.

.....

Bc. Věra Slaninová

V Českých Budějovicích dne 26. 4. 2012

Acknowledgement

First, I would like to express my gratitude to my supervisor Alena Krejčí for confidence she put into me, for all her help and guidance during last the two years. Then I thank to my colleagues: Matej, Pavel, Jirka, Andrea and Aida and the other crew of our lab: Alex, Vasanth and Peter for their support, consultations and nice atmosphere.

I would like to acknowledge MUDr. Jan Trnka from 3rd faculty of medicine in Prague for his help with functional study of metabolism.

Finally, a huge thanks belongs to my family for everything they have done for me, this part in Czech...

Svým rodičům bych chtěla poděkovat za jejich obrovskou podporu, morální i finanční. Mami, tati, díky že jste to se mnou nevzdali a vždy mě podrželi ve chvílích, kdy jsem to nejvíc potřebovala. Mému bráškově patří dík za jeho občasné uštěpačné poznámky které mě držely nohama na zemi a často i pobavily. Strejdovi a Olince za jejich podporu a nocleh při provádění pokusů v Praze. Zbytku své rodiny za příjemně strávené chvíle v průběhu celého studia.

Table of contents

1	Introduction.....	1
1.1.	Metabolism of a cell.....	2
1.2.	Metabolism of the cancer cells.....	4
1.2.1.	Warburg effect.....	4
1.2.2.	Factors influencing Warburg effect.....	6
1.3.	Notch signalling.....	7
1.3.1.	The role of Notch signalling in development.....	9
1.3.2.	Regulation of Notch signalling.....	10
1.3.3.	Notch target genes.....	13
1.3.4.	Notch and cancer.....	14
2	Aims.....	16
3	Material and methods.....	18
3.1.	Selection of potential Notch target genes involved in metabolism.....	18
3.2.	Analysis in cell lines.....	22
3.2.1.	Testing Su(H) enhancers in the luciferase assay.....	22
3.2.2.	Analysis of the mRNA expression profile after the activation of the Notch pathway using Q-RT-PCR.....	28
3.3.	Analysis <i>in vivo</i>	31
3.3.1.	Q-RT-PCR from the wing discs.....	32
3.3.2.	<i>In situ</i> hybridization in imaginal wing discs.....	32
3.4.	Measurement of metabolism.....	35
4	Results.....	38
4.1.	Selection of potential Notch target genes involved in metabolis.....	38
4.2.	Analysis in cell lines.....	43
4.2.1.	Testing Su(H) enhancers in the luciferase assay.....	43
4.2.2.	Analysis of the mRNA expression profile after the activation of the Notch pathway using Q-RT-PCR.....	45
4.3.	Analysis <i>in vivo</i>	49
4.4.	Measurement of metabolism.....	54
5	Conclusions.....	61
6	Discussion.....	62
6.1.	Su(H), a transcription factor of the Notch signalling pathway, binds potential enhancer regions of several metabolic genes.....	62

6.2.	Metabolic genes show transcriptional response <i>in vitro</i> and <i>in vivo</i> to activation of Notch signalling pathway.....	63
6.3.	Notch activation and the transcriptional response of the Notch target genes has functional connection to cell metabolism.....	65
6.4.	Notch signalling pathway drives expression of metabolic genes directly.....	66
7	Bibliography.....	68
8	Supplement.....	74

1 Introduction

Many forms of life have developed during evolution, from primitive unicellular organisms to complex organisms composed of billions of cells. Nowadays, tens of millions of species are living and inhabiting different ecological niches. What is common to all these organisms is their need for a source of outside energy in the form of nutrients. However, most of these nutrients can not be used in the form they are excepted from the environment. Various metabolic pathways developed in the bodies of all living organisms which process these nutrients to basal components that can be then either further utilized or stored.

Moreover, formation of multicellularity required establishment of new orders. Individual cells of system needs to stay in touch, communicate with surroundings, cooperate, follow some rules for the sake of preservation of the organism as the whole. For this purpose, signalling pathways developed. We know relatively few of these pathways but they mediate whole range of physiological responses. For example they trigger gene expression, start metabolic processes, participate in cell differentiation, immune response or apoptosis. It is their combination and the overall cellular context that defines the final signalling output.

One of those signalling pathways that is conserved in all multicellular organisms is the Notch pathway. This signalling is mainly active during the development but it plays the role also in the adult organism where it takes part in the proliferation of regularly renewing tissues such as gut epithelium (1). The dysfunction of this pathway can lead to many diseases, e.g. lymphoid neoplasm or breast cancer, lung cancer, cancer of skin or colorectal cancer (2) multiple sclerosis (3), cerebral autosomal dominant arteriopathy with subcortical infarcts and leukoencephalopathy (CADASIL) (4) or Alagille syndrome (5).

Even small disorders in either metabolic or signalling pathways often have fatal consequences. They result in the development of hundreds of diseases and malformations. In fact lots of diseases involve both metabolic and signalling dysfunctions. For example, diabetes is a classical example of such a disease that effects millions of people (6). Moreover, various cancers show a special type of metabolism different from the one in most of the other cells in the body, called the Warburg effect. The cancerous growth is in may cases caused by defects in cell signaling directing changes in cellular metabolism towards the Warburg effect. However, as proposed by Otto Warburg nearly 80 years ago, metabolic changes might be the primary cause of cancerous growth that are accompanied by changes in

cell signalling (7). Nowadays, many of the techniques in tumor treatment work with this reality and metabolic, as well as signalling pathways become popular targets of therapeutics (8–12).

In this study, I am looking into the connection of the Notch signalling pathway and cell metabolism, primarily the glycolysis and Krebs cycle. Our data suggest that the Notch pathway controls directly the expression of several genes involved in metabolism in various *Drosophila* tissues. By this way the Notch pathway influences the cellular metabolic profile. By describing the regulation of new Notch target genes involved in metabolism we may also provide an explanation how the Notch pathway triggers the Warburg effect in cancer cells.

1. 1. Metabolism of a cell

The word metabolism expresses a set of chemical reactions which take place inside cells and which are vital for the survival of the organism. During catabolism, nutrients are decomposed to smaller units and this is the way how energy is gained, mostly in the form of high energy phosphates, e.g. adenosine triphosphate (ATP). On the contrary, anabolic reactions consume energy for building of the structural subunits such as proteins, lipids, sugars or nucleic acids (13). The main sources of nutrients for a mammalian cells are glucose, glutamine and lipids.

Glucose is metabolized during the glycolysis in the cytoplasm followed by the pyruvate decarboxylation, Krebs cycle, and finally respiratory chain leading to oxidative phosphorylation in mitochondria to gain most of energy per unit of glucose. Up to 36 molecules of ATP can be formed from one molecule of glucose this way (13). In glycolysis one molecule of glucose is gradually remodeled to two molecules of pyruvate, two molecules of ATP and two molecules of NADH. Pyruvate is then transferred through mitochondrial membranes to mitochondrial matrix. Here, pyruvate is changed to acetyl coenzyme A (acetyl CoA) by pyruvate dehydrogenase. Acetyl CoA is the main substrate for Krebs cycle where further NADH molecules, H₂O, CO₂ and FADH₂ are formed.

In the respiratory chain in mitochondria electrons are removed from NADH or succinate and they are transmitted between different complexes by ubiquinone (coenzyme Q). During their transfer, there is a large amount of protons flowing through the complexes (except complex II) from mitochondrial matrix through the inner membrane into intermembrane space. This is the way how proton gradient is set up across the inner

membrane. At the end of the electron transport chain, electrons are passed on the oxygen and water is formed. Protons are pumped through the ATP syntase back to the mitochondrial matrix powering the ATP syntase which makes ATP (14).

Beside the glucose, another important energy source for rapidly dividing cells (as well as cancer cells) is glutamine, the most abundant amino acid in the mammalian plasma. Glutamine is degraded in a process called glutaminolysis, to glutamate, aspartate, CO₂, pyruvate, lactate, alanine and citrate. These metabolites are then used as building blocks for the synthesis of nucleic acids, polysaccharides or glutathione. It also mimicks part of the Krebs cycle which provides important metabolites to rapidly dividing cells where Krebs cycle does not run effectively (15).

Metabolism of lipids is also connected to energy production. Lipids are the major source of energy for liver and heart and they are decomposed during β-oxidation to acetyl coenzyme A which is the substrate for Krebs cycle. During this decomposition, molecules of FADH₂ and NADH are also produced (13).

One should note that none of the above described metabolic pathways is able to work independently, without the help of the other metabolic pathways. Metabolic processes are deeply connected and all of them cooperate to produce the ATP (fig.1).

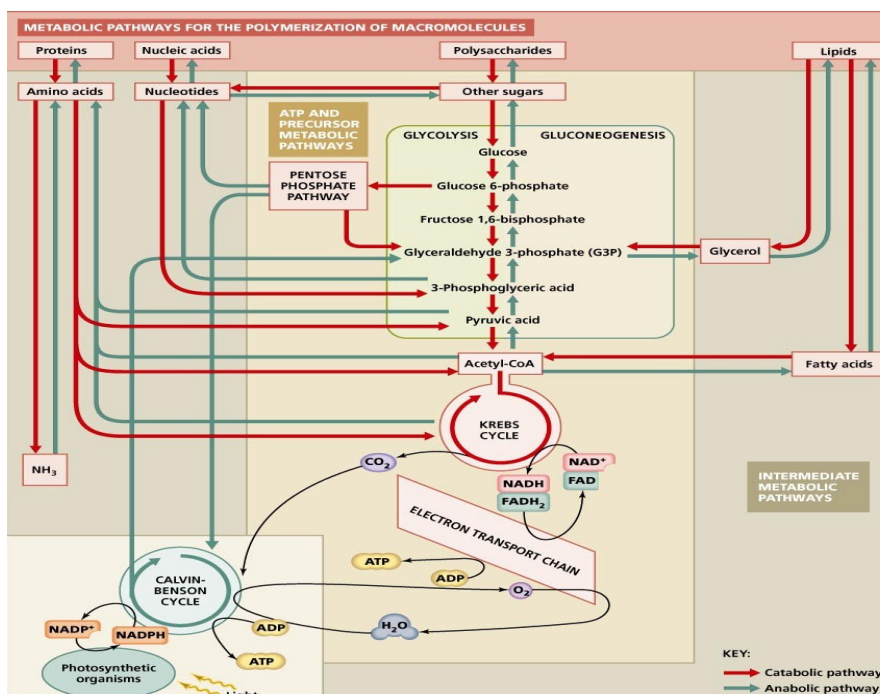


Fig.1: Connection of metabolic pathways (<http://biology-pictures.blogspot.com/2011/11/cellular-metabolism-summary.html>). Metabolism of glucose, aminoacids, lipids, Krebs cycle and other metabolic pathways provides building blocks for respiratory chain.

1. 2. Metabolism of cancer cells

The metabolism of cancer cells (and to a large extent also of any other rapidly dividing cells) is very different from that present in adult differentiated tissue. Cells of multicellular organisms live in a nutrient rich environment and their uptake is driven by signalling pathways (like the insulin pathway or by pathways triggered by growth factors). In other words, normal cells do not accept nutrients continuously, they need an instruction to do it. But cancerous cells were able to get around this signal-dependent induction of nutrients intake. For example, they accumulate mutations in signalling pathways that lead to the upregulation of glucose transporters. This way there is a constant supply of energy needed for the synthesis of proteins, lipids and nucleic acids to allow the rapid cellular growth and divisions (16). Tumorous cells produce energy nearly solely through glycolysis, with only a limited use of the Krebs cycle and the respiratory chain, even in the presence of oxygen. This phenomenon is known as the Warburg effect (17).

1. 2. 1. Warburg effect

In the 20th decade of the 20th century, Otto Warburg found that cancer cells gain energy mostly by glycolysis even though the oxygen levels inside the cell is sufficient (Fig.2). It was really unexpected because glycolysis as the main energy producing pathway was only known in cells suffering by hypoxia. He evolved a theory saying that respiration and mitochondrias as a whole are probably damaged in cancer cells or that quantity of mitochondrias is reduced so these cells don't have a choice but gain the energy through glycolysis (7).

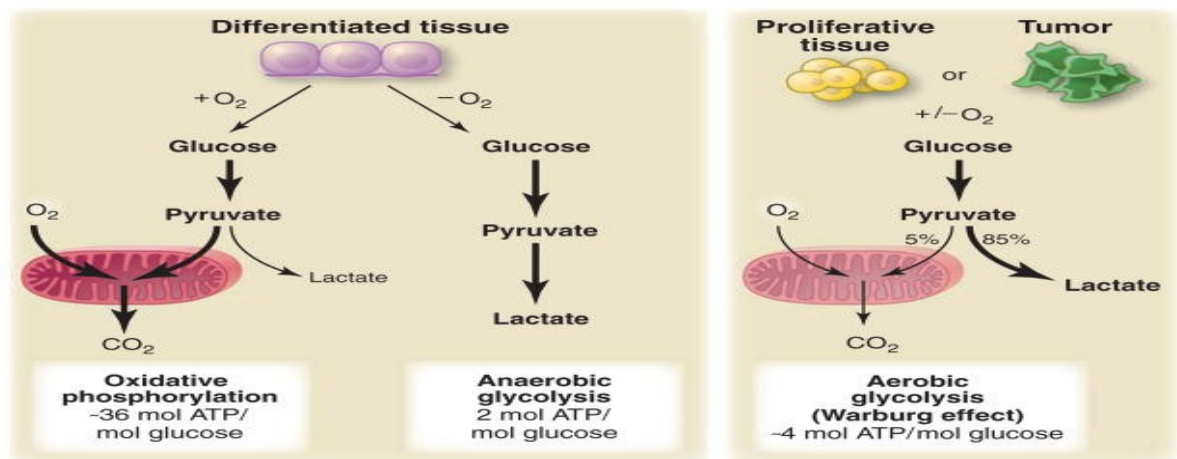


Fig. 2: Warburg effect scheme (Matthew G. Vander Heiden et al. Science 2009). Normal tissues gain energy from electron transport chain, cancerous and proliferating tissues use glycolysis as a source of energy

Now we know that this hypothesis was incorrect. Aerobic glycolysis as a source of energy is used not only by tumor cells but also by all highly proliferative cells (17). Additionally, even cancerous cells have functional respiratory chain (it is only suppressed). This was supported by experiments wherein restriction of glycolysis lead to almost normally working respiratory chain (18). So why cancerous cells upregulate glycolysis? Why instead of going to the Krebs cycle the pyruvate is converted to lactate and secreted outside the cell, wasting a valuable source of energy? Several explanations have been proposed:

The oldest explanation says that glycolysis is the main metabolic pathway in the rapidly dividing cells because the precursors for biosynthesis of amino acids, nucleic acids and fatty acids can be easily gained from glycolysis (17). Proliferative cells need to reproduce their genome and synthesize proteins and lipids for new cell quickly (19) and glucose metabolites are essential for it. The precursor for nucleic acids, ribose-5-phosphate, is derived from glucose-6-phosphate. Phosphoenolpyruvate, pyruvate, 3-phosphoglycerate and glucose-6-phosphate are needed for aminoacid synthesis. And cytosolic production of acetyl CoA is vital for fatty acid biosynthesis (17).

Second theory connects aerobic glycolysis with protection of cells against oxidative stress. Rapidly metabolizing cells produce much more reactive oxygen species (ROS) than those which gain energy through respiratory chain. One of the metabolites of glycolysis, pyruvate, is catching molecules of hydrogen peroxide and transform them to water. Glucose-6-phosphate is the substrate for pentose cycle where nicotinamide adenine dinucleotide phosphate is produced. NADPH is a cofactor for glutathion reductase which reduces

glutathion disulfide to glutathion and the latter takes O_2^- and changes it to water.

The newest hypothesis basically interconnect both of the previously mentioned theories. It says that cells are using Warburg effect as a source of energy to get a fast biosynthesis of metabolic precursors and simultaneously to protect themselves from reactive oxygen species. This hypothesis is supported by experiments in which investigated cancer cells are slowing their division with decreased glycolysis rate and they are dying through oxidative stress when glycolysis is completely off (18).

1. 2. 2. Factors influencing Warburg effect

According to previously mentioned theory we can suppose that Warburg effect is not just a byproduct of cancer growth. On the contrary, it seems that it is an essential requirement for it. Thompson recently developed a model in which mutations in signalling pathways responsible for glucose uptake lead to general deregulation of nutrient intake and thus trigger the Warburg effect and cancer cells proliferation (20).

In normal, non-dividing cells glycolysis is overactivated only during hypoxic conditions by a transcription factor called HIF-1A (Hypoxia inducible factor 1A) which regulates expression of glycolytic genes (21). Oxygen and α -oxoglutarate are used as cosubstrates of HIF prolyl-hydroxylase which hydroxylates HIF-1A on a proline residue. Hydroxylated HIF-1A is then recognized by an E3 ubiquitin ligase and labeled for degradation in proteasome. But if oxygen level is low, HIF prolyl-hydroxylase is inhibited which leads to the stabilization of HIF-1A and the expression of glycolytic genes (22).

Even though the oxygen uptake is unchanged in tumor cells metabolism can be switched from oxidative to substrate phosphorylation. Regulation of the metabolism by HIF-1 is connected with high oxygen levels in cancer cells and tissues (23). Mutated components of signalling pathways such as Akt, Myc, Src or H-Ras can lead to HIF-1 activation despite of the adequate amount of oxygen in the cell (21, 24). In addition, HIF-induced glycolysis might be triggered by mutations in succinate dehydrogenase (SDH) or fumarate hydratase (FH) (21). On top of that, increased metabolism of glucose leads to higher ROS production and glycolytic metabolites accumulation and it can either influence HIF-1 stability and therefore contribute to Warburg effect (17).

Nevertheless cancer cells can set off glycolysis even without stable HIF-1. For instance the transcription factor myc activates the expression of nearly all glycolytic

enzymes (21). Increased activation of myc also leads to higher ROS production and thus antioxidation potential of glycolysis is required (21). The activation of PI3K/AKT pathway upregulates the expression glucose transporters (25). One of the most well known tumor suppressor, p53, works the opposite way - it stimulates oxidative phosphorylation (24).

According to our hypothesis, Notch signalling can also directly influence the expression of genes involved in glycolysis thus contributing to the development of Warburg effect in Notch dependent cancers.

1. 3. Notch signalling pathway

Notch signalling pathway is highly conserved among all Metazoan species. It influences various cellular processes, e.g. triggers differentiation, supports or suppresses cell proliferation or induces cell death. It is dependent on cell contact but no second messengers or other mediators are needed (26). Despite of the level of conservation of the Notch signalling pathway as a whole, number of receptors and ligands exist in different organisms. The most simple system is present in *Drosophila* where there is only one receptor (called Notch) and two ligands (Delta, Serrate). That is one of the reasons why we chose this model organism for our experiments.

An interesting property of the Notch signalling pathway is its dependency on several proteolytic cleavages. First cleavage (S1) takes place in Golgi apparatus where the furine like protease cleaves newly emerged polypeptide to extracellular and intracellular domain, connected by disulfidic bonds in the transmembrane region (although this might not be true for *Drosophila*). Second cleavage (S2) comes when ligand is bound to a receptor. In this point, the extracellular domain is cleaved off by a metalloproteases from the ADAM family. Notch extracellular truncation (NEXT) is created and it is the substrate for the third and four cleavages (S3 and S4) when γ -secretase separates the intracellular domain from the membrane. Notch intracellular domain (NICD) is released and goes to the nucleus (1). There is another cleavage site within the NICD (S5) that was identified as the site for the mitochondrial intermediary peptidase (MIPET). This cleavage results in a decrease in cell viability and mitochondria membrane potential which suggests a novel mechanism by which Notch signalling can be regulated (27).

Notch receptor signalling pathway possesses only one known transcriptional factor called CSL [CBF1/RBP κ in mammals, Su(H) in *Drosophila*, Lag-1 in *C. elegans*] which binds to its consensus binding site (CGTGGGAA) in the enhancer regions of Notch target genes and in the absence of Notch signalling it recruits a corepressor complex (see below) to repress the expression of Notch target genes. After the Notch pathway is activated, NICD goes to the nucleus, displaces the corepressor complex from CSL protein and triggers the assembly of a coactivator complex (see below) to start the expression of the target genes (1) (fig.3 and fig.4). It should be noted that not all Notch target genes must be occupied by CSL (and actively repressed by it) before Notch pathway activation (28).

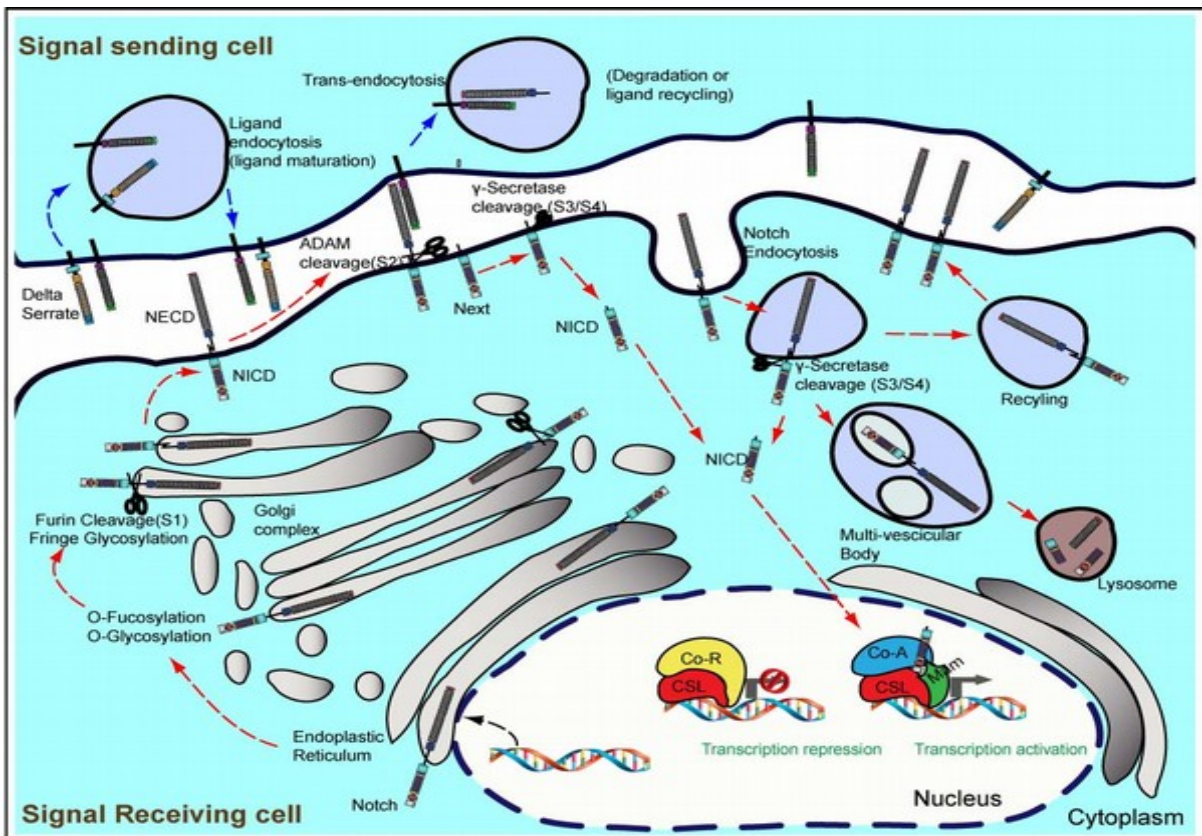


Fig.3: Scheme of activation of Notch receptor and Notch signalling pathway (http://www.bsse.ethz.ch/egg/research/research_gunter/notch_pathway_legend).

1. 3. 1. The role of Notch signalling in development

During development the Notch pathway participates in processes such as lateral inhibition or lateral induction, boundary formation and lineage specification.

Lateral inhibition drives the competition between group of cells which are initially equal and which can all choose different fate. It is typical for the specification of neurons in *Drosophila*. In the beginning all cells in the proneural cluster express about the same amount of Notch receptor and ligand. They all also express proneural genes *Achaete* (*Ac*) and *Scute* (*Sc*) so they all have the potential to become neurons. Over the time one of the cells expresses more ligand than the others which leads to the activation of the Notch pathway in the surrounding cells (activating genes of the *Enhancer of split complex that repress Ac/Sc*) but inhibition of it in the ‘winning’ cell in the middle. This way neuronal differentiation in the neighbouring cells is stopped and instead they develop into epithelial cells. Lateral inhibition drives for example bristle patterning in *Drosophila* (29), neurogenesis in *Drosophila* and vertebrates or inner ear patterning in vertebrates (30).

Lateral induction works in similar situations as lateral inhibition but controls the expression of Serrate (Jagged) ligands in the neighbouring cells by a positive feedback loop by mutual Notch dependent inductive signals amongst the neighbouring cells. However, Notch signalling is still blocked in the middle cell by the regulator Numb. This leads to the situation very similar to lateral inhibition in the way that in a cluster of cells the one in the middle has low Notch activity and the surrounding cells have high activity of Notch pathway. This process takes place in differentiation of lens fibres (31), contributes to assembly of arterial walls (32) or specification of prosensory domains of mammalian inner ear (33) (while lateral inhibition drives their differentiation into sensory hair cells (29)).

The formation of a boundary between two populations of cells that can segregate two groups of cells and/or that can establish an organizer can also be controlled by Notch as it happens in the *Drosophila* wings (34) or intestine, midbrain organiser in chicken embryo (35)

Notch also drives specification of f.e. stem cell or sensory organ precursor (SOP) lineages (36). Here, Notch regulators like Numb are unequally inherited during assymetric cell divisions leading to Notch signalling being active only in certain cells, participating this way in the specification of specific cell subtypes. Other examples of Notch being involved in

this process is specification of projection neuron precursors (PN) (37) or specification of cells from hematopoietic progenitors (38, 39)

1. 3. 2. Regulation of Notch signalling

Notch pathway must have very complex regulatory mechanisms since it works differently in various cells and tissues, influences different set of genes in a context dependent manner. Although still poorly understood, several mechanisms determining this context dependent specificity were proposed.

First step in this complex regulation can be the ligands and receptors themselves. For example ubiquitinylation is needed for the activation of the ligands as well as the receptors. E3 ligases like mindbomb or neuralized are necessary in this process and the regulation of their expression and activity sets a context to the Notch signalling (40). Another posttranslational modification, fucosylation, contributes to spatial regulation of Notch signalling (41). Further modifications of the receptor by the specifically expressed glycosyl transferase Fringe are responsible for differential interactions of the receptor with its ligands (42). Moreover, both the receptor and ligand need to be cleaved. While cleaving of receptor is well understood, the purpose and role of cleaved ligand remains elusive (43).

Another layer of regulation comes with the selection of target genes and the transcriptional events before and during Notch signalling. Although there are thousands of potential binding sites for CSL proteins within the genome (consensus CGTGGGAA) only a few hundreds of them is occupied in highly tissue and context dependent manner (44). It is not strictly true that the occupation of DNA binding sites by CSL proteins dictates the target gene selection. Many genes bind Suppressor of Hairless (Su(H)) only after Notch pathway activation which challenges the 'textbook' model of Notch signalling. This also implies that not all Notch target genes need to be repressed by Su(H) and cell response to Notch signaling pathway is highly dynamic process (44).

Both the corepressor and coactivator complexes are composed of many different proteins (fig.4) in a context dependent manner and therefore subject of specific regulation (45) mammals, two proteins are common to both the complexes: transcription factor CSL (mammalian homolog of the Drosophila Su(H)) which binds DNA and then SKIP (Ski-interacting protein, Bx42 in Drosophila) which bridges interactions between either CSL and corepressors or CSL and NICD. Other partners are unique for either corepressor or

coactivator complex. Corepressor complex engages other proteins such as ETO (Eighty-one), CtBP (C-terminal binding protein), Gro (Groucho) or SMRT (Silencing Mediator for Retinoid and Thyroid hormone receptor) which recruit histone deacetylases (HDACs, SAP30 (Sin3A associated protein 30 kDa), Sirt1) or demethylases (LSD1) via linker proteins such as CIR (CBF1 interacting corepressor, binds CBF-1, HDACs and SAP30) or SHARP (SMRT and HDAC associated repressor protein). In *Drosophila*, similar corepressor complex is assembled. Su(H) interacts with its repressor Hairless (homologue of SHARP) (46) which in turn recruits its corepressors groucho (Gro) and CtBP. Another proteins such as histone chaperons Asf1 (anti-silencing factor-1) or NAP1 complex (nucleosome assembly protein-1 complex) are involved too (42).

The coactivator complex composes of three key proteins: CSL, NICD and mastermind (MAML). Together, they recruit histone acetyltransferases like p300 or PCAF and H2B ubiquitinase (Bre1) to activate transcription of Notch target genes. This ternary complex is highly unstable on DNA where its rapid turnover is mediated by recruitment of the cyclin dependent kinase 8 (CDK 8) which phosphorylate NICD and thus tag it for ubiquitination and decomposition (47). At least in mammals, NICD molecules multimerize in cytoplasm after Notch activation where SKIP protein is attached to them. This complex goes to the nucleus where MAML is recruited to it and together they form a preactivation complex. Preactivation complex then binds CSL, forcing the corepressor complex to detach from CSL. During this process, one NICD molecule dissociates from the preactivation complex leaving just one NICD to be part of the activation complex associated with CSL and MAM (fig. 5) (48). NICD can also dimerize directly on DNA if two CSL binding sites are in close to each other (49).

Major part of tissue specificity of Notch signalling is taken by its cooperation with other signalling pathways. For example in *Drosophila* Su(H) can cooperate synergistically with NF- κ B (50), TGF- β (51) or growth factor / cytokine signaling (52). Importantly, cooperation with transcription factors like grainy head (45) or twist (53) defines target gene selectivity in specific tissues.

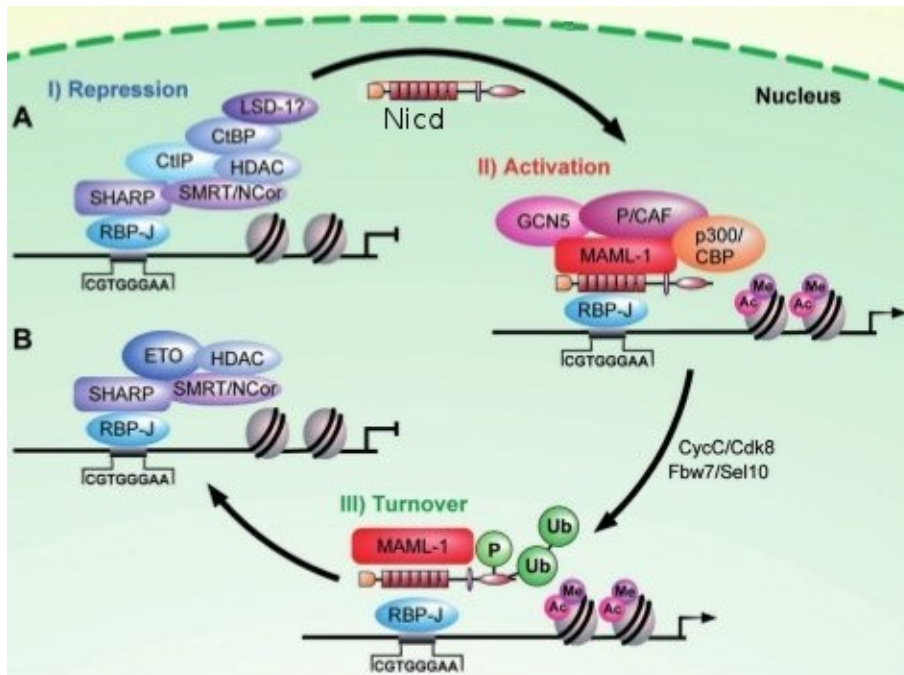


Fig. 4: Composition of the mammalian corepressor and coactivator Notch complexes recruited by CSL (Borggreffe and Oswald, 2009). RBP-J is different name for CBF-1, the mammalian homologue of CSL.

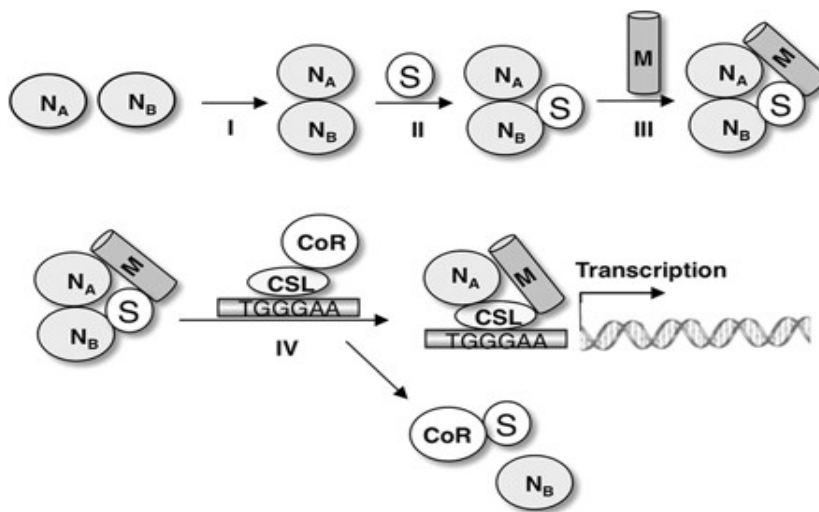


Fig.5: Assembly of the Notch coactivator complex involves multimerization of NICD in the cytoplasm (Vasquez-Del Carpio and col, 2011).

1. 3. 3. Notch target genes

Notch signaling target genes have been studied for quite a long time. The best known target of Notch pathway in *Drosophila* is *Enhancer of split* complex (it is composed of 10 highly homologous genes in a cluster). In mammals there are homologues of these proteins called HES genes (*Hairy/Enhancer of split*). They work as transcriptional repressors mediating many major effects of Notch signaling pathway (54).

Recently, several publications focussed on the identification of new Notch target genes in different tissues using genome wide approaches. For example Krejčí et al. searched the *Drosophila* genome looking for the changes in mRNA expression and for sites occupied by Su(H) after activation of Notch in *Drosophila* muscle progenitor cells. Interestingly, they found that genes encoding core components of different signaling pathways such as RTK, TGF- β , Wnt and also Notch itself are with high probability direct targets of Notch signaling. They also found that Notch stimulates the expression of certain genes and also of their repressors, creating a negative feed-forward loops (44). Meier-Stiegen and col. found huge amount of Notch 1 target genes in murine stem cells including transcription factors, lineage determinants, cell cycle regulators, intracellular signaling mediators, receptors and ligands (55).

A problem during the identification of the Notch target genes is to distinguish between the primary and secondary targets. For example, when a transcriptional profile is compared between normal tissue and a tissue where NICD was overactivated, it is difficult to truly distinguish between a primary response caused by the direct signalling of Notch to CSL and a secondary or tertiary responses caused by a mediator in between. A few methods to distinguish primary and secondary targets might be used. For example, stopping protein translation by cycloheximide can be useful in experiments using cell lines (but not tissues, (56)) although secondary responses might still be mediated by a pre-made protein mediator. Inhibiting γ -secretase is another way to identify Notch targets but again, a secondary response can not be excluded. The best approach is to combine the expression studies with the bioinformatic/computational approach (*in silico* prediction of CSL binding sites within the genome) and chromatin immunoprecipitation (ChIP) that identifies elements occupied by a transcription factor *in vivo* (57). Only genes whose mRNA is upregulated in response to Notch stimulation and that have Su(H) or NICD bound in their enhancers at the same time can be considered as true primary targets (44).

1. 3. 4. Notch and cancer

The relationship between Notch signalling and cancer is known for a long time. It is a known cause of carcinomas of T-cells, breast tissue, colon,... However, depending on the context it can be considered both an oncogene as well as an oncosuppressor. Here are several examples how aberrant Notch activity arises in differentiated cells to promote their cancerous growth:

In 1980's, translocation t(7;9) connected with small group of T lymphocytes were found by Skalar's group (44). This translocation cause non-regulated expression of several tumor-specific 5' deleted mRNA transcripts of NOTCH 1. Damaged Notch signalling then influences proliferation and survival of imperfectly differentiated T-lymphocytes which leads to blood cancer called lymphoid neoplasm of T-all (2, 58).

Another mechanism causing a heritable and very aggressive type of breast cancer is an insertional mutagenesis caused by the Mouse Mammary Tumor Virus (MMTV). This virus inserts itself into Int-3 region inside of the Notch 4 gene, close to LIN12. Loss of regulation sequence of extracellular domain then cause higher expression of the active form of Notch 4 and therefore higher proliferation of these cells (59).

Notch signalling plays a role in colorectal cancer too. It is the vital gatekeeper for maintenance of proliferative cells. It's function is necessary for renewal of Lieberkühn's crypts. But constitutive activation of Notch in gut epithelium leads to an accumulation and subsequent proliferation of non-differentiated epithelial cells (60).

Notch doesn't act only as an oncogene though. In many types of cells it plays a role as a tumor suppressor; its inactivation is essential for tumorigenesis (59). For example the Achaete-scute homolog-1 (ASH-1) protein is inevitable for the differentiation of the neuroendocrine cells of the lung or neuronal tissue. In epithelial cells, Notch activates the expression of the HES protein which binds the *ASH-1* promoter and suppress its expression. In lung cancerous cells, the inhibition of notch signalling and huge overexpression of ASH-1 protein takes place (59).

Another typical example of Notch as a tumor suppressor is the cerevical cancer. Notch signalling suppresses activities dependent on the Human Pappilomavirus (HPV). In healthy cells or in those with low content of virus we can detect a huge amount of Notch-1 and its ligands on the surface of the cells. But the number of receptors and ligands is

decreasing with increasing volume of virus in affected cells. And in fully transformed, cancer cells we can't detect any receptors or ligands (2).

A little bit different case is the formation of meduloblastoma. This type of cancer is provoked by a malformation in Sonic hedgehog signalling pathway (Shh). Nevertheless, in subsequent studies it was found that Notch is continuously activated in meduloblastoma cells. The most probable explanation is that Notch signalling is triggered by Shh. Notch negatively regulates Numb which is a suppressor of Shh (60).

Notch can contribute to cancerous growth by many distinct mechanism. Its effect on tumor suppressors or oncogenes were found. For example, gene *Myc* (regulator of cell growth, proliferation, metabolism, differentiation, apoptosis and one of the well known protooncogenes) was recently proven to be one of the direct targets of Notch signalling pathway. Therefore, over-activated Notch pathway leads to higher expression of *Myc* and thus causing cancerous growth (61). There is even connection with the major tumor suppressor, p53. This connection proved to be complex because p53 can be either suppressed by Notch signalling (62) or, in directly opposite manner, it can down-regulate Notch1 signalling pathway (63). Notch pathway also influences expression of *phosphatase and tensin homologue (PTEN)*, a tumor suppressor involved in the regulation of the cell cycle and most importantly AKT, preventing cells from growing and dividing too quickly. In prostate adenocarcinoma, Notch-1 signalling is lost and *PTEN* expression is decreased (64).

We believe (and our data point to it) that Notch can work as an oncogene by influencing cell metabolism, mainly glycolysis, thus provoking Warburg effect which can cause or at least promote the cancerous growth.

2 Aims

In this master thesis I am trying to prove the connection between Notch signalling pathway and cell metabolism. According to our hypothesis, Notch signalling is one of the pathways able to modify metabolic status of the cell, influencing especially glycolysis and Krebs cycle. This way it can cause Warburg effect or at least contribute to its manifestation.

Specific aims:

1. To identify potential Notch target genes involved in the regulation of metabolism.

Analysis of the Chip-chip experiment with the Su(H) antibody in several cell lines as well as tissues looking for peaks of Su(H) binding in the vicinity of metabolic genes

2. To investigate the effect of Notch pathway activation on the expression of selected metabolic genes *in vitro*

- *Are there functional Su(H) binding sites in the potential regulatory regions of selected metabolic genes?*

Method: Luciferase assay of transfected cells to look for the response of enhancers activated by the overexpression of Notch intracellular domain.

Cloning of the enhancer regions into the pGL3-basic vector in front of a minimal promoter and a luciferase reporter. Transfection of S2 Drosophila cell line to perform the luciferase assay. Mutation of Su(H) binding sites within the cloned enhancer region to see if the response of the luciferase reporter is really Notch dependent.

- *Is there a transcriptional response of the selected metabolic genes to the activated Notch pathway in cell lines and if so how long does it take to see it?*

Method: Q-RT-PCR analysis of S2N, KC167 and DmD8 cells in a time course experiment.

Activation of the Notch pathway in selected cell lines by a short pulse of EDTA, extraction of RNA, preparation of cDNA, real time PCR analysis.

3. To investigate the effect of Notch pathway activation on the expression of selected metabolic genes in vivo

- *Will the expression of selected metabolic genes be affected in the wing discs where we activate / suppress Notch pathway?*

Methods: a) Q-RT-PCR analysis of mRNA from imaginal wing discs where the Notch pathway was upregulated / downregulated in the *patched* domain. Dissection of imaginal wing discs, extraction of RNA, preparation of cDNA, real time PCR analysis.

b) In situ hybridization of imaginal wing discs where the Notch pathway was upregulated / downregulated in the *patched* domain to see the changes in the endogenous expression pattern of the genes of interest

4. To analyze metabolic changes associated with activation of the Notch pathway in vitro and in vivo

- *Is there a functional connection between the Notch activation and the transcriptional responses of the Notch target genes involved in metabolism?*

Method: Measurement of the rate of glycolysis and respiration on the Seahorse XF extracellular flux analyser in S2N, Kc167 and DmD8 cells as well as in imaginal wing discs with the overactivation of Notch pathway.

3 Material and methods

3.1. Selection of potential Notch target genes involved in metabolism

The selection of genes potentially regulated by the Notch pathway was based on the published (44) as well as unpublished data set of Alena Krejčí and colleagues who performed ChIP-chip experiments searching the genome for regions bound by the Suppressor of Hairless (Su(H)) in different cell lines and tissues. Su(H) is a transcription factor that occupies the Notch target gene enhancers and is the only and therefore crucial DNA binding effector of the Notch pathway in the nucleus. Experiments were performed with three *Drosophila* cell lines (*BG2* – neural cells progenitors, *Kc167* – hemolymph progenitors, *DmD8* – muscle progenitors) and three types of the *Drosophila* imaginal wing discs (*yw* – control, 'Giant Su(H)' –overexpression of Su(H) in the *patched* domain, 'Giant NICD' – overexpression of NICD in large clones of cells throughout the discs, basically filling the discs). Data were analyzed as previously described (44) and visualized by the Integrated genome browser software (65). We searched for peaks of Su(H) binding in the vicinity of metabolic genes listed in tab.1 in any of the cell lines or discs described above. Ideally we wanted to see these peaks to overlap with the computationally predicted Su(H) binding sites (predicted by a weight matrix or using a set of experimentally verified Su(H) binding sequences (which we call a 'dictionary')).

Several genes showed Su(H) peaks in their vicinity and we chose seven of them to be studied in more detail (see results, tab. 8). These were either genes with the most profound peaks or genes that play critical roles in the glycolysis or Krebs cycle. These genes were then used for the *in vitro* and *in vivo* studies with *Drosophila* cell lines and third instar larvae.

We tested the responsiveness of their enhancers to the Notch pathway in luciferase assays, we quantified the upregulation of their mRNA by real time PCR after the Notch pathway stimulation in cells and wing discs, we looked on the upregulation of their mRNA in the imaginal wing discs by *in situ* hybridizations and we measured the metabolic parameters of several cell lines and wing discs on the Seahorse FX analyser.

Tab 1: List of metabolic genes tested for the presence of Su(H) peaks in their vicinity.

Carbohydrate metabolism					
Gene	Symbol	Function	Gene	Symbol	Function
6-phosphofructo-2-kinase	Pfrx	transfers phosphate from ATP to fructose-6-phosphate	Phosphoglycerate mutase 87	Pgym87	converts 3-phosphoglycerate to 2-phosphoglycerate
Aldolase	Ald	cleaves Fructose 1,6-bisphosphate to dihydroxyacetone phosphate and glycerol-3-phosphate	Phosphogluconate dehydrogenase	Pgd	changes 6-phosphogluconate and NADP to ribulose 5-phosphate and NADPH
Ecdysone-inducible gene L3	Impl3	predicted lactate dehydrogenase, converts lactate to pyruvate	Triose phosphate Isomerase	Tpi	converts glyceraldehyde-3-phosphate to dihydroxyacetone phosphate
Enolase	Eno	converts 2-phosphoglycerate to phosphoenolpyruvate	Pyruvate kinase	Pyk	phosphorylates pyruvate to phosphoenolpyruvate
Glucose dehydrogenase	Gld	oxidizes D-glucose to D-gluconolactone	Trehalase	Treh	converts trehalose to glucose
Glucose transporter 1	glut1	transfers glucose to the cell	Phosphorylase kinase gamma	PhK gamma	converts between different kinds of phosphorylases
Glucose transporter 3	glut3	transfers glucose to the cell	Zwischenferment	Zw	predicted glucose 6-phosphate dehydrogenase
Glucose-6-phosphate dehydrogenase	G6PD	catalyzes conversion of glucose 6-phosphate to 6-phosphogluconolactone	X	CG5432	predicted fructose-bisphosphate aldolase
Glyceraldehyde 3 phosphate dehydrogenase 1	Gapdh1	catalyzes oxidation of glucose 3-phosphate to 3-phosphoglycerate	X	CG7059	predicted phosphoglycerate mutase
Glyceraldehyde 3 phosphate dehydrogenase 2	Gapdh2	catalyzes oxidation of glucose 3-phosphate to 3-phosphoglycerate	X	CG7140	predicted glucose 6-phosphate dehydrogenase
hexokinase A	Hex-A	converts D-hexose to D-hexose 6-phosphate	X	CG9010	predicted glucose 3-phosphate dehydrogenase
hexokinase C	Hex-C	converts D-hexose to D-hexose 6-phosphate	X	CG9961	predicted phosphoglycerate kinase
hexokinase T1	Hex-t1	converts D-hexose to D-hexose 6-phosphate	X	CG12229	predicted pyruvate kinase
hexokinase t2	Hex-t2	converts D-hexose to D-hexose 6-phosphate	x	CG11249	predicted pyruvate Kinase
Maltase A1	LvpH	catalyzes hydrolysis of maltose to glucose	X	CG30410	predicted ribose 5-phosphate isomerase
Maltase A2	LvpD	catalyzes hydrolysis of maltose to glucose	X	CG4747	predicted 3-hydroxyisobutyrate dehydrogenase
Maltase A3	LvpL	catalyzes hydrolysis of maltose to glucose	X	CG10924	predicted phosphoenolpyruvate carboxykinase
Phosphoglucose isomerase	Pgi	catalyzes conversion of glucose 6-phosphate to fructose 6-phosphate	X	CG17333	predicted 6-phosphogluconolactolase
Phosphoglycerate kinase	Pgk	transfers phosphate from 3-phosphoglycerate and ATP to form ADP and 1,3-bisphosphoglycerate	X	CG7024	predicted pyruvate dehydrogenase phosphatase
Phosphoglycerol mutase	Pglym78	converts glucose 2-phosphate to glucose 3-phosphate	X	CG7362	predicted pyruvate kinase
Phosphoenolpyruvate carboxykinase	Pepck	converts oxaloacetate and GTP to CO ₂ , GDP and phosphoenolpyruvate	X	CG13334	predicted lactate dehydrogenase
Phosphofructokinase	Pfk	phosphorylates fructose 6-phosphate to fructose bisphosphates	X	CG7069	predicted pyruvate kinase

Krebs cycle					
Gene	Symbol	Function	Gene	Symbol	Function
Isocitrate dehydrogenase	ldh	converts isocitrate to α -ketoglutarate	X	CG4095	predicted fumarate hydratase
Neural conserved At 73 EF	Nc73EF	predicted oxoglutarate dehydrogenase	X	CG5214	predicted dihydro-lipoyllysine residue succinyl-transferase
Pyruvate dehydrogenase phosphatase	PDK	activates pyruvate dehydrogenases	X	CG6140	predicted fumarase
skpA associated protein	skap	converts succinate and coenzyme A to succinyl-CoA	X	CG5261	predicted dihydro-lipoyllysine residue acetyltransferase
Succinate dehydrogenase B	SdhB	oxidizes succinate to fumarate	X	CG6439	predicted isocitrate dehydrogenase
Succinate dehydrogenase C	sdhC	oxidizes succinate to fumarate	X	CG10749	predicted L-malate dehydrogenase
succinate-CoA ligase	Sucb	converts succinate and coenzyme A to succinyl-CoA	X	CG1544	predicted oxoglutarate dehydrogenase
Malate dehydrogenase 1	MDH1	catalyzes the conversion of malate into oxaloacetate	X	CG33791	predicted oxoglutarate dehydrogenase
X	CG4706	predicted aconitase	X	CG7998	predicted malate dehydrogenase 2
X	CG14740	predicted citrate (Si)-synthase	X	CG10748	predicted L-malate dehydrogenase
X	CG5599	predicted dihydro-lipoamide acyltransferase	X	CG1516	predicted pyruvate carboxylase
X	CG7430	Predicted dihydro-lipoyl dehydrogenase	X	CG5718	predicted succinate dehydrogenase
Others					
Gene	Symbol	Function	Gene	Symbol	Function
Protein kinase B	AKT	phosphorylates proteins	DNA damage-binding protein 1	DDB1	large subunit of protein repairing UV-damaged DNA
C terminal binding protein	CtBP	transcriptional co-factor	Spaghetti squash	sqh	encodes light chain of nonmuscle myosin
SNF1A/AMP-activated protein kinase	SNF1A	nutrient and cellular energy sensor and regulator; determinant of cell polarity'	Target of rapamycin	TOR	serine/threonine protein kinase regulating motility, proliferation, protein synthesis,...
Hairy	h	transcriptional factor	Sirtuin 2	Sir2	(histone)deacetylase
Insuline like receptor	InR	triggers response to insuline	Sirtuin 4	Sirt4	(histone)deacetylase
nicotinamide amidase	d-NAAM	hydrolyses nicotinamide to nicotinate	Sirtuin 5	Sirt5	(histone)deacetylase
Nicotinamide mononucleotide adenyltransferase	Nmnat	biosynthesis of NAD	Sirtuin 6	Sirt6	(histone)deacetylase
Nucleoporin 133	Nup133	protein for building of nuclear pore	Sirtuin 7	Sirt7	(histone)deacetylase
Phosphatase and tensin homolog	PTEN	phosphoprotein phosphatase activity	Tarsal-less	Tal	involved in morphogenesis, differentiation,...
Poly-(ADP-ribose) polymerase	PARP1	NAD+ ADP-ribosyltransferase 1	X	CG15093	predicted 3-hydroxy-isobutyrate dehydrogenase
Liver kinase B1	lkb1	phosphorylates proteins	X	CG9467	predicted oxidoreductase
Slimfast	slif	cationic amino acid transmembrane transporter	X	CG11294	predicted sequence-specific DNA binding transcription factor

Function of genes studied and their connection to diseases

The genes we selected to study are connected to cell metabolism but they are also associated with disease such as cancer of metabolic syndromes.

Hexokinase-A (Hex-A) is an important enzyme of glycolysis. It phosphorylates hexoses to hexoses phosphates. In flying insect, it is one of the most expressed genes because of the sugar needed for flight. *Drosophila* hexokinase coding sequences *DM1* and *DM2* have extensive homology (up to 45%) to human *Hexokinase* genes (66). Moreover, connection between human *Hexokinase* and cancer has been discovered. Human Hex II, if connected to inner mitochondrial membrane, prevents apoptosis of cancer cells (67). And interconnection between high *Hex II* expression in human brain metastases of breast cancer and poor survival of patients had been revealed (68).

Another players involved in glucose metabolism are proteins from the glucose transporter family. Amongst them, *glucose transporter 1 (Glut1)* is the one with connection to human tumorous diseases such as renal cell carcinoma, melanoma, hepatocarcinoma, breast cancer, etc. Higher expression of *Glut1* is present in 69,6 % of these types of cancer (69). Moreover, there is high similarity (68%) between *Drosophila melanogaster* and mammals amino acid sequences (70). There is some connection between higher glucose metabolism and immune response too. Singer had found that higher expression of *Glut-1* is correlated to lower amount of CD8+ T-cells in the renal cell carcinoma tissue (71).

Drosophila lactate dehydrogenase, *ecdysone-inducible gene L3*, is a protein needed for embryogenesis, larval and somatic muscle development, imaginal discs morphogenesis, and it shows 53-61% amino acid homology to human lactate dehydrogenase (LDH) (72). There is another predicted *Drosophila* lactate dehydrogenase, a protein coded by the gene *CG13334* which also showed Su(H) binding according to the ChIP-chip experiments and therefore we included it in our studies. Human *lactate dehydrogenase* was found to be connected to renal cell carcinoma, melanoma and hepatocarcinoma (71, 73) and it is said that the higher level of serum LDH before treatment the worse the prognosis is (73, 74).

Another enzyme connected to sugar metabolism is trehalase (Treh). Its function is to convert trehalose (sugar to be found in algae, fungi, insect...) to glucose. Trehalase deficiency is a rare disease causing health problems such as vomiting, abdominal pain and diarrhea after the food containing trehalose is eaten (75).

One representative of enzymes engaged in the Krebs cycle is the isocitrate dehydrogenase (IDH). Mutations in *IDH 1* and *IDH 2* are known to be involved in most cases of gliomas, glioblastomas and in 8% of cases of acute myelogenous leukemias. Mutations in *IDH 1* causes lower affinity of IDH to isocitrate and higher to NADPH and α -ketoglutarate which leads to higher production of 2-hydroxyglutarate which is not normally produced in healthy cells (76, 77). Accumulation of this 'oncometabolite' is thought to cause the activation of the hypoxia-responsive pathway (via HIF-1 α) and up-regulation of the glycolytic enzymes necessary for continued cancer cell growth.

Last but not least, we also tested another potentially very interesting Notch target gene, *hairy (h)*. It is a transcriptional repressor which in *Drosophila* has an important role in the segmentation of embryos and bristle patterning in adults (78). It also acts as a metabolic switch in hypoxic conditions: *h* is upregulated in *Drosophila* exposed to low oxygen level whereas some metabolic genes are downregulated compared to control flies. Interestingly, its binding elements were found in regulatory region of these metabolic genes (79). In mammals, its misregulation is present in many type of cancer (80).

3. 2. Analysis in cell lines

3. 2. 1. Testing Su(H) enhancers in the luciferase assay

To investigate the responsiveness of the selected metabolic genes to the Notch pathway, their enhancers were tested in a luciferase assay.

The enhancers were cloned into a slightly modified pGL3-Basic vector containing the luciferase reporter gene and a Hsp70 minimal promoter (pGL3-min, fig.6) and transfected into the S2 cells together with a vector coding for a copper inducible Notch intracellular domain. If the cloned enhancers contained functional binding sites for Su(H) they triggered the expression of the luciferase gene after the induction of NICD. Cells transfected with the reporter alone set the background.

Two individual reporter enzymes (luciferase and renilla) were expressed simultaneously within one experiment. The luciferase is an enzyme responding to Notch activation of enhancers and renilla serves as an internal control of experimental variability such as different viability of the cells, transfection efficiency or pipetting errors. The same

amount of pRL-TK-Renilla (Promega) plasmid was cotransfected with the luciferase reporters in each well.

Luciferase and renilla were measured sequentially from a single sample by adding different substrates (fig.7) using the Dual-luciferase reporter assay system (Promega). The luminiscence of the luciferase was measured first by the addition of the Luciferase assay reagent II. This reaction was subsequently stopped by Stop & glo reagent which also produced a signal of renilla luminescence (81).

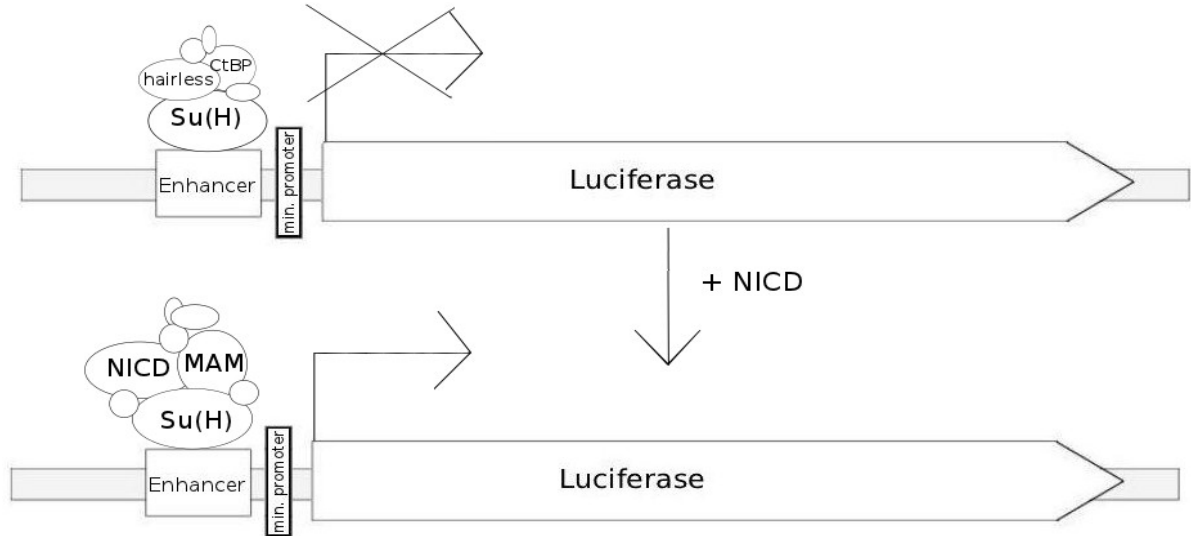


Fig.6: Principle of the luciferase enhancer assay: If the cloned DNA functions as an enhancer, a coactivator complex is assembled on the DNA after the Notch pathway induction and transcription of the *luciferase* starts.

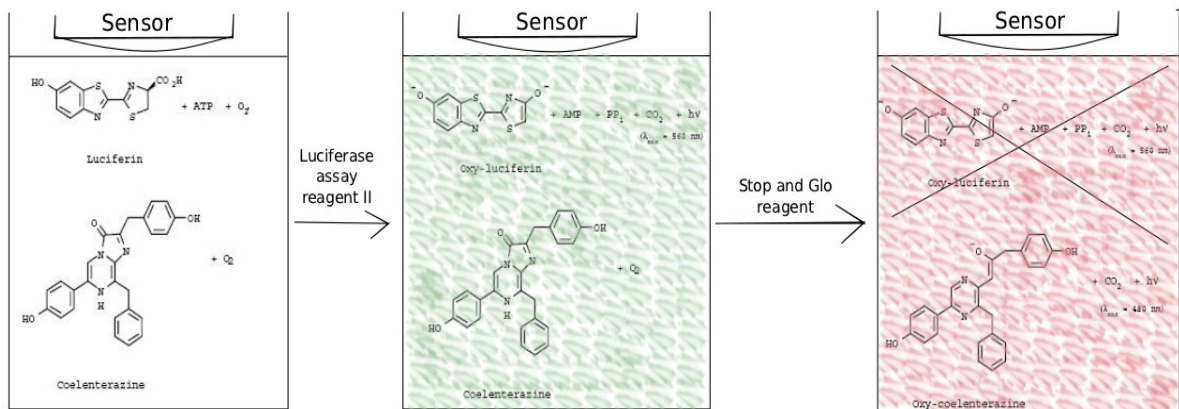


Fig.7: Bioluminescent reaction catalyzed by firefly and Renilla luciferase. Luciferin and coelenterazin are both present in the sample. After Luciferase assay reagent II is added luciferin is changed to oxyluciferin. Subsequently added Stop and Glo reagent stop luciferine reaction and coelenterazin is converted to oxy-coelenterazin.

PCR amplification of enhancers

In case some genes contained more than one 'good' Su(H) peaks more enhancer regions were amplified and cloned from the same gene. In total, eleven enhancer regions were amplified from seven originally selected genes. The lengths of the amplified sequences varied from 152 bp to 641 bp.

For the polymerase chain reaction, BioTaq polymerase (Bioline) and oligonucleotides (Sigma) listed in table 2. were used. Template DNA was isolated from the *yw* line of *Drosophila* according to the protocol described below. Primers were designed by Primer3 software (82). A unique 5 bp sequence was added upstream to the restriction site (RE I) to enable a good binding of the restriction enzyme. PCR was performed according to the protocol in tab. 3 and 1% agarose gel electrophoresis was used to check the products.

Table 2: Oligonucleotides and restriction endonucleases (RE I) used for cloning of enhancers

Gene	Primer Name	Sequence	RE I
CG13334	Kpn1 CG13334_1fw	gatca GGTACC ctgctccattgctgttgac	KpnI
	Bgl2 CG13334_1rev	gactc AGATCT tccgaaacgaaaacgaaaac	BglII
	Mlu1 CG13334_2fw	gactc ACGCGT ccctggatacagacgattgc	MluI
	Bgl2 CG13334_2rev	gactc AGATCT cctttggctgtttgtctgc	BglII
	Mlu1 CG13334_3fw	gactc ACGCGT tggacgcaaccatcatattc	MluI
	Bgl2 CG13334_3rev	gactc AGATCT tactccacgaaagcgaacc	BglII
Glut1	Kpn1 Glut1_fw	gatca GGTACC Gaagacgacgacatgactgc	KpnI
	Bgl2 Glut1_rev	gactc AGATCT cgaggatgctgactttgaatc	BglII
Hairy	Kpn1 hairy_fw	gatca GGTACC agcaacaacaccaaccac	KpnI
	Bgl2 hairy_rev	gactc AGATCT caccgcgttactcatacgc	BglII
Hex-A	Kpn1 Hex-A_1fw	gatca GGTACC tgtgctacaagcgaagcag	KpnI
	Bgl2 Hex-A_1rev	gactc AGATCT tccaaggagtgcattgg	BglII
	Kpn1 Hex-A_2fw	gatca GGTACC cagcaccgaatggaaattg	KpnI
	Bgl2 Hex-A_2rev	gactc AGATCT ttggcttcgtctttgaacc	BglII
	Kpn1 Hex-A_3fw	gatca GGTACC gcgacgcataagggttcc	KpnI
	Bgl1 Hex-A_3rev	gactc AGATCT cggcatggttgagatatg	BglII
Treh	Kpn1 Treh_fw	gatca GGTACC cgtaaacgaaagaaaagtgc	KpnI
	Bgl2 Treh_rev	gactc AGATCT ttctgcctccttttctgc	BglII
IDH	Mlu1 ldh_fw	gactc ACGCGT gtaaatactggcggaatg	MluI
	Kpn1 ldh_rev	gatca GGTACC ccggtaacattcacttttg	KpnI
ImpL3	Bgl2 ImpL3_fw	gactc AGATCT tcagttctgtttgggagag	BglII
	Kpn1 ImpL3_rev	gatca GGTACC gcttaatatcgcagtcgatcg	KpnI

Table 3: Polymerase chain reaction protocol

Reaction mix protocol		Three-step cycling	
Components	Volume	protocol	
10x NH ₄ reaction buffer	5 µl	<u>94°C</u>	<u>90 s</u>
50mM MgCl ₂ solution	1,5 µl	94°C	40 s
100mM dNTP mix	1 µl	56°C	40 s
Primer mix (10mM each)	2,5 µl	72°C	40 s
Water	up to 50 µl		
Template	1 µl (150 ng)		30x
BIOTAQ	0,5 µl		

Genomic DNA extraction protocol

- 1) homogenize 50 *Drosophilas* in 500 µl H-buffer
- 2) add 25 µl of 10 mg/ ml proteinase K and 50 µl 10% SDS, incubate at 55 °C over-night
- 3) extract by 500 µl of phenol:chlorophorm:isoamylacohol, vortex and spin 5 min at 4 °C (Repeat twice)
- 4) clean with chlorophorm:isoamylacohol, vortex and spin 5 min at 4°C
- 5) add 1 ml of 100% ethanol and 40 µl of sodium acetate and put to the -80°C for a few hours, than spin 20 min at 4°C, discard a supernatant
- 6) wash pellet with 70% ethanol, spin 5 min at 4°C, discard a supernatant
- 7) dry the pellet and resuspend it in adequate volume of water

Cloning of enhancers

PCR product was cleansed by phenol:chlorophorm extraction and precipitated in ethanol by sodium acetate and pelete was resuspended in 20 ul of H₂O. Whole amount of cleansed PCR product and 5 µg of cloning vector were cleaved with the appropriate restriction endonucleases according to tab.2 overnight at 37°C with suitable buffers and BSA (if needed). Cleaved vectors were treated with alkaline phosphatase (Roche) to prevent religation. The ligation reaction was accomplished overnight at 16°C with T4 DNA ligase (Roche) and the transformation of competent DH 5α *E. coli* was carried out by a heatshocked at 42°C for 45 seconds. The verification of colonies after the transformation was

performed by PCR using a forward primer from the enhancer region and a reverse primer RV3 from the vector (see tab. 2). Plasmids from the positive colonies were purified by High-speed plasmid mini kit (Geneaid) and sequenced.

Mutagenesis

To prove that the effect we observe in a luciferase assay is really dependent on the activity of the Notch pathway we decided to mutate the Su(H) binding sites in the reporter vectors to see the loss of the NICD dependent response. Sometimes the enhancers we cloned contained more than one predicted Su(H) binding site. In such cases the most conserved Su(H) site was chosen for the mutagenesis or a site that overlapped with both the computationally predicted sites using the weight matrix as well as by using the 'dictionary' (see above).

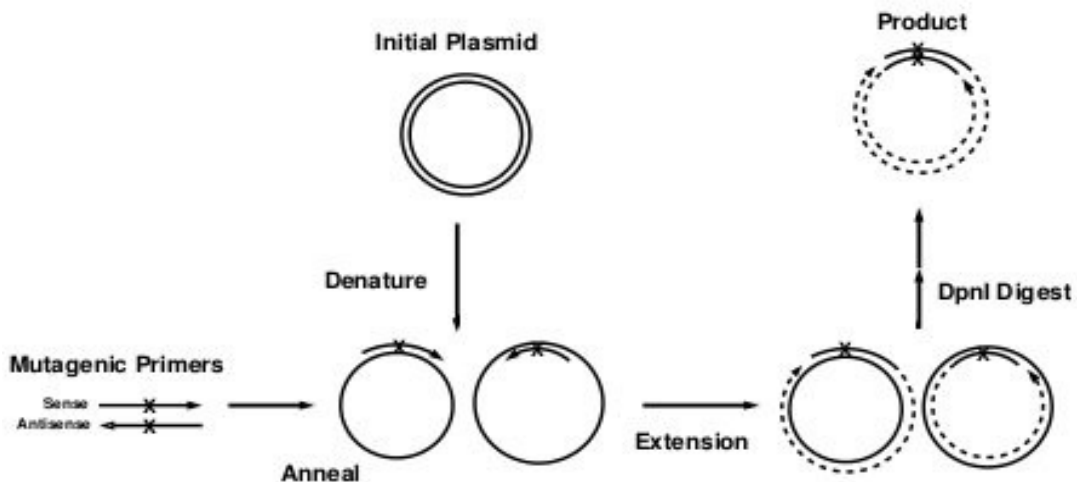


Fig. 8: Principle of the mutagenesis protocol (www.stanford.edu/~loening/protocols/Site_Directed_Mutagenesis.pdf): Initially cloned enhancers were mutated within the Su(H) binding site using 47 bp mutagenic primers and a proofreading Pfx polymerase. Nonmutated plasmids were then removed from the PCR product by the DpnI restriction enzyme.

Primers for mutagenesis were 47 bp long (7bp of the Su(H) binding site of which 3 base pairs were mutated and 20 bp at each side to allow good annealing). For the PCR amplification proofreading Pfx Platinum polymerase was used according to a protocol provided by the supplier (Invitrogen). Originally cloned plasmids containing enhancer regions were used as a template. After the amplification, the PCR products were treated by the Dpn I restriction endonuclease (specifically recognizing only its methylated DNA recognition sequence) to remove the original (nonmutated) plasmids isolated from bacteria

and therefore methylated. DH 5 α *E. coli* was used for transformation. Plasmids were isolated by High-speed plasmid mini kit (Geneaid) and sequenced.

After the verification, plasmids were purified using the Plasmid midi kit (Quiagen). Transfections of S2 cells with both the mutated and nonmutated plasmids were performed and luciferase was measured with the Dual-luciferase reporter assay system (Promega, see below).

Luciferase assay

Luciferase assay was performed with the *Drosophila* S2 cell line using Fugene transfection reagent (Roche) to deliver the plasmids into the cells. For each well in a 24-well dish total amount of 1200 ng of DNA was used (200 ng pRL-TK-Renilla (Promega), 500 ng reporter plasmid, 200 ng pMT-Nicd and 300 ng empty pMT) in the following protocol:

1. For each sample mix 40 μ l of Opti-MEM (Invitrogen) with 200 ng of pRL-TK-Renilla and 500 ng of the luciferase reporter plasmid containing the enhancer of interest.
2. Add 200 ng of pMT-NICD (coding the copper inducible Notch intracellular domain) and 300 ng of the empty pMT plasmid (or 500 ng of pMT plasmid as a negative control without pMT-NICD).
3. In another vial mix 25 μ l of Opti-MEM with 3 μ l of FuGENE, vortex lightly and let stand for 5 minutes on RT
4. Combine vials 1 and 2, vortex lightly and incubate on RT for 30 minutes
5. Suck off medium from the cells, keep only 250 μ l in the dish
6. Add transfection mix into medium by drops
7. After 6 hours replace medium for medium containing 600 μ M CuSO₄ to activate the NICD expression
8. After 24 hours suck off the medium, and lyse the cells in 50 μ l of 1x Lysis buffer.
9. Samples were 5x diluted and 10 μ l of this diluted sample used for the measurement on the Orion II microplate luminometer (Titertek-Berthold) according to the following protocol:
 - a) adding 50 μ l of the Luciferase assay reagent II
 - 2,05 s delay
 - 10 s measurement of *luciferase*
 - 10 s delay

- adding 50 μ l Stop & glo reagent
- 2s delay
- 10s measurement of *renilla*

If necessary, lysed cells were stored at -20 °C to the next day or at -80 °C for longer time before the measurement. All transfections were prepared in duplicates and at least three independent biological replicates were performed on separated days.

3. 2. 2. Analysis of the mRNA expression profile after the activation or the Notch pathway using Q-RT-PCR

To investigate the Notch dependent mRNA induction of our genes of interest we decided to do a time course analysis of their expression in S2N, Kc167 and DmD8 cells. The S2N cell line are S2 cells stably transfected by a copper inducible full length *Notch* construct. Here, the expression of *Notch* was triggered by 600 μ M overnight and the Notch pathway activated by 2 mM EDTA in PBS (28). Our initial attempts to activate cells by adding EDTA directly to the medium failed (data not shown). Therefore we decided to activate cells for 15 minutes with EDTA in PBS as a compromise between good induction of mRNA and the possibility of starvation by the lack of media during the activation. The 6-well plate was used for this assay and 6 samples from every cell line were collected according to the following scheme (fig.9):

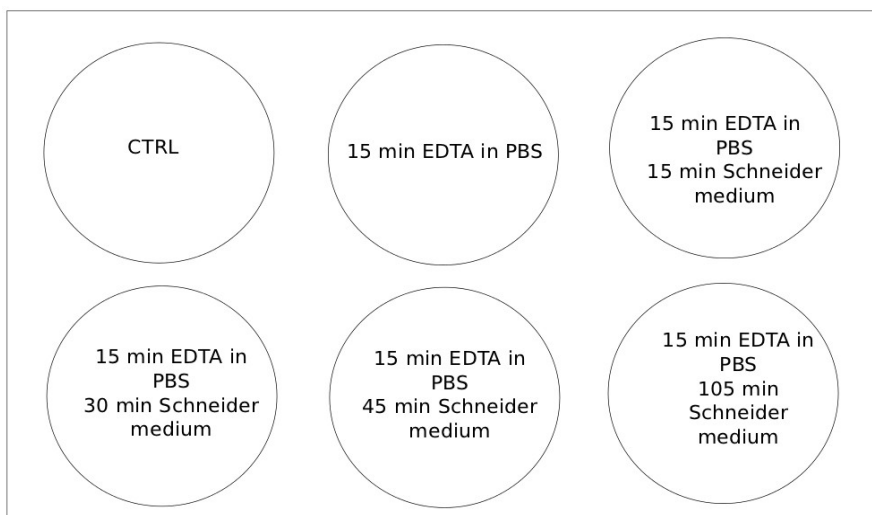


Fig.9: Scheme of the time course experiment

Table 4: Used Q-PCR primers

Gene	Primer name	Sequence
CG13334	CG13334RT_Fw	ACTCCAAGGATTCCGATGTG
	CG13334RT_Rev	ACTGAGCTCCACCAGTTTGG
glut1	Glut1RT_Fw	TCGACCATGGAGCTGATATG
	Glut1RT_Rev	TGAACAGCGACGTGGAATAG
hex-A	Hex-ART_Fw	GATGTGCACAGCATCAATCC
	Hex-ART_Rev	CTTCGGAATCCTGTCCATTG
treh	TrehRT_Fw	CACCAACGATGACAAGTTCG
	TrehRT_Rev	GAATCGCGGTACACACACAG
idh	IDHRT_Fw	TTGCTTATGCCATGAAGTCG
	IDHRT_Rev	ATAGCAGCACGGAGGTCATC
ImpL3	ImpL3RT_Fw	TGGTCTGGAGTGAACATTGC
	ImpL3RT_Rev	AGCTTGATCACCTCGTAGGC
hairy	HairyRT_Fw	ACAAATTCAAGGCCGGATTG
	HairyRT_Rev	TCTTAACGCCATTGATGCAG
CG42807	CG42807RT_Fw	TTGTGCCAAACCATTCTTCA
	CG42807RT_Rev	GCCAGGGACTCCATTATCAA
CG42808	CG42808RT_Fw	AATGCGAAACCGAAACAAAC
	CG42808RT_Rev	ATGCCAGGGATTATGCAGAG
rp49 (normalizing control)	Rp49 real new s	CCGCTTCAAGGGACAGTATC
	Rp49 real new a	TTCTGCATGAGCAGGACCTC
m3 (positive control) E(Spl) gene	M3 real sense	AGCCCACCCACCTCAACCAG
	M3 real antisense	CGTCTGCAGCTCAATTAGTC
m7 (positive control) E(Spl) gene	M7_sense	CGTTGCTCAGACTGGCGATG
	M7.6	ATCAGTGTGGTTCCAAAAGC

Additional two genes were included for the analysis on top of the seven originally selected genes. As the enhancer for the *CG13334* could potentially belong also to the *CG13335* gene we decided to test its expression too. However, based on the new release 6 of the *Drosophila* genome the *CG13335* gene was split into two genes (*CG42807* and *CG42808*) so we included both of them into our analysis.

3. 3. Analysis *in vivo*

To investigate the effect of overexpression / down regulation of the Notch pathway on selected genes *in vivo* we performed *in situ* hybridizations and Q-RT-PCR in the wing discs of four *Drosophila* strains (tab.5). Here the Notch pathway was activated by NICD overexpression in the *patched* domain of the disc or silenced by RNAi induced downregulation of the Notch receptor in the same part of the disc. The *Su(H)-VP16* fusion (a fusion with the *VP16* activation domain) was used to induce the expression of all Su(H) bound genes in the *patched* domain (fig. 10). The same lines were used for both the Q-RT-PCR analysis and the *in situ* hybridization.

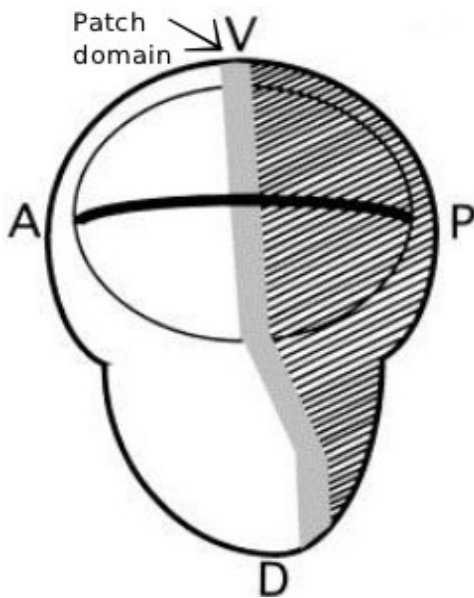


Fig. 10: *Drosophila* wing imaginal disc

The *patched* expression domain is marked by an arrow. A – anterior side of the disc, P – posterior side of the disc, D – dorsal side of the disc, V – ventral side of the disc.

Table 5: *Drosophila* strains used for the Q-RT-PCR and *in situ* hybridization

<i>Drosophila</i> strain (cross)	Description
UAS-N ^{RNAi} ; Ptc-Gal4; Tub-Gal80 ^{ts}	Down regulation of Notch in the <i>ptc</i> region of <i>Drosophila</i> wing disc, thermosensitive
Ptc-Gal4, Tub-Gal80 ^{ts} (II.); UAS-Nicd/TM6	Overexpression of NICD in the <i>ptc</i> region of <i>Drosophila</i> wing disc, thermosensitive
If/cyo; Su(H)-VP16 (III.) x Ptc-Gal4, Tub-Gal80 ^{ts} (II.)	Overexpression of <i>Su(H)-VP16</i> in the <i>ptc</i> region of <i>Drosophila</i> wing disc, thermosensitive

Gal4 is a transcription activator protein binding the upstream activation sequence (*UAS*) that works as a tetramere. Gal80 protein replaces one or more of Gal4 protein in this tetramere and therefore inhibits its function. In our study, thermal sensitive mutant of *Gal80* (*Gal80^{ts}*) was used. Larvae were exposed to heat shock temperature (29°C) for two days before dissection. This destroys Gal80^{ts} so the Gal4 complex is activated and the expression of target gene is induced.

3. 3. 1. Q-RT-PCR from the wing discs

RNA had been isolated from 60 *Drosophila* imaginal wing discs of selected phenotypes using TRI Reagent (Sigma) and treated with DNAFree kit to remove traces of genomic DNA (Ambion). SuperScriptII reverse transcriptase (Invitrogen) and random primers (Promega) were used for preparation of cDNA according to the attached manuals. Q-PCR analysis was performed with the same primers and protocol as for the time course analysis (chapter 3.2.2.).

3. 3. 2. In situ hybridization in imaginal wing discs

Digoxygenine labeled RNA probes were synthesized and *in situ* hybridization was performed according to the following protocol:

For the probe synthesis the sense or the antisense oligonucleotides with T7 promoter attached to their 5' ends (tab.6) to create either a sense or antisense RNA probes was used. BioTaq polymerase (Bioline) was used for the PCR reaction to amplify products from 555 to 717 bp long.

Table 6. Primers used for PCR amplification of DNA used for synthesis of RNA probes

Gene	Primer name	Sequence of primer
<i>CG13334</i>	CG13334 probe s	TCCGGAATCTCACCAAGAAC
	T7 CG13334 a	T7 + TGTCTGGATTCCGTTTAGG
	T7 CG13334 s	T7 + TCCGGAATCTCACCAAGAAC
	CG13334 probe a	TGTCTGGATTCCGTTTAGG
<i>Glut1</i>	Glut1 probe s	GGAGATAGCGCCACTGAA
	T7 Glut1 a	T7 + ATTAGCGGAATGGACACGAG
	T7 Glut1 s	T7 + GGAGATAGCGCCACTGAA
	Glut1 probe a	ATTAGCGGAATGGACACGAG
<i>ImpL3</i>	ImpL3 probe s	GTGTGCCTCATCGATGTCTG
	T7 ImpL3 a	T7 + CCCAGGAGGTGTATCCCTTT
	T7 ImpL3 s	T7 + GTGTGCCTCATCGATGTCTG
	ImpL3 probe a	CCCAGGAGGTGTATCCCTTT
<i>IDH</i>	IDH probe s	CCAGGTCACCATTGACTGTG
	T7 IDH a	T7 + TGCACATCACCGTCGTAGTT
	T7 IDH s	T7 + CCAGGTCACCATTGACTGTG
	IDH probe a	TGCACATCACCGTCGTAGTT
<i>Treh</i>	Treh probe s	AACGGCGGTCGAGTCTACTA
	T7 Treh a	T7 + CCTTCACCCACAGTGGAGAT
	T7 Treh s	T7 + AACGGCGGTCGAGTCTACTA
	Treh probe a	CCTTCACCCACAGTGGAGAT
<i>Hex-A</i>	Hex-A probe s	TGTGTACAAGGAGCGTTTGC
	T7 Hex-A a	T7 + GGCTCGTCAGCTTCAATT
	T7 Hex-A s	T7 + TGTGTACAAGGAGCGTTTGC
	Hex-A probe a	GGCTCGTCAGCTTCAATT
<i>Hairy</i>	Hairy probe s	TGCTACAGCACCTGAGCAAC
	T7 Hairy a	T7 + ATGTGTGCGAGTTGGATGAG
	T7 Hairy s	T7 + TGCTACAGCACCTGAGCAAC
	Hairy probe a	ATGTGTGCGAGTTGGATGAG

Amplified DNA was purified by phenol:chloroform extraction and precipitated in ethanol. RNA probes were prepared with T7 RNA polymerase and DIG RNA labeling mix (both Roche) according to the following protocol:

Preparation of the RNA probes:

1. Mix: 1 µg of PCR product
2 µl of DIG RNA labeling mix
2 µl of 10x transcription buffer
x µl of H₂O RNase free
2 µl of T7 RNA polymerase
0,5 µl of RNAsin
final volume 20 µl
2. Incubate 4 hours at 37 °C
3. Add 2 µl of DNase I, incubate 15 min at 37°C
4. Add 1 µl of 0,5 M EDTA (pH 8) to stop the reaction
5. To precipitate the probe add 1,28 µl of LiCl and 75 µl of 100% ethanol
6. Incubate on ice for 60 min, centrifuge at 13200 rpm at 4 °C for 30 min
7. Remove the supernatant, dry the pellet and resuspend it in 20 µl of DEPC H₂O

For *in situ* hybridizations 30 larval heads were dissected in 1x PBS (15 for antisense probe and 15 for sense probe). Heads were dissected immediately to 4% formaldehyde in PBS and fixed for 30 minutes in total at room temperature. After fixation, heads were washed three times in PBT-Tween 0,1% for 5 minutes, fixed again in 4% formaldehyde in PBT-Tween 0,1% for 20 min and washed three times in PBT-Tween 0,1% for 5 min once more. Another wash step in 50% Hybridization solution (HS) in PBT-Tween 0,1% for 5 min was included. At the end heads were put into the pure HS and frozen in -20 °C where they were kept until hybridization with probes.

Before prehybridization, heads were washed with HS for 10 minutes and then incubated in fresh HS at least 3 hours at 55 °C. 7 µl of probe had been mixed with 100 µl of HS, incubated 10 minutes at 80 °C and chilled on ice to prevent renaturation. After that, HS was removed of the heads and incubation with probe at 55 °C over-night was performed.

Next day, probe was removed and heads were washed according to the following steps: 5 min with SH at 55 °C

15 min with SH at 55 °C

5 min with 70% HYBE in 30% PBT-Tween 0,1% at 55 °C

5 min with 50% HYBE in 50% PBT-Tween 0,1% at 55 °C

5 min with 30% HYBE in 70% PBT-Tween 0,1% at 55 °C
4x 10 min with PBT-Tween 0,1% in agitation

After washing steps, heads was incubated with PBT-BSA for 30 min at RT and then incubated with digoxigenine antibody in PBT-BSA for 2 hours. This was followed by washing in PBT-Tween 0,1% for 10 minutes (4x) in agitation. Heads were washed with staining solution for 15 minutes in agitation and then incubated with NBT / BCIP (Roche) in staining solution until an expression was seen or until the staining did not shown any progress. Reaction was stopped by washing the heads with PBT-Tween 0,1% for 5 minutes (3x) in agitation. Heads were then washed with 30%, 50% and 70% glycerol and imaginal wing discs were dissected.

Solutions:

saline-sodium citrate (SSC) buffer:

3 M sodium chloride
300 mM trisodium citrate
adjust pH to 7.0 with Hcl

HYBE:

50% Formamide
50% 5X SSC buffer

Hibridization solution (HS):

50% Formamide
5X SSC buffer
100µg/ml DNA salmon sperm
50µg/ml Heparine
0,1% Tween20

Staining solution:

100mM NaCl
50mM MgCl₂
100 mM TrisHCl
adjust pH to 9,5
0,1% Tween 20

3. 5. Measurement of metabolism

Metabolic status of cells and imaginal wing discs was measured by the XF24 Extracellular Flux Analyzer (Seahorse Bioscience). Three different parameters were measured in the medium surrounding cells or tissues: oxygen consumption rate (OCR), extracellular acidification rate (ECAR) and proton production rate (PPR) where OCR is an indicator of the activity of the respiratory chain and both ECAR and PPR are indicators of the rate of glycolysis. Medium without sodium bicarbonate have to be used instead of the normal Schneider medium (Sigma, S9895). In our experiments, metabolic status of three cell lines (S2N, DmD8, KC167) and imaginal wing discs from two different *Drosophila* strains was measured (tab. 7). Because of technical limitations of the Seahorse machine all

measurements were performed at 26°C.

S2N cells were treated with 600 µM over-night and all cell lines were activated with 2mM EDTA in 1x PBS for 15 min. After this time, PBS with EDTA was exchanged for medium without bicarbonate and basal metabolism of cells was measured for 2 hours, followed by the addition of respiration blocking reagents (see bellow). Both the control (non-activated) and experimental (activated) cells were measured in triplicates. Background was measured in wells without any cells. Three-step cycle (1 min of mixing, 2 min delay and 3 min of measuring) was performed 20 x to measure basal metabolic status. Then, three inhibitors were subsequently added: 2 µM oligomycin (inhibits ATP synthase by blocking its proton channel; by blocking ATP production in mitochondria glycolysis should start running faster to compensate for the loss of ATP production), 1 µM (0,4 µM respectively) carbonyl cyanide-p-trifluoromethoxyphenylhydrazone (FCCP, ionophor stimulating respiration in mitochondria by transporting H⁺ across the membrane without coupling it with ATPase) and 1 µM antimycin (binds to the Qi site of cytochrome c reductase and therefore inhibits completely electron transport chain). After the addition of each drug metabolic parameters were recorded in three loops of 1 min mixing, 2 min delay and 3 min measurement.

Drosophila imaginal wing discs were attached to the bottom of the wells by Poly – L-lysine hydrobromide (Sigma). Polylysine was applied to the bottom of the cells 90 minutes before dissection of the discs according to the following protocol:

- put 50 µl of 1,5 x dipping solution at the bottom of each well of 96-well plate
- let stand at room temperature for 15 minutes
- suck of 45 µl the polylysine
- put into 55°C for 15 minutes
(repeat 3x)
- let dry at room temperature for 1 hour, put into the fridge if plate isn't used immediately

Discs were both dissected and placed in medium without bicarbonate. Dissection of the 48 discs takes on an average 50 minutes (for measuring in triplicates). To minimize the variability caused by different times when discs were 'sitting' in the medium, larvae were dissected alternately (discs from one control larvae → discs from one 'giants' larvae → discs from one control larvae...). The same three-step protocol for the measurement of OCR,

ECAR and PPR was used as for cell lines except that baseline metabolism was measured only for 18 minutes (3 times).

Both cells and imaginal wing discs were further normalized to the amount of proteins. Cells and discs were lysed in the plate by 100 μ l of RIPA lysis buffer, shaken on ice for 15 min and placed into -20°C . Next day, cells and discs were scratched from the plate and transferred into pre-cooled eppendorfs and spinned for 5 min at 14 000 g in 4°C . After centrifugation, 25 μ l of lysate was transferred into a 96-well plate. For the determination of the amount of protein Biquinonic acid kit for protein determination (Sigma) was used. After reaction mix was added samples were incubated for 30 min at 37°C and measured on SpectraMax 340PC384 Absorbance Microplate Reader (Molecular Devices) at 562 nanometes. All samples were measured in triplicates.

Tab. 7: *Drosophila* strains used for metabolic analysis

UAS-GFP Su(H) (II.) x Ptc-Gal4 (II.)	Overexpression of Su(H) in the ptc, so called 'giants'
YW x Ptc-Gal4 (II.)	Control

4 Results

4.1. Selection of potential Notch target genes involved in metabolism

We took advantage of the available published and unpublished ChIP-chip data from several cell lines (30 minute activation of Notch) and tissues to look for peaks of Su(H) binding in the regulatory regions of genes involved in the regulation of cellular metabolism (see Methods for the complete list). Interestingly, more than twenty genes were found to contain binding sites for Su(H) in their vicinity (potential enhancers in the promoter regions, in the introns or at the 3' end of the genes). Of those, we decided to pick seven genes that either had the most profound peaks or an important role in metabolism. These were *hexokinase-A*, a key regulatory enzyme of the glycolysis, two predicted lactate dehydrogenases (*Impl3* and *CG13334*), *glucose transporter 1*, *trehalase* and *isocitrate dehydrogenase* (tab. 8 and fig.11-17). We also decided to involve the transcription factor *hairy* into our analysis because it has been shown to be a master regulator of cellular metabolism during hypoxia (79).

The Nimblegen genomic tiling microarrays used in this experiment covered the whole *Drosophila* genome with 50-75 bp long probes in 55bp intervals (60-bp probes distributed in 300-bp intervals for DmD8 cells) and peaks were defined using the Tamalpais program with a minimum cut-off of 5 adjacent probes and p-value<0.05. Due to the distribution of genomic fragments after the sonication in the ChIP experiment each peak should have a characteristic 'hill' shape with the Su(H) binding site pulled down in the ChIP experiment most probably located in the top (middle) of the peak. Sometimes the peak was rather broad indicating that there was more than one Su(H) binding site in the area. For cloning into the luciferase vector we selected regions 152 - 641 bp long around the top of the peaks containing also a high predicted Patser or 'dictionary' site(s). When some genes showed more than one interesting ChIP peak we decided to test more than one region in the luciferase assay. Also, one cloned fragment often contained more than one predicted Su(H) binding site. In total eleven regions were cloned (fig. 11-17, genomic localization of cloned fragment according to release 5 of the *Drosophila* genome).

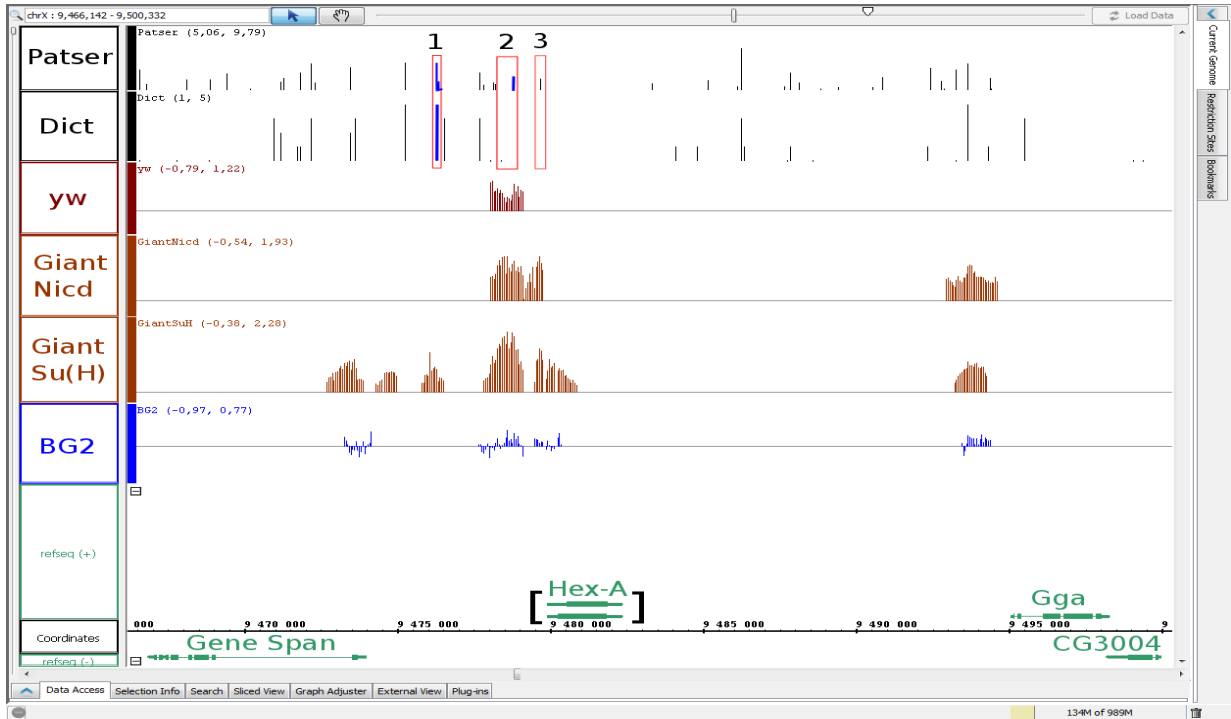


Fig.11: *Hexokinase-A (Hex-A)*. ChIP-chip data from BG2 cells and imaginal wing discs from larvae with over-expression of Nid or Su(H) and yw as a control with Su(H) antibody. Red rectangles represent regions cloned into the luciferase vector. 1: genomic localization 9476155-9476474; 2: genomic localization 9478335-9478834; 3: genomic localization 9479614-9479765. Su(H) sites mutated for the luciferase assay are coloured in blue.

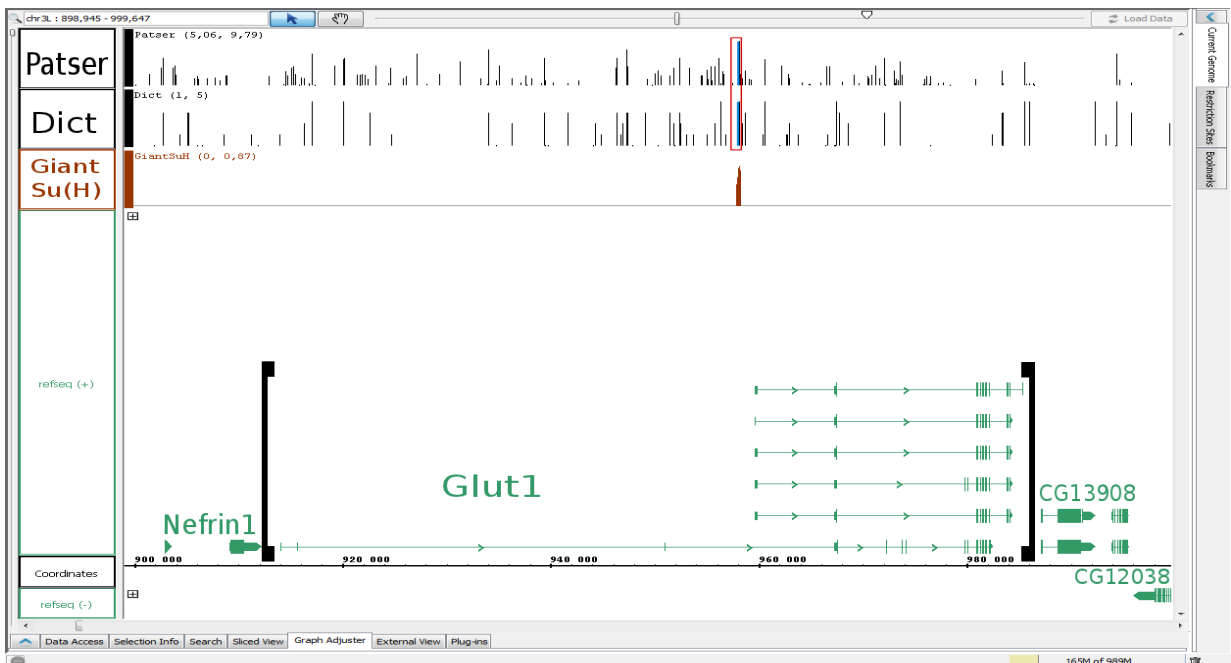


Fig.12: *Glucose transporter 1 (Glut1)*. ChIP-chip data from imaginal wing disc from larvae with over-expression of Su(H). Red rectangles represent regions cloned into the luciferase vector. Genomic localization 958044-958332. Su(H) sites mutated for the luciferase assay are coloured in blue.

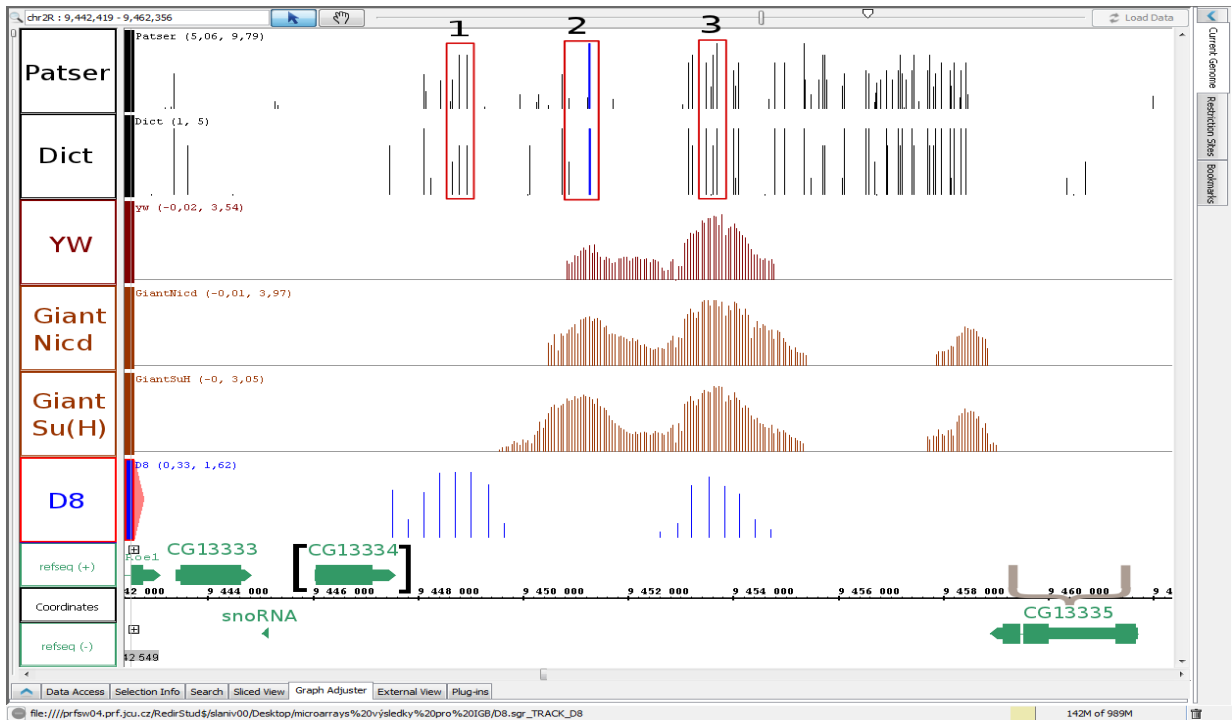


Fig.13: CG13334. ChIP-chip data from BG2 cells and imaginal wing discs from larvae with over-expression of Nicd or Su(H) and *yw* as a control with Su(H) antibody. Red rectangles represent regions cloned into the luciferase vector. 1: genomic localization 9448588-9449012; 2: genomic localization 9450850-9451334; 3: genomic localization 9453421-9453750. Su(H) sites mutated for the luciferase assay are coloured in blue.



Fig.14: Ecdyson-inducible gene L3 (*ImpL3*). ChIP-chip data from imaginal wing disc from larvae with over-expression of Su(H) or NICD. Red rectangles represent regions cloned into the luciferase vector. Genomic localization 958044-9583326280455-6281092. Su(H) sites mutated for the luciferase assay are coloured in blue.

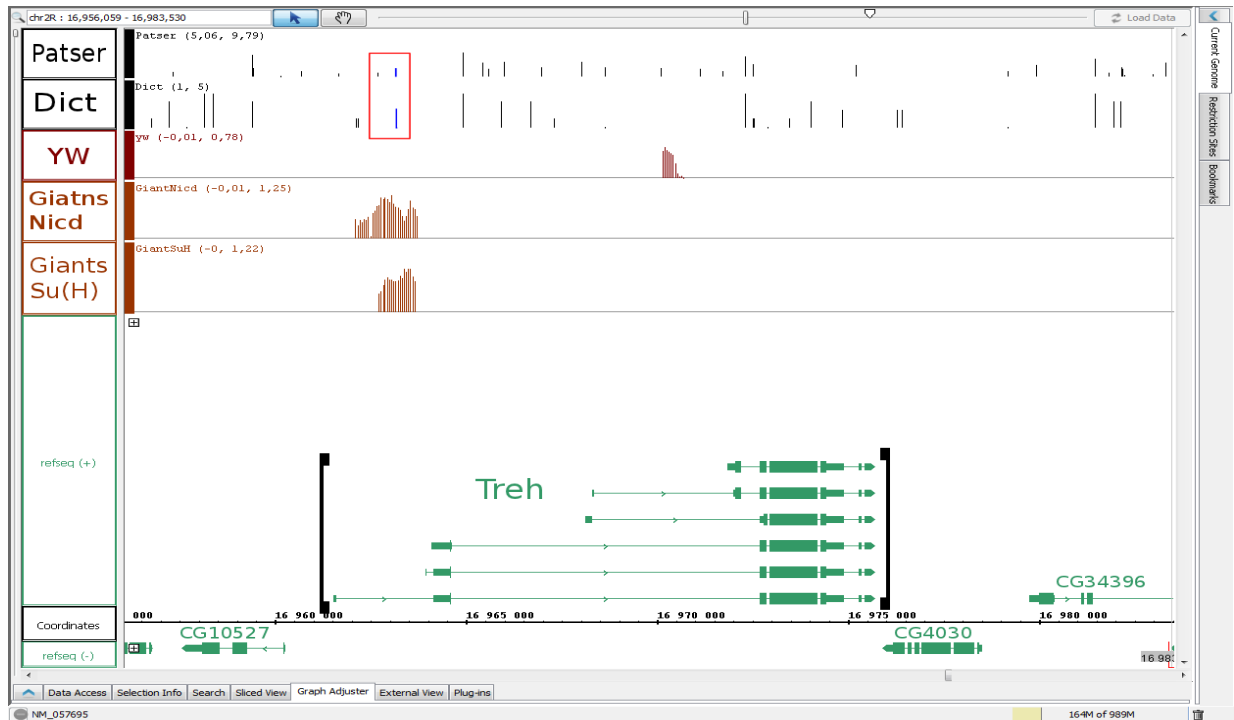


Fig.15: *Trehalase (Treh)*. ChIP-chip data from imaginal wing disc from larvae with over-expression of Su(H) or NICD. Red rectangles represent regions cloned into the luciferase vector. Genomic localization 16962603-16963243. Su(H) sites mutated for the luciferase assay are coloured in blue.

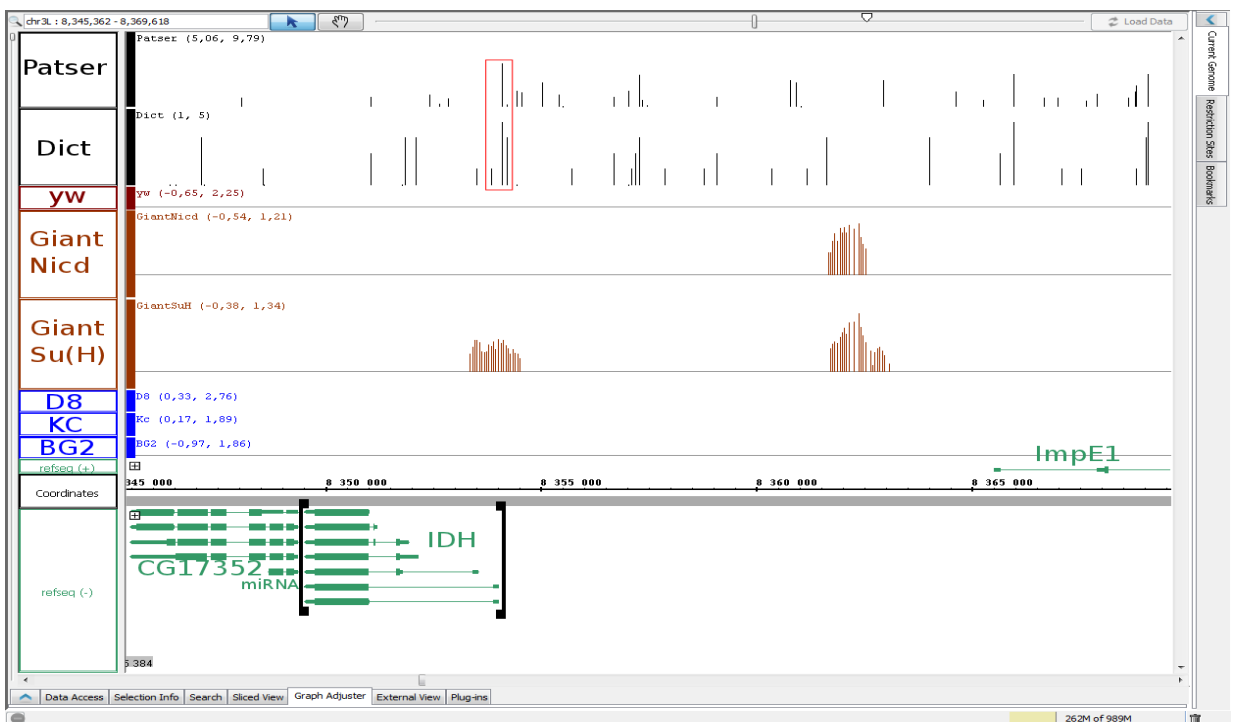


Fig.16: *Isocitrate dehydrogenase (IDH)*. ChIP-chip data from imaginal wing disc from larvae with over-expression of Su(H). Red rectangles represent regions cloned into the luciferase vector. Genomic localization 8353800-8354290. Su(H) sites mutated for the luciferase assay are coloured in blue.

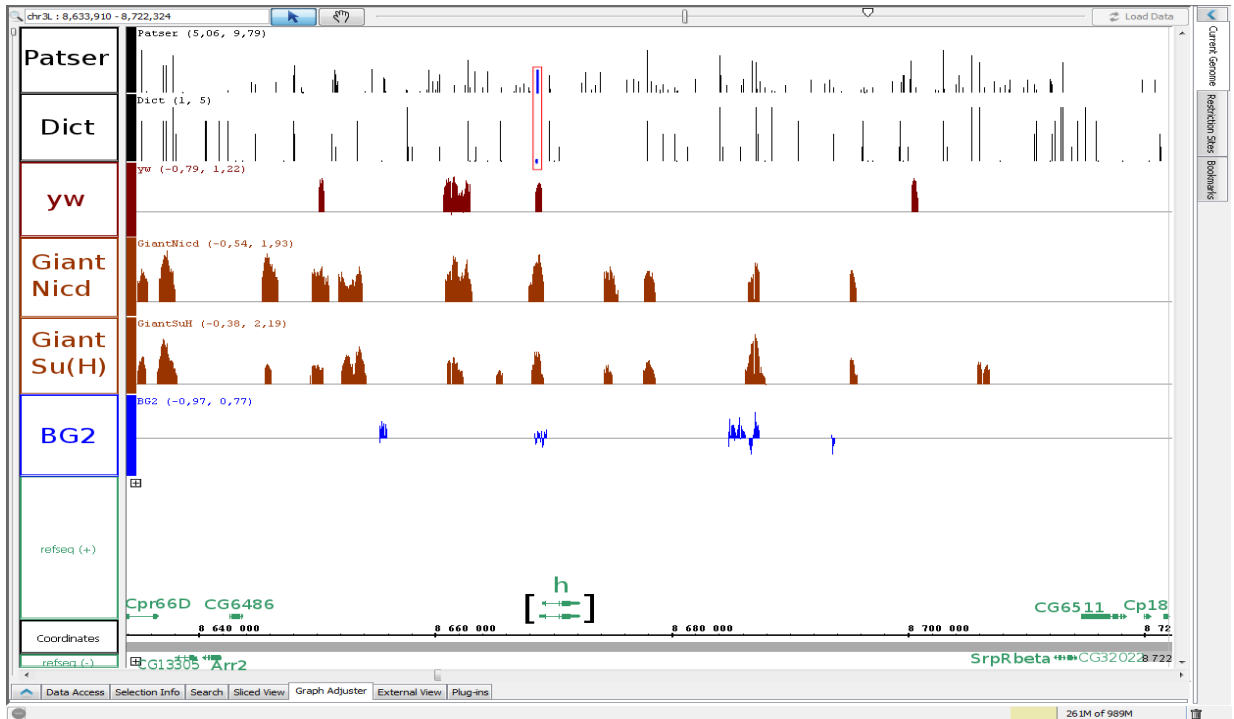


Fig.17: Hairy (h). ChIP-chip data from BG2 cells and imaginal wing discs from larvae with over-expression of Nidc or Su(H) and yw as a control with Su(H) antibody. Red rectangles represent regions cloned into the luciferase vector. Genomic localization 8668458-8668677. Su(H) sites mutated for the luciferase assay are coloured in blue.

Table8: Genes selected for further analysis

Name of the gene	symbol	Function
<i>Hexokinase A</i>	<i>Hex-A</i>	Phosphorylates glucose to Glucose-6- phosphate
<i>Glucose transporter 1</i>	<i>Glut1</i>	Transfers glucose through plasma membrane
<i>CG13334</i>	-	Predicted L-lactate dehydrogenase activity, converts pyruvate to lactate
<i>Ecdysone-inducible gene L3</i>	<i>ImpL3</i>	Predicted L-lactate dehydrgenase, converts pyruvate to lactate
<i>Trehalase</i>	<i>Treh</i>	Converts trehalose to glucose
<i>Isocitrate dehydrogenase</i>	<i>IDH</i>	Decarboxylates isocitrate to α -ketoglutarate
<i>Hairy</i>	<i>h</i>	Transcription factor, regulator of cellular metabolism during hypoxia

4. 2. Analysis in cell lines

4. 2. 1. Testing *Su(H)* enhancers in the luciferase assay

Eleven predicted enhancer regions were amplified by PCR (see supplement 1 for sequences) and cloned into the pGL3 vector in front of a luciferase reporter gene and a minimal promoter. After the ligation, 8-16 colonies were screened by PCR with gene-specific forward primer in combination with vector-specific reverse primer (RV3). Fig 18 shows the PCR products before cloning and the result of fig. 19 is an illustration of a typical result we obtained after screening the colonies after transformation.

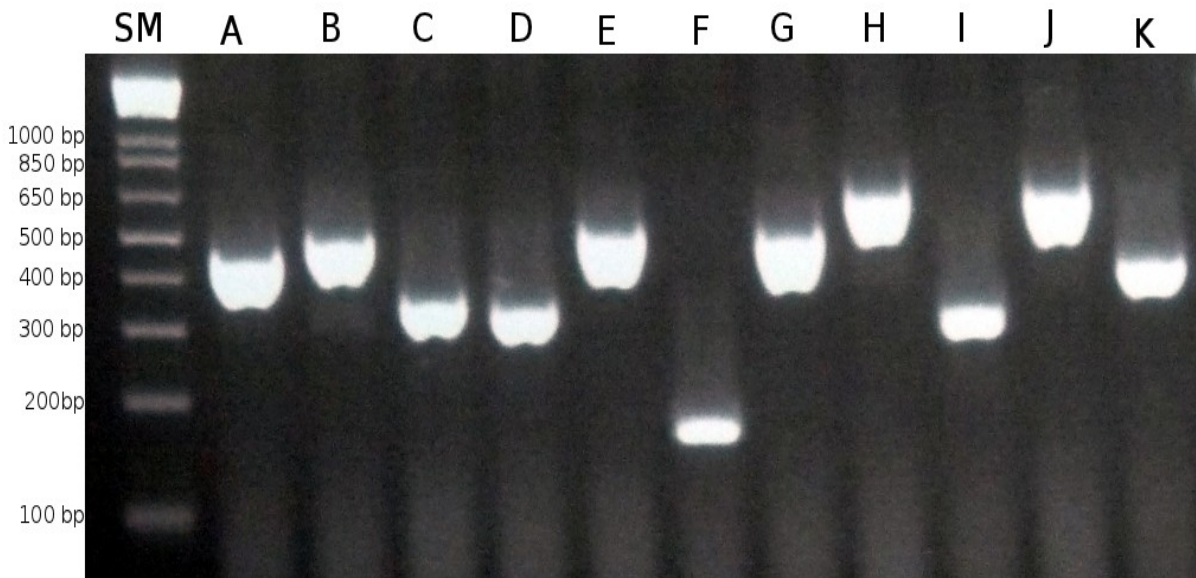


Fig.18: PCR amplified enhancer regions separated by gel electrophoresis. SM – Size marker (1kb plus DNA ladder (Invitrogen)), A – CG13334(1) (432 bp), B – CG13334(2) (485 bp), C – CG13334(3) (330 bp), D – Hex-A (1) (320 bp), E – Hex-A (2) (500 bp), F – Hex-A (3) (152 bp), G – IDH (491 bp), H – Treh (641 bp), I – Glut1 (289 bp), J – ImpL3 (638 bp), K – h (420 pb)

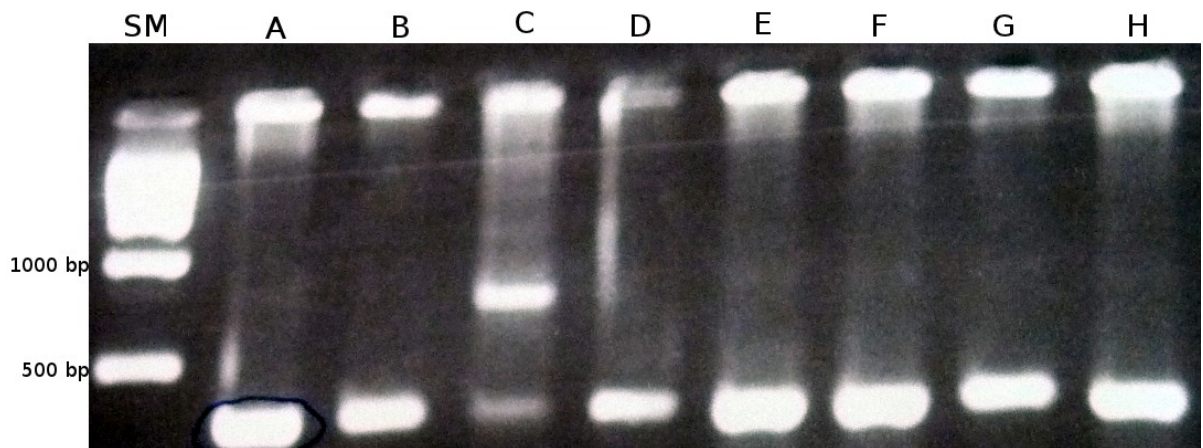


Fig.19: Verification of cloned product for *Glut1* by PCR. SM – size marker (Mass DNA ladder (Neb)), A-H – different colonies of cloned *Glut1* enhancers taken into the analysis using reverse gene specific Bgl2 CG13334_3rev primer and vector specific RV3 primer (see tab.2). Expected product from positive colonies should be 409 bp.

Luciferase assays were performed in duplicates in at least three independent experiments on separate days. As a positive control a vector containing the Su(H) dependent enhancer from the *m3* gene was used. As a negative control we used a plasmid containing *grainyhead* binding sites and four mutated non-functional Su(H) binding sites (called 1.1). Out of the eleven cloned regions six showed a signal above the background, corresponding to the genes *Hex-A*, *Glut1*, *CG13334* and *hairy* (fig.20).

We then decided to mutate the predicted *Su(H)* sites within all the responding enhancers to see if the luciferase response we saw is really dependent on Su(H) binding. In case a fragment contained more than one predicted Su(H) site we chose to mutate the one that overlapped between the dictionary and Patser or that had the higher score in either of the prediction methods. In *Hexokinase-A* fragment1 we mutated two sites, one common for both computationally predicted and experimentally verified and one that was only computationally predicted. The fragments from *Hex-A 1*, *Glut1* and *hairy* significantly lowered their response to NICD suggesting that we are working with the true Notch dependent enhancers (see the T-test values in tab.9). The mutation of the fragments for *CG13334* is still in progress but we hope to see the same trend. We also decided to mutate fragments that did not respond to NICD to serve as controls. As expected, none of the *Hex-A2*, *trah* or *Idh* fragments significantly changed their responses. However, in case of *Impl3* we saw a decrease in the luciferase response suggesting that this may still be a true Notch enhancer. Data showed in

graph is the average of all measurements. For T-test, mutated versions of plasmids were calculated as a percentage to nonmutated plasmids.

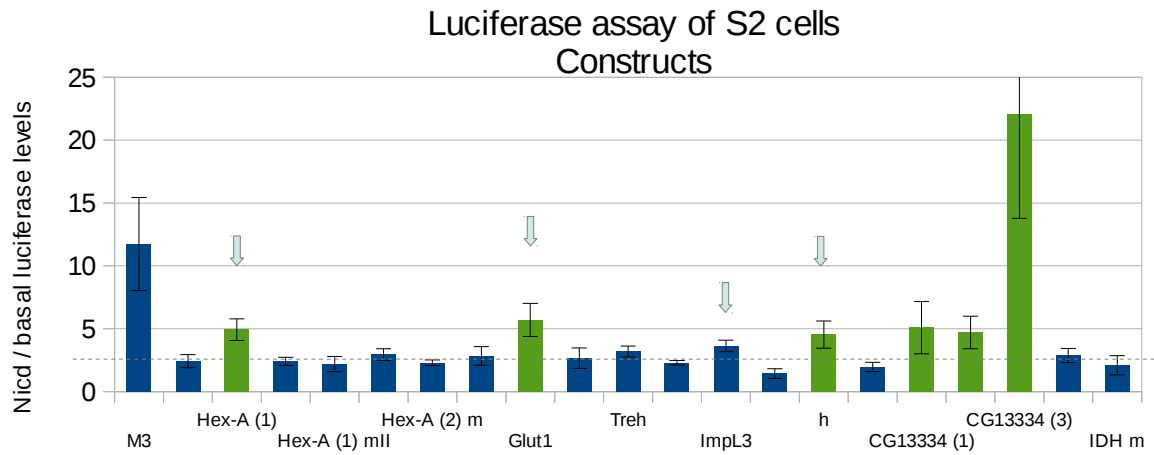


Fig.21: Luciferase assays with selected enhancer regions. *M3* - positive control; *1.1* – negative control. ‘*m*’ - mutated version of the plasmid (for construct Hex-A (1) two different Su(H) binding sites were mutated - mI, mII); responding genes are showed in green. arrows mark the fragments that lost their responses to Nictd after their Su(H) binding sites were mutated.

Tab.9: T-test analysis comparing luciferase experiments with the mutated and nonmutated Su(H) sites within the cloned enhancer regions.

Gene	T-test value
<i>Glut1</i>	0,024
<i>Hex-A (1)_I</i>	0,032
<i>Hex-A (1)_II</i>	0,042
<i>ImpL3</i>	0,041
<i>h</i>	0,007
<i>Treh</i>	0,135
<i>Hex-A (2)</i>	0,752

4. 2. 2. Analysis of the mRNA expression profile after the activation of the Notch pathway using Q-RT-PCR

In the luciferase assay we proved that there are functional Su(H) binding sites in the potential regulatory regions of our genes. However, do they really regulate the expression of these genes? One of the indirect ways to test this is to see if the genes respond to Notch pathway in cell lines (and in imaginal discs, see chapter 4.3.) .

The usual way we activate Notch receptor in cell lines is to incubate them with 2mM EDTA in PBS for 30 minutes (and we know that PBS itself activates Notch to some extend). In order to minimize the possible starving effect of having PBS on the cells instead of a medium we tried to activate cells by adding EDTA directly to the media. However, the efficiency of this approach was very low and the concentrations of EDTA that gave a moderate level of Notch activation were toxic for the cells (data not shown). From our previous unpublished work we know that even a 5 minutes pulse of EDTA in PBS triggers the response of most of the same Notch target genes as with the 30 minutes incubation although a few genes respond to lower extend. As a compromise between good mRNA induction and possible starving effects we decided to activate cells with EDTA in PBS but only for 15 minutes. Then we followed mRNA expression of our seven selected genes in 15, 30, 45, 60 and 120 min time points.

We observed changes in expression of all genes although they were dependent on the cell line used and the timing of their induction was different among the genes, too. In S2N cells Glut1 showed an increase of expression from 45 minutes onwards. Similar was the response of CG13334 and the neighbouring two genes previously reported as CG13335 (CG42807 and CG42808). Impl3 showed a sharp but short increase in expression at 15 minutes. Unexpectedly, Hex-A and hairy were downregulated, with hairy possibly showing an early upregulation at 30 minutes followed by a downregulation. In dmD8 and Kc167 cells did no respond in all cases but if they did the trends were similar, except for Impl3 gene that seems to go up in S2N and Kc167 cells but it goes down in DmD8 cells.

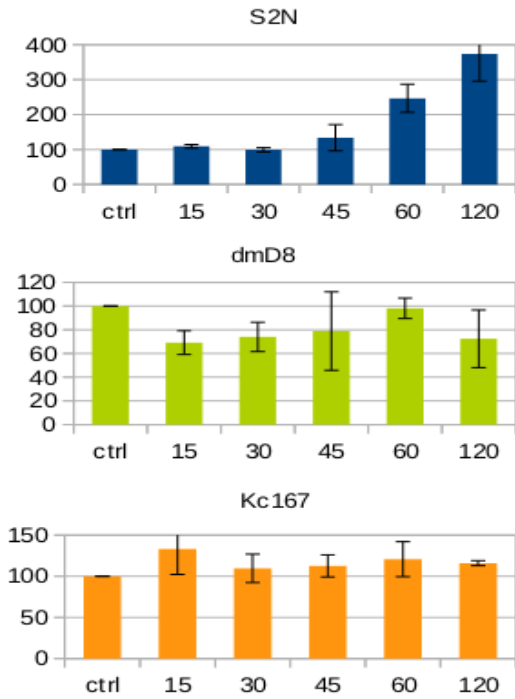
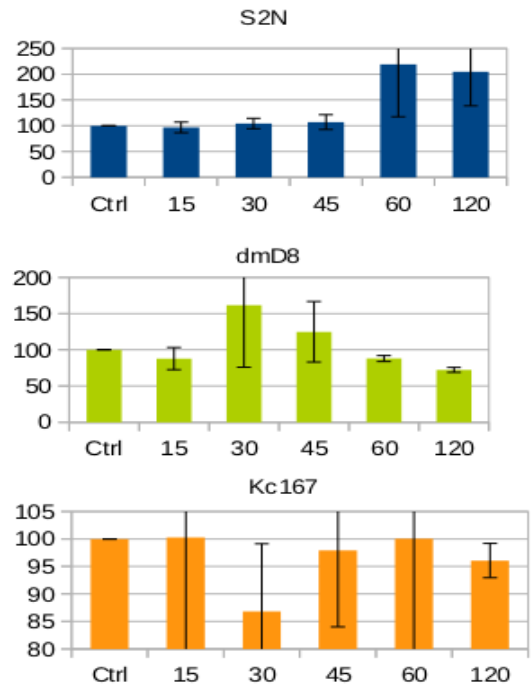
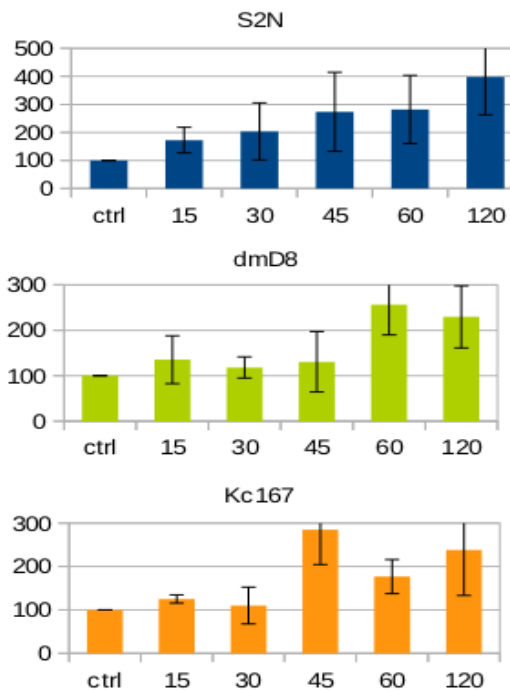


Fig.22:

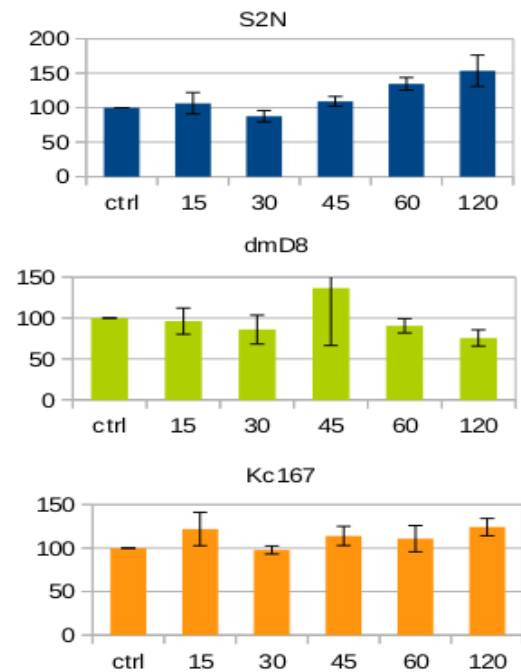
Glucose transporter 1 (Glut1): Expression in S2N, DmD8 and Kc167 cells 15 - 120 minutes after the activation of Notch pathway. Axis X gives time in minutes.



CG13334: Expression in S2N, DmD8 and Kc167 cells 15 - 120 minutes after the activation of Notch pathway. Axis X gives time in minutes



CG42807: Expression in S2N, DmD8 and Kc167 cells 15 - 120 minutes after the activation of Notch pathway. Axis X gives time in minutes



CG42808: Expression in S2N, and Kc167 cells 15 - 120 minutes after the activation of Notch pathway. Axis X gives time in minutes

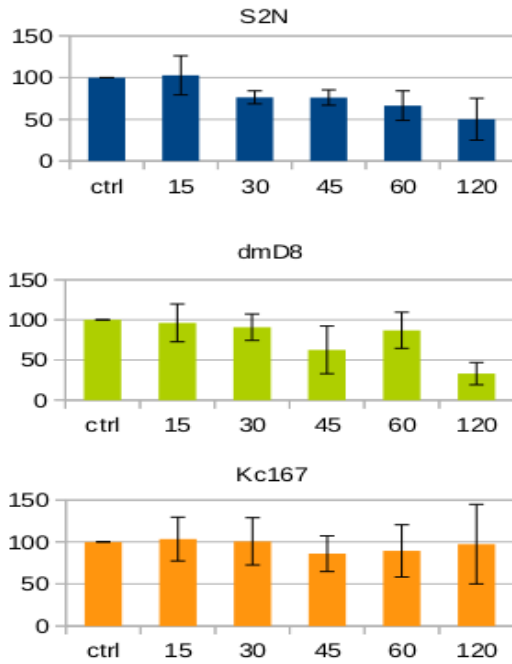


Fig.26: Hexokinase-A (Hex-A): Expression in S2N, DmD8 and Kc167 cells 15 - 120 minutes after the activation of Notch pathway. Axis X gives time in minutes.

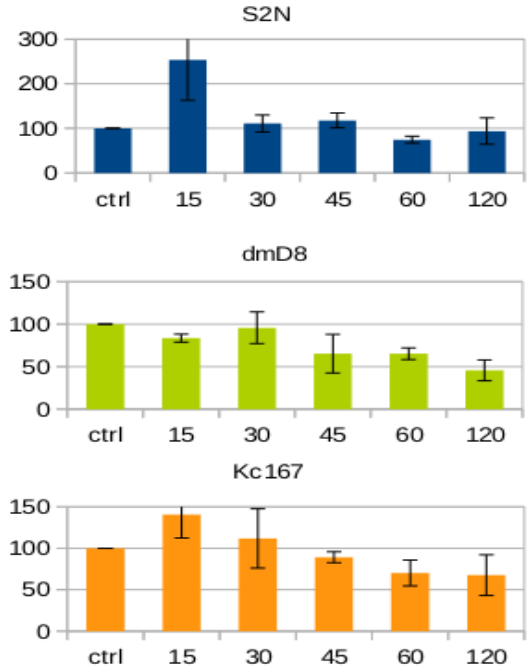


Fig.27: Ecdison inducible gene L3 (ImpL3): Expression in S2N, DmD8 and Kc167 cells 15 - 120 minutes after the activation of Notch pathway. Axis X gives time in minutes.

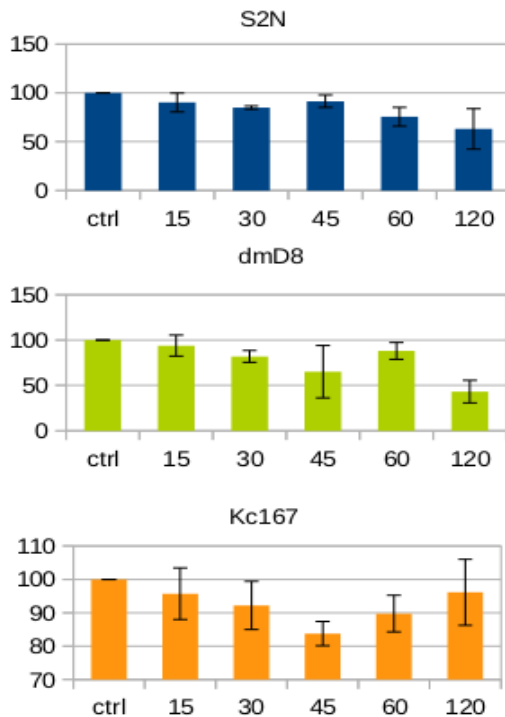


Fig.28: Trehalase (Treh): Expression in S2N, DmD8 and Kc167 cells 15 - 120 minutes after the activation of Notch pathway. Axis X gives time in minutes.

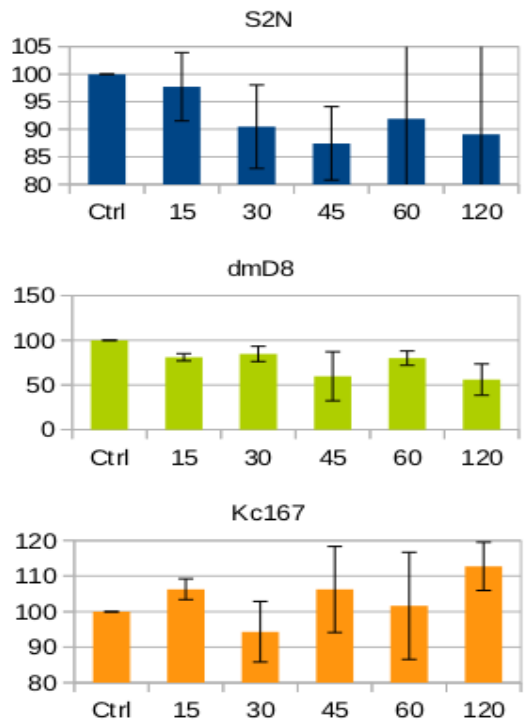


Fig.29: Isocitrate dehydrogenase (IDH): Expression in S2N, DmD8 and Kc167 cells 15 - 120 minutes after the activation of Notch pathway. Axis X gives time in minutes.

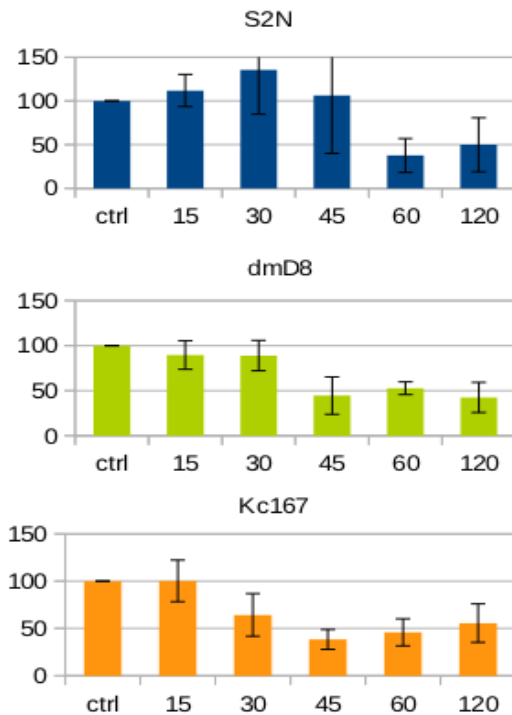


Fig.30: Hairy (h): Expression in S2N, DmD8 and Kc167 cells 15 - 120 minutes after the activation of Notch pathway. Axis X gives time in minutes.

4. 3. Analysis *in vivo*

We showed that selected metabolic genes respond to Notch activation in cell lines. But are they regulated by Notch also *in vivo*? We used two approaches to answer this question.

First, we performed *in situ* hybridization in imaginal wing discs where Notch pathway was upregulated or downregulated in the *patched* domain. Larvae of three phenotypes were used. We first tried to downregulate Notch receptor by RNAi in the *patched* domain but as we realized the discs changed their morphology so as the wing pouch was divided by a ‘dip’ in the A/P boundary and the signals from both the antisense and sense probe gave there a weaker signal (see fig. 31 for illustration of a typical result). Secondly, we overexpressed NICD in the *patched* domain which gives an overgrowth of the A/P part of the discs (see fig.32-34). *In situs* with probes against *Hex-A*, *Glut1* and *hairy* were tried but we did not see a convincing reproducible difference in the signal. Finally, we overexpressed SuH-VP16 fusion protein in the *patched* domain which gives relatively strong overgrowth of the A/P part of the disc. Here the *in situ* hybridizations with probes against *Hex-A*, *CG13334* and *hairy* showed upregulation of their mRNA in the A/P region (fig 35-37). With *hairy*, the whole A/P region of the pouch showed upregulation of the mRNA. However, the signal from *Hex-A* and *CG13334* was mostly upregulated only in the dorsal and ventral part of the A/P

region. It is this ventral region where the most of the Notch dependent overgrowth happens. We did not see any effect with the probe against *Glut1*. However, we should note here that none of our probes were designed to distinguish against specific transcriptional variants of the selected genes.

Secondly, we extracted mRNA from the discs of the same phenotypes and investigated the changes in expression of the selected genes. This experiment was performed only once so preliminary results are presented. We can say that *CG13334* and *CG42808* showed a robust response when SuH-VP16 was overexpressed in the patched domain (fig. 38). However, the responses of other genes differ hardly more than twice between the control and flies where Notch pathway was manipulated which is within the experimental error. This experiment is technically rather challenging since the yields of RNA from the discs are small but its repetition is in the progress and it will give us the definitive answers.

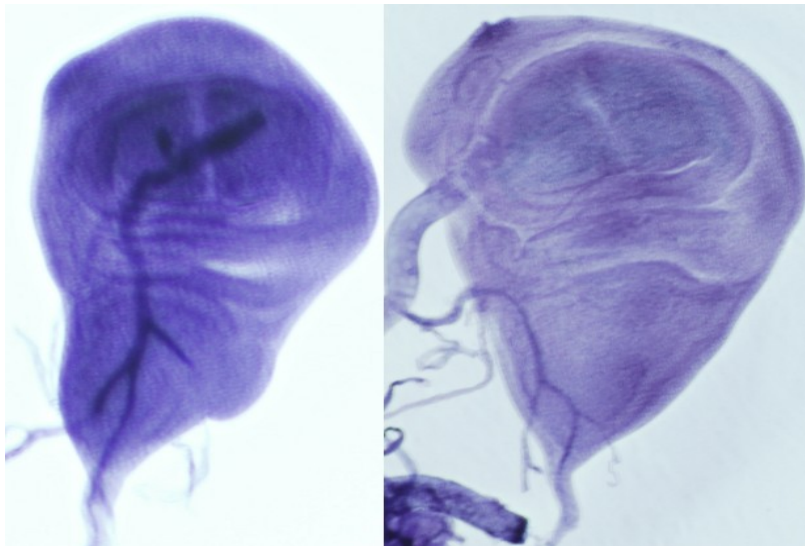


Fig. 31: *In situ* hybridizations of UAS-N^{RNAi}; Ptc-Gal4; Tub-Gal80^{ts}, gene *Hex-A*, antisense probe on the left, sense probe on the right.

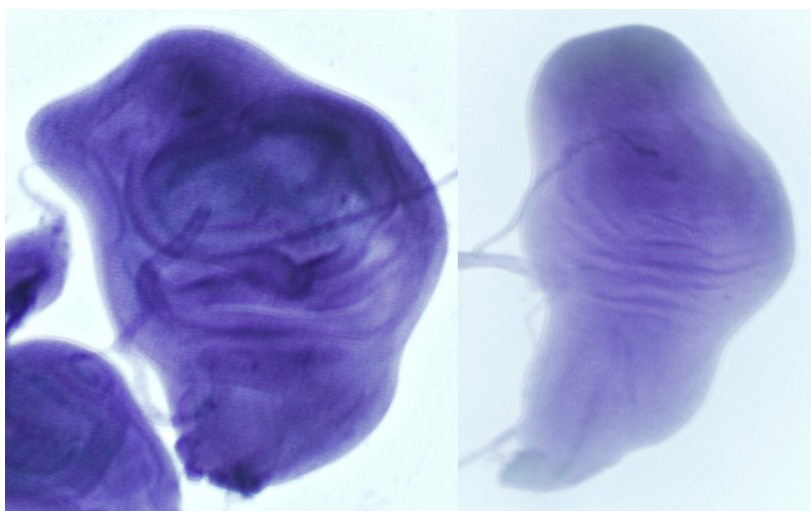


Fig. 32: *In situ* hybridizations of Ptc-Gal4, Tub-Gal80^{ts} (II); UAS-Nicd/TM6; gene *Hex-A*, antisense probe on the left, sense probe on the right.

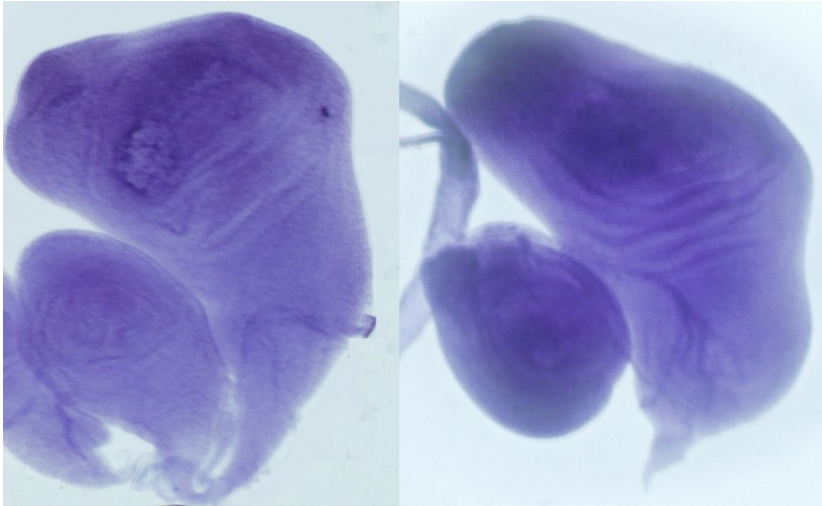


Fig. 33: *In situ* hybridizations of **Ptc-Gal4, Tub-Gal80^{ts} (II.); UAS-Nicd/TM6;** gene *Glut1*, antisense probe on the left, sense probe on the right.

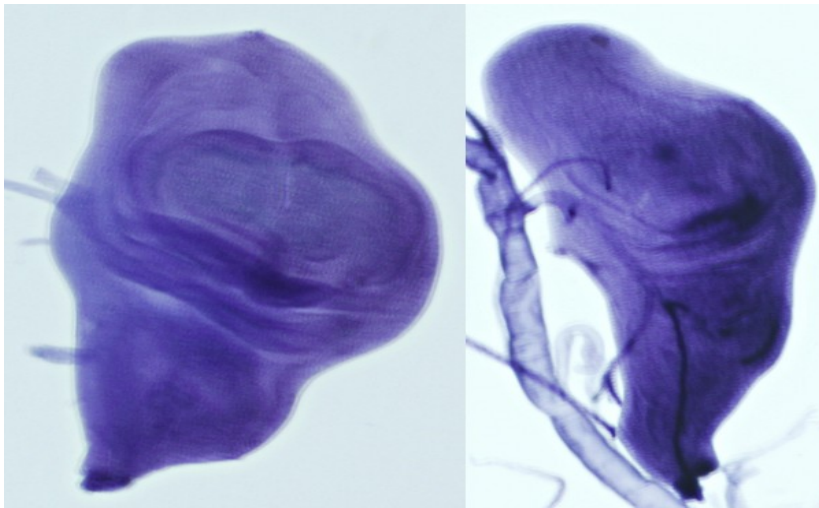


Fig. 34: *In situ* hybridizations of **Ptc-Gal4, Tub-Gal80^{ts} (II.); UAS-Nicd/TM6;** gene *hairy*, antisense probe on the left, sense probe on the right.

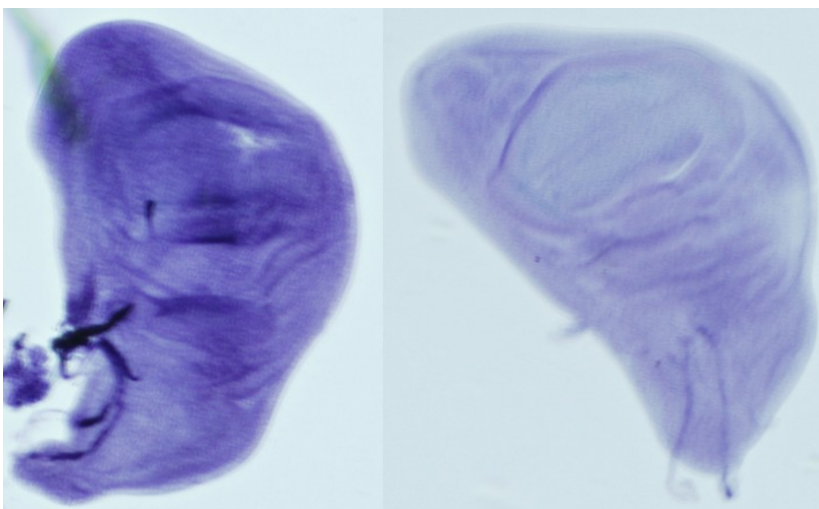


Fig.35: *In situ* hybridizations of **If/cyo; Su(H)-VP16 (III.) x Ptc-Gal4, Tub-Gal80^{ts} (II.);** gene *Hex-A*, antisense probe on the left, sense probe on the right.

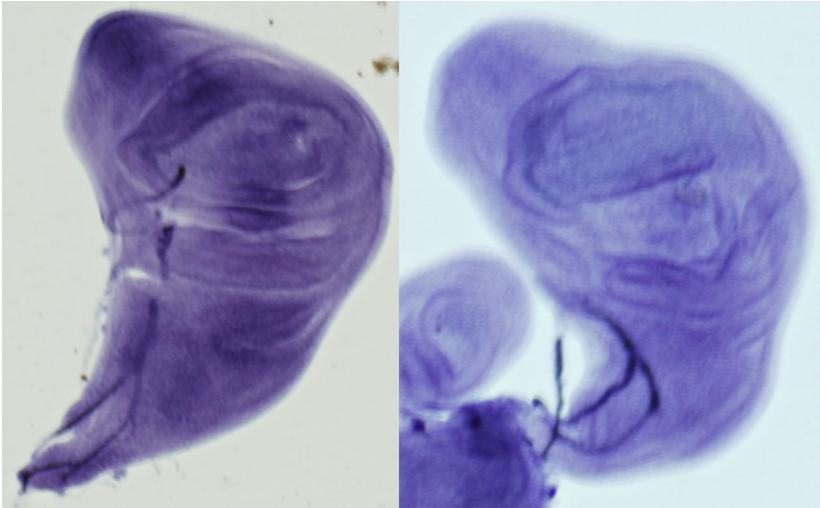


Fig.36: *In situ* hybridizations of **If/cyo; Su(H)-VP16 (III.) x Ptc-Gal4, Tub-Gal80^{ts} (II.)**; gene *CG13334*, antisense probe on the left, sense probe on the right.

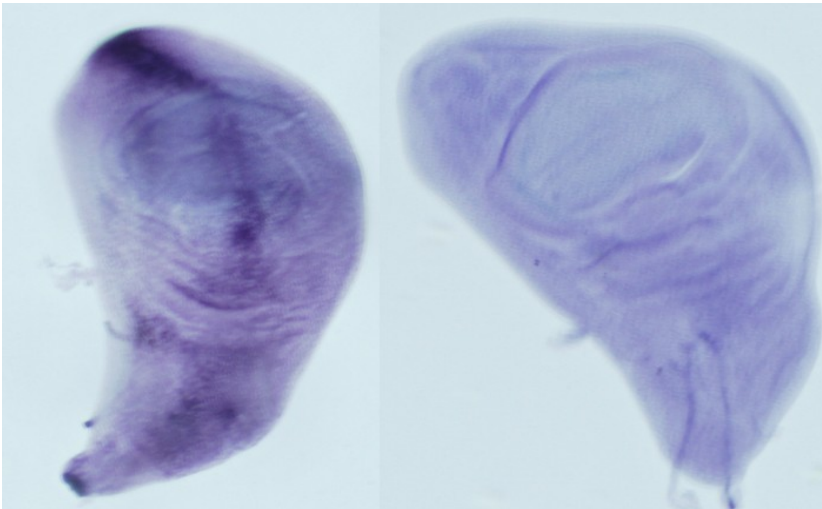


Fig.37: *In situ* hybridizations of **If/cyo; Su(H)-VP16 (III.) x Ptc-Gal4, Tub-Gal80^{ts} (II.)**; gene *hairy*, antisense probe on the left, sense probe on the right.

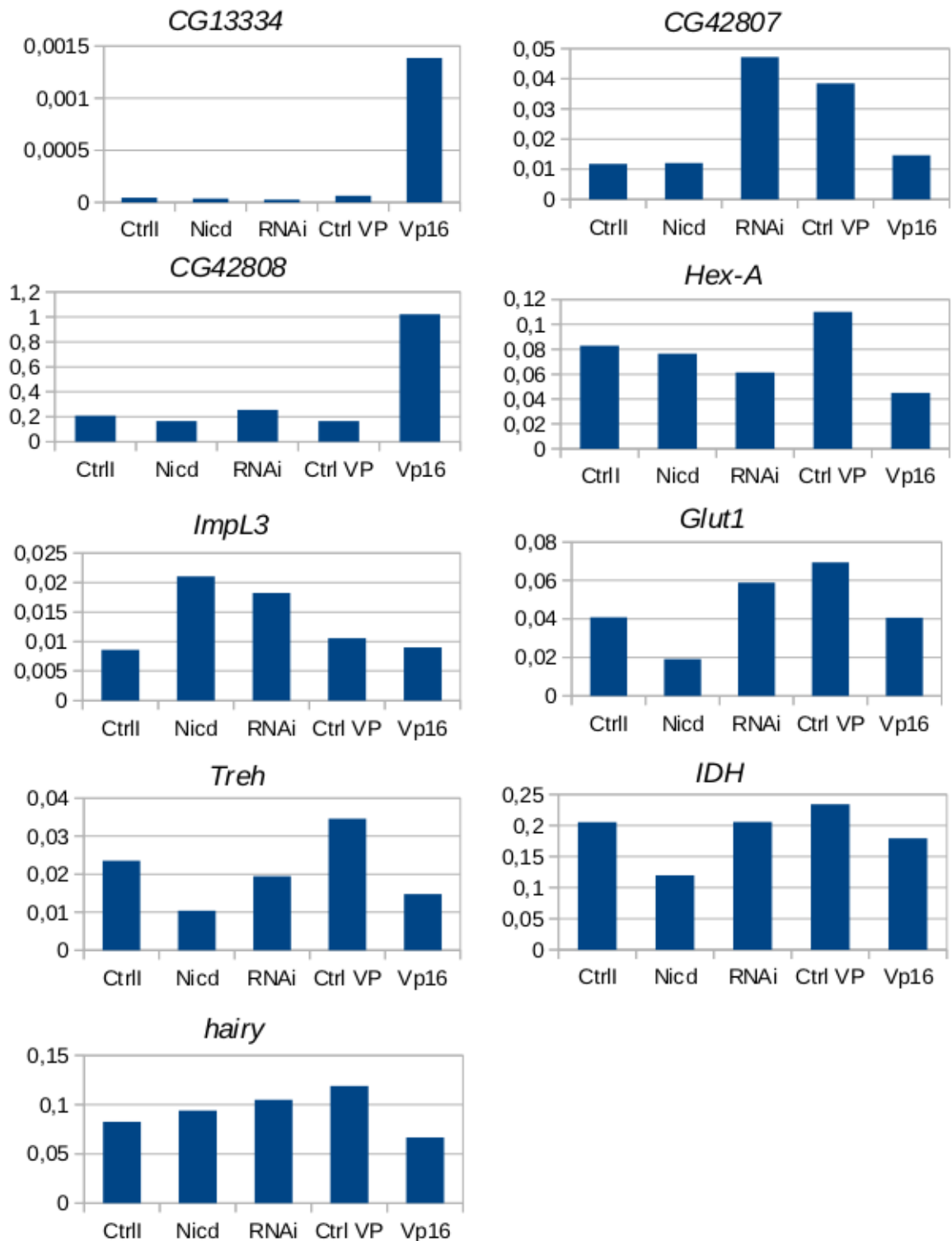


Fig 38: Expression of genes of interest in imaginal wing discs: Ctrl I (*yw x ptc gal4 tub gal 80^{ts}*) – control for Nicd and RNAi, Nicd (*PtcGal4, TubGal80^{ts}; UAS-Nicd/TM6*) – flies with overexpression of Nicd in *patched* domain, RNAi (*UAS-NRNAi; Ptc-Gal4; Tub-Gal80^{ts}*)- flies with downregulation of Notch in *patched* domain Ctrl VP (*yw x ptc gal4 tub gal 80*) – control for Su(H)-VP16, Vp16 (*If/cyo; Su(H)-VP16 x Ptc-Gal4, Tub-Gal80^{ts}*) flies with overexpression of Su(H)-VP16 in *patched* domain.

4. 4. Measurement of metabolism

At least some of the selected genes showed responses *in vitro* and *in vivo*, as described in previous chapters. If more mRNA is made as a response to the Notch pathway there should also be more protein made which will then influence the metabolic status of the cell. To investigate the functional consequences of Notch dependent upregulation of metabolic genes we took advantage of availability of the Seahorse flux analyser at the 3rd faculty of medicine in Prague at the laboratory of MUDr. Jan Trnka. This device is able to measure oxygen consumption reflecting the rate of respiration (OCR), acidification of medium reflecting the rate of glycolysis (ECAR; because the lactate created during glycolysis is to some extent transported outside the cell) and proton production rate also reflecting the rate of glycolysis (PPR; an alternative to measurement of ECAR, but unlike ECAR, PPR counts for variations in buffer capacity and volume). Before the deadline for submitting this thesis we managed to do only one round of the experiments, with no time for optimization of various parameters (the machine is design primarily for mammalian systems and so far there is no publication of measurements in *Drosophila*). We still decided to present this data as part of the thesis because they are interesting. However, we are aware of the fact that this experiment still needs to be optimized and repeated more times before any conclusions will be made.

We measured basal metabolism of three types of *Drosophila* cell lines (both activated and non-activated) for 2 hours. After this period three inhibitors to restrict the respiratory chain and therefore induce glycolysis were added (see Methods).

The oxygen consumption rate of Kc and especially S2N cells was decreased after the activation of Notch pathway (fig. 40) suggesting that their respiration was lower, as one would expect in cells with the Warburg effect. The S2N cells did not respond to FCCP at all indicating that their respiration chain was completely out of function. DmD8 cells showed an increase in respiration after EDTA but this difference was not observed with a second repeat of the same experiment on the next day where there was no change between cells before and after activation. The S2N and Kc results were reproducible.

The basal rate of glycolysis (assessed by the measurement of the acidification of the media) was rather low for all the cell lines. After the addition of drugs inhibiting respiration we expected to see an increase in ECAR because glycolysis should run faster to compensate for the low supply of ATP from the respiratory chain. We saw an increase in ECAR in S2N

cells in this case but only in the first of the three repeats of each measurement. Activated S2N cells showed a higher increase indicating that their glycolysis has the capacity to run faster than in cells without the activated Notch pathway, again as in one would expect in cells with the Warburg effect. However, the second and third measurements after the addition of the drugs were low again. In total, measurement of ECAR and PPR didn't show the trend we have expected (fig. 39). As we mention in the Discussion this might possibly be because of the upregulation of the lactate dehydrogenases *Impl3* and *CG13334* that metabolize lactate and therefore it can not be excreted outside the cell where we can detect it as ECAR (fig. 41) or PPR (fig. 42).

The same experiment as in cell lines was performed with imaginal wing discs from larvae from two different strains of *Drosophila* (giant overgrown discs from the Su(H) overexpression in the patched domain and an appropriate control) to see the response *in vivo*. Triplicates were prepared but these were not entirely comparable because the first set of disc spent more time outside the larvae in the measuring medium than the second or third set of discs which may have influenced the metabolic parameters of the tissues (the difference between the first and last disc was 50 minutes). Nevertheless, it appears that the giant discs may have lower respiration and higher glycolysis than the control discs (fig. 43-45). The FCCP did not seem to work on these tissues so the measurements of its effect (and therefore also of the effect of antimycin) is probably irrelevant. However, these data are very preliminary and we show them just because they would fit into the whole 'story'. Again, this need to be repeated and measuring parameters optimized before we can make any conclusions.

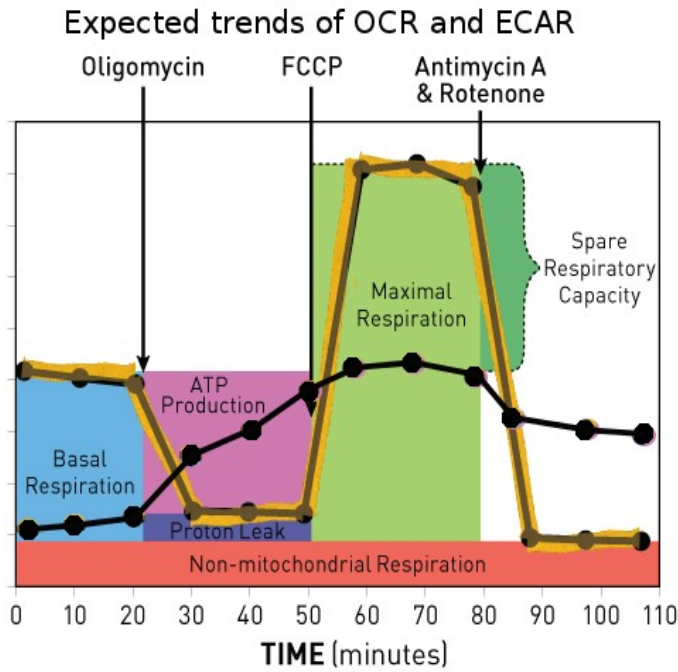


Fig.39: Expected trends of OCR / ECAR measurement (<http://www.seahorsebio.com/products/consumables/kits/cell-mito-stress.php>). Yellow curve gives expected trend of OCR, black curve gives expected trend of ECAR. When oligomycin is added, OCR goes down and ECAR up. After addition of FCCP, OCR goes up (higher than basal level) and ECAR stays at the same level or goes slightly up. Antimycin A or Rotenone block respiration completely, ECAR stays at the same level or goes slightly down.

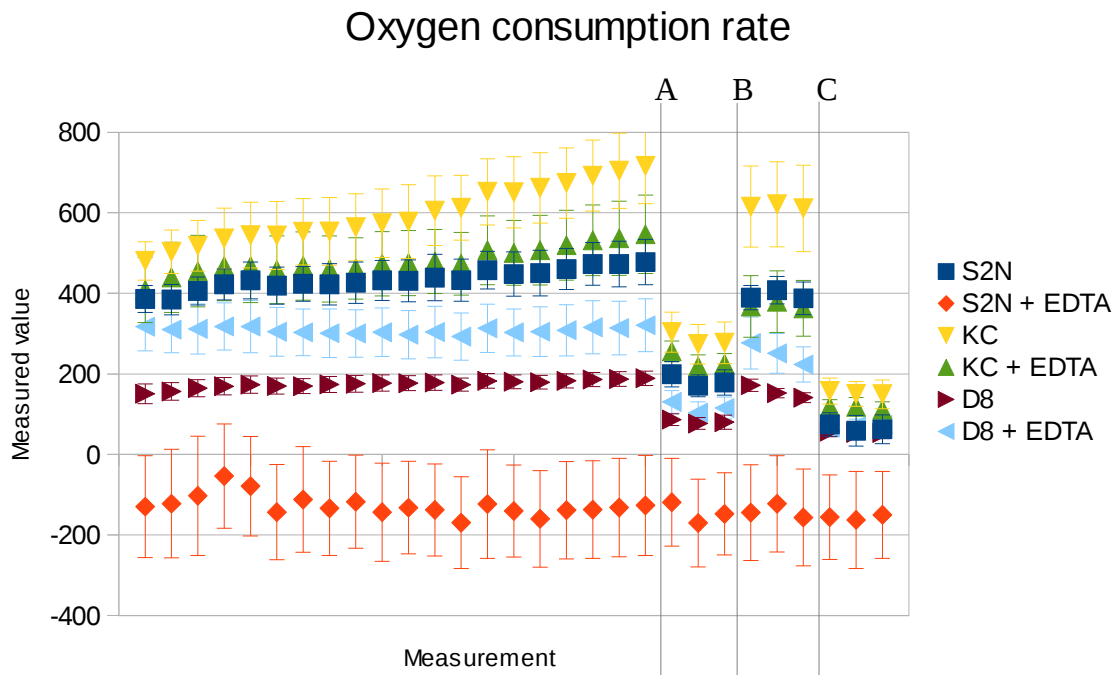


Fig.40: Oxygen consumption rate (OCR) in cell lines. A – injection of 2 μM oligomycin, B – injection of 1 μM FCCP, C – injection of 1 μM antimycin. Axis X gives individual measurements, spacing of two measured points is 6 minutes.

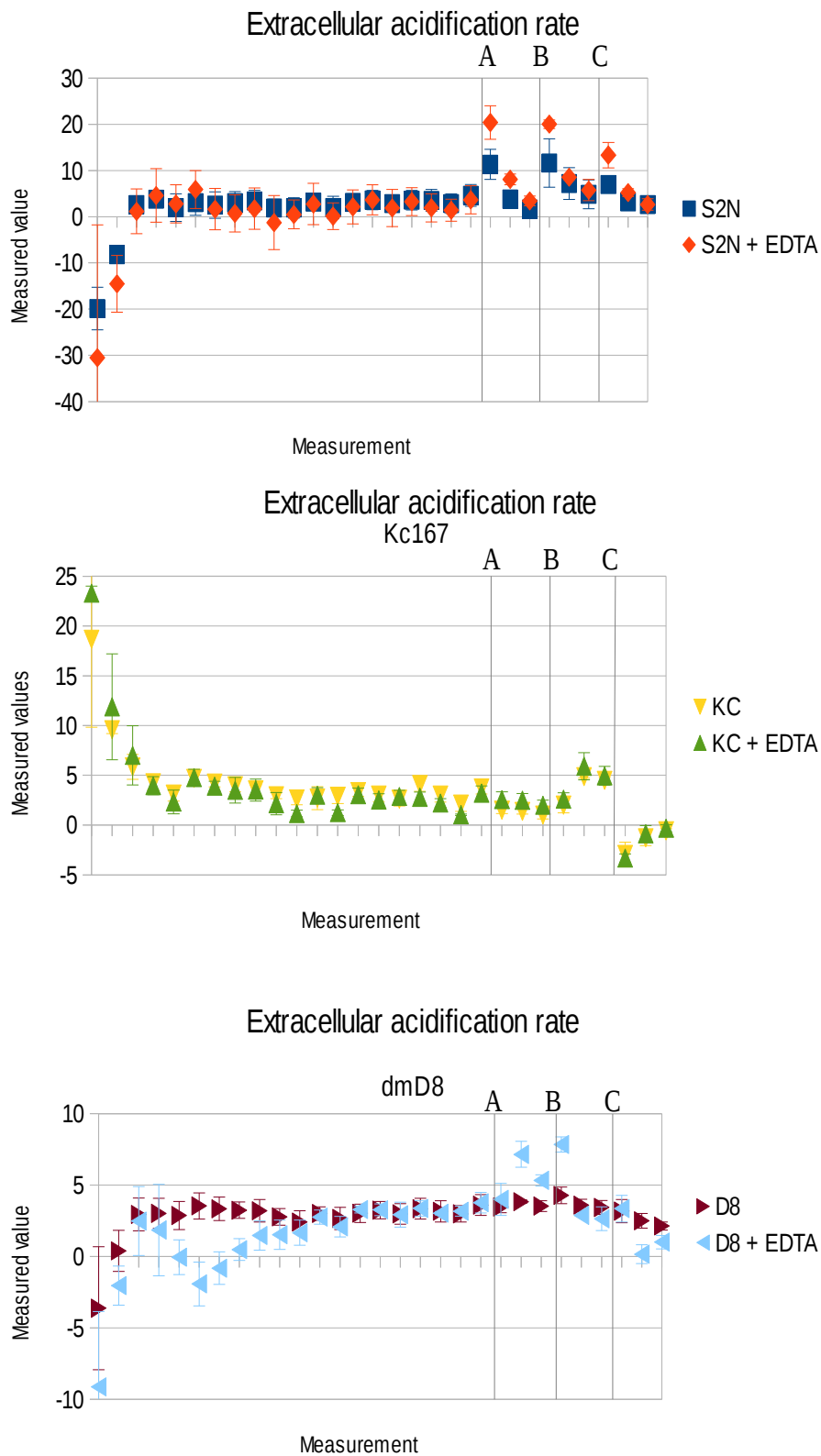


Fig.41: Extracellular acidification rate (ECAR) in cell lines. A – injection of 2 μ M oligomycin, B – injection of 1 μ M FCCP, C – injection of 1 μ M antimycin. Axis X gives individual measurements, spacing of two measured points is 6 minutes.

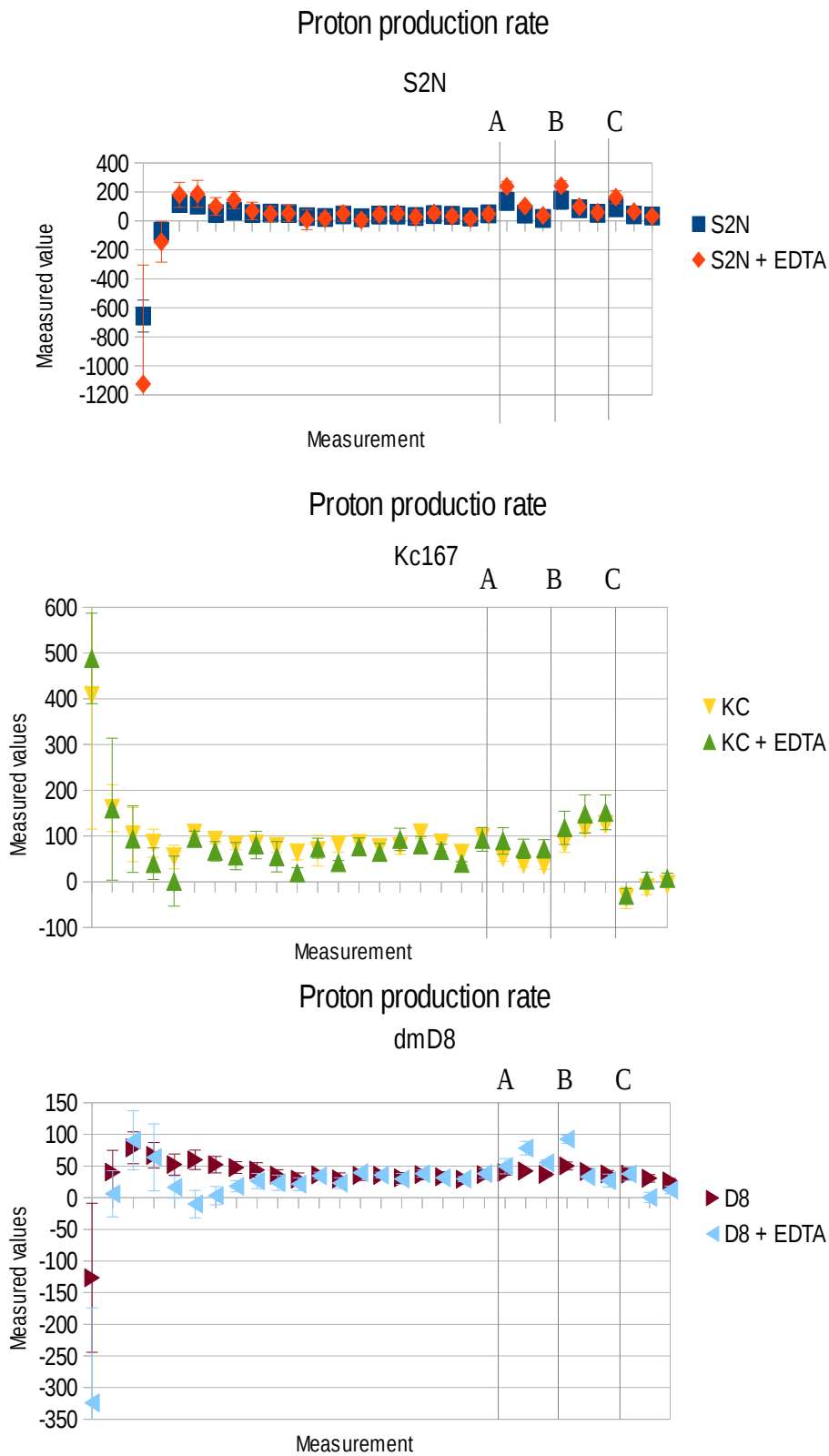


Fig.42: Proton production rate (PPR) in cell lines. A – injection of 2 μM oligomycin, B – injection of 1 μM FCCP, C – injection of 1 μM antimycin. Axis X gives individual measurements, spacing of two measured points is 6 minutes.

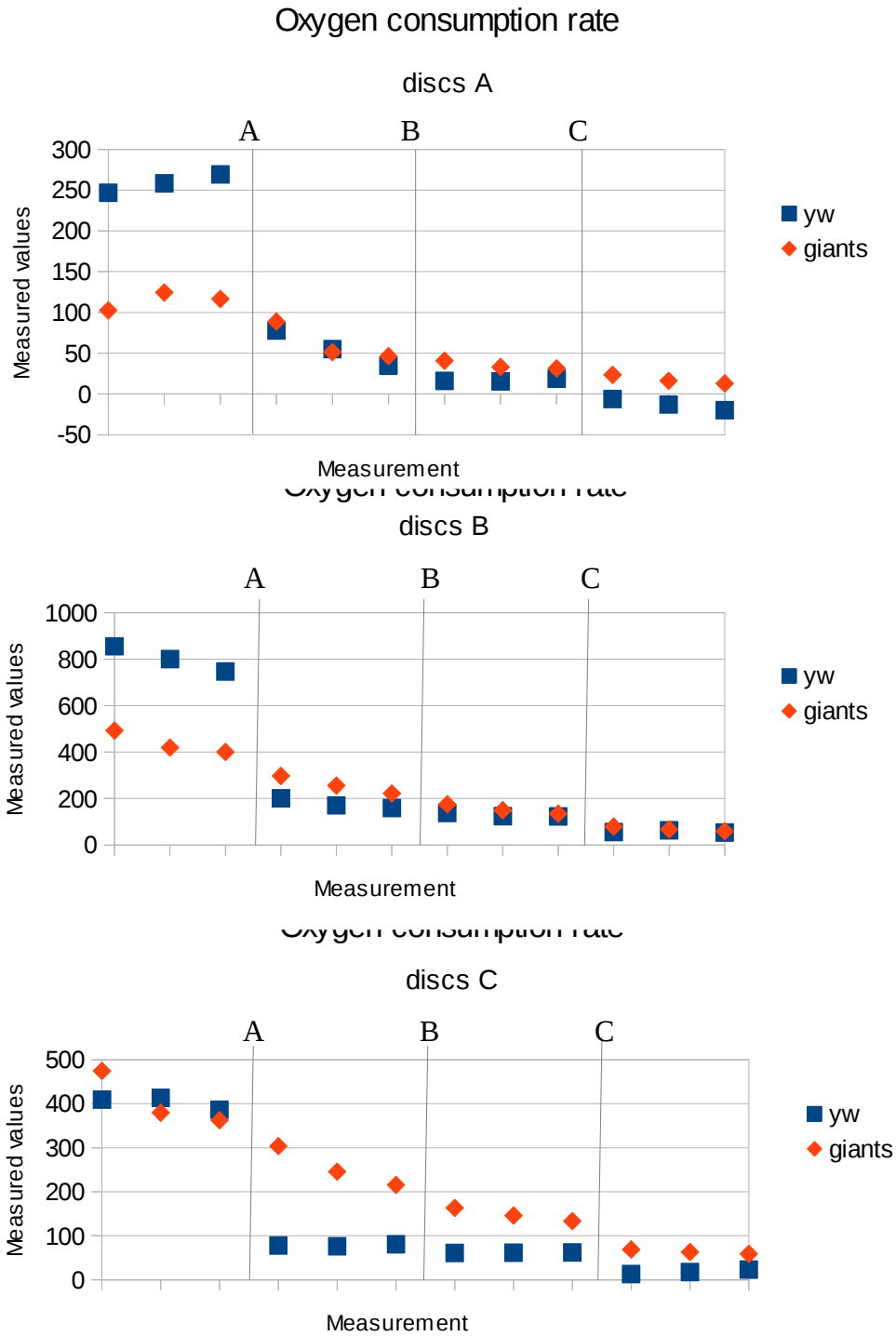


Fig.43: Oxygen consumption rate (OCR) in imaginal wing discs. Discs A – group of discs dissected as first, discs B – group of discs dissected as second, discs C – group of discs dissected as third. A – injection of 2 μM oligomycin, B – injection of 1 μM FCCP, C – injection of 1 μM antimycin. Axis X gives individual measurements, spacing of two measured points is 6 minutes.

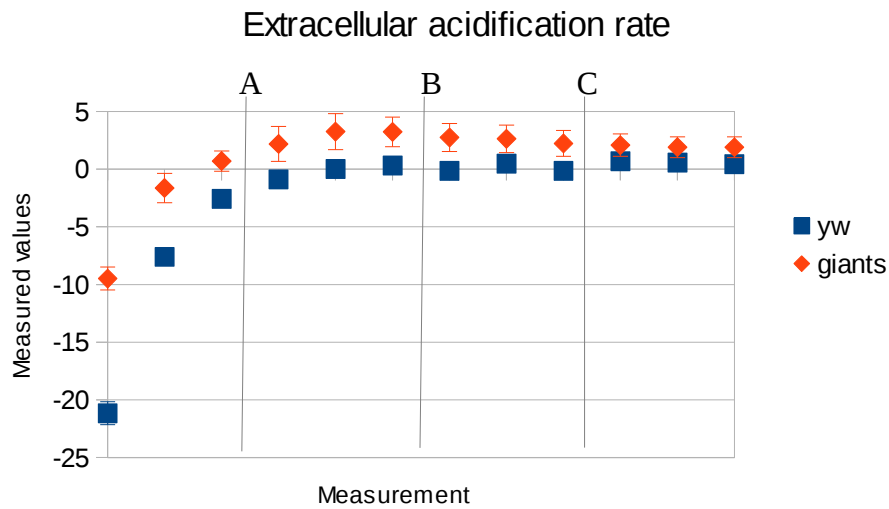


Fig.44: Extracellular acidification rate (ECAR) in imaginal wing discs. Graph gives average values of all three measurement. A – injection of 2 μM oligomycin, B – injection of 1 μM FCCP, C – injection of 1 μM antimycin. Axis X gives individual measurements, spacing of two measured points is 6 minutes.

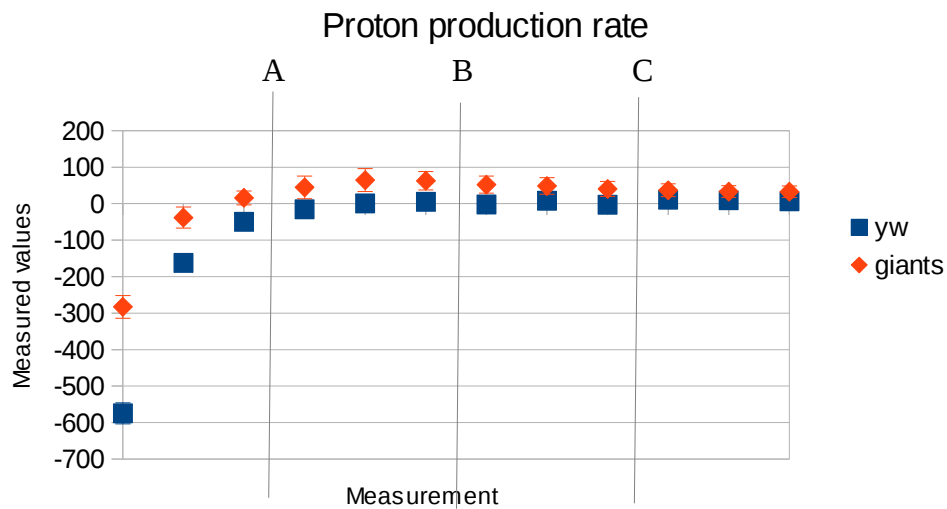


Fig.45: Proton production rate (PPR) in imaginal wing discs. Graph gives average values of all three measurement. A – injection of 2 μM oligomycin, B – injection of 1 μM FCCP, C – injection of 1 μM antimycin. Axis X gives individual measurements, spacing of two measured points is 6 minutes.

5 Conclusions

Are there functional Su(H) binding sites in the potential regulatory regions of selected metabolic genes?

Cloning of the enhancer regions predicted to contain Su(H) binding sites and mutagenesis of these binding sites in a luciferase assay confirmed that five metabolic genes possess functional Su(H) binding sites in their potential regulatory regions. These were *Hex-A*, *Glut1*, *CG13334*, *ImpL3* and *hairy*.

Is there a transcriptional response of the selected metabolic genes to the activated Notch pathway in cell lines and if so how long does it take to see it?

Most of the selected metabolic genes proved to be transcriptionally upregulated or downregulated as a response to the activated Notch signalling pathway in cell lines. This response appeared 15-60 minutes after the activation of Notch pathway.

Will the expression of selected metabolic genes be affected in the wing discs where we activate / suppress Notch pathway?

The upregulation of *Hex-A*, *CG13334* and *hairy* was shown by *in situ* hybridization experiments in discs with overactivated Notch pathway. The upregulation of *CG13334* was also seen by Q-RT-PCR analysis.

Is there a functional connection between the Notch activation and the transcriptional responses of the Notch target genes involved in metabolism?

Upregulation of metabolic genes after activation of Notch signalling pathway *in vitro* and *in vivo* appears to have functional connection to the changes in cellular metabolism. Measured by Seahorse XF extracellular flux analyser, cell lines S2N, Kc167 and *Drosophila* imaginal wing discs showed lowered oxygen consumption when Notch pathway was active. Higher rates of glycolysis might have been observed too but experiments need to be repeated.

6 Discussion

Drosophila melanogaster is a perfect model organism for the examination of Notch signalling pathway. This pathway is conserved within all metazoan species, consisting of virtually the same proteins and effectors and triggering very similar intracellular processes. Unlike mammals, where four receptors and five ligands exist, *Drosophila* possesses only one Notch receptor and two ligands (Delta and Serrate). Analysis are therefore much simpler to do compared to those in vertebrates.

Moreover, we are using a simple way to activate Notch pathway that works very well in *Drosophila* and that allows a precise timing of the start of the signalling. This helps us to distinguish between the primary and secondary targets of the pathway. So far only a few Notch target genes were well characterized (44, 54, 55). Here, we identified and characterized new targets that prove a direct connection between Notch signalling pathway and the regulation of metabolism.

6. 1. Su(H), a transcription factor of the Notch signalling pathway, binds potential enhancer regions of several metabolic genes

The CHIP-chip data we used to search for metabolic genes regulated by Notch were a powerful tool to base our selection on. Only a few Notch targets identified by this approach have been published but a lot of the results reminded unverified. Through these data, by “data mining” approaches, we selected seven genes containing Su(H) binding site that had a connection to cell metabolism for our analysis. Eleven predicted Su(H) containing enhancer regions were cloned and six of them (all three cloned regions from *CG13334*, one region from *Hex-A*, *Glut1* and *hairy*) responded to Notch activation in a luciferase assay and we proved by mutational analysis that the response is Su(H) dependent. The potential enhancer by *Impl3* gene did not show a significant increase in the luciferase assay but its response still went down after mutating its Su(H) sites suggesting this might still be a functional Notch enhancer. Taken together, the luciferase results tells us that the genomic fragments we tested are capable of Su(H) binding and responding to Notch but this assay can not say to which genes these enhancers belong, in other words which genes are regulated by them in the genomic context.

For example, the genes *CG13334* and former gene *CG13335* (classified as *CG42807* and *CG42808* in the latest release 6 of the genome) lie next to each other and the Su(H) peaks are in between them. So despite the fact we tested positively these regions in the luciferase assay we can not say if they regulate *CG13334* or one of the *CG42807* or *CG42808* genes. Published data from DmD8 cells identified *CG13335* as a Notch target (44) because the mRNA for *CG13335* was upregulated following Notch activation (*CG13334* was not examined on the arrays). However, it is still possible that *CG13334* and former *CG13335* genes have common enhancers or that from the three peaks of Su(H) binding in between them some belong to *CG13334* and some to *CG42807* or *CG42808*. Our results suggest this is the case because all the three genes show transcriptional response after Notch pathway activation in cell lines, on a very similar time scale. We also proved the regulation of *CG13334* *in vivo* in wing discs by *in situ* hybridization.

6. 2. Metabolic genes show transcriptional response *in vitro* and *in vivo* to activation of Notch signalling pathway.

Three different approaches were used to investigate if our genes of interest transcriptionally respond to Notch pathway.

In the time course experiment in cell lines all genes except *Treh* and *Idh* showed some transcriptional response. However, these responses differ according to cell line used which is not unexpected because these cell lines originate different tissues and we know that Notch signalling pathway works in tissue dependent manners (45). What is surprising is the fact that some genes were downregulated following Notch activation (*hairy* and *Hex-A*) despite the fact that in luciferase assay and in *in situ* hybridizations in wing discs higher expression of these genes was observed. At least in case of *hairy* there seems to be a phase of upregulation at 30 minutes followed by the downregulation (in S2N cells) suggesting primary upregulation of Notch followed by a secondary repression by another mechanism. From our unpublished data we suspect *E(spl)* genes to be responsible for this later phase of repression. *Hex-A* might follow a similar scenario so we would like to make a more detailed timing experiment to verify this (take samples every 5 minutes for the first half an hour). Another unexpected result was the fact that *Glut1*, *CG1334*, *CG42807* and *CG42808* were upregulated quite late, only after 45-60 minutes after Notch activation (most of the primary Notch targets come within 30 minutes). This could mean these genes are rather secondary

than primary Notch targets. We can not discriminate these options in our experiments but we know there are other examples of Notch primary targets that respond late (like *EGFR* in DmD8 cells, (44)).

In the Q-RT-PCR analysis of gene expression from imaginal wing discs only *CG13334* showed a robust upregulation in the *Su(H)-VP16* overexpressing discs. The changes of expression amongst the other genes were small so this experiment needs to be repeated (since it was done just once) to get definitive answers. One should also remember that only a subset of cells in the disc show (or might show) upregulation of their mRNA. As RNA is then isolated from the whole disc the level of upregulation may be 'diluted' by the rest of the non-responding cells which express relatively high levels of these genes (judges by *in situ* hybridizations all the metabolic genes are expressed ubiquitously throughout the disc). For this reason we now decided to take *Drosophila* strains with Notch over-expression / down-regulation in larger area of the wing disc for this type of experiments.

In the *in situ* hybridizations we see Notch dependent upregulation of *Hex-A*, *CG13334* and *hairy* mRNA (no change in *Glut1*, the rest of the genes have not been tested) in discs where *Su(H)-VP16* was overexpressed in the patched domain. *Hairy* showed clear upregulated expression in the whole *patched* domain but genes *Hex-A* and *CG13334* showed higher expression only in dorsal and ventral part of the region. We know that it is the ventral part of the patched domain where the Notch dependent overgrowth happens so cells divide quickly and need energy for that. So this fits with the observation that our metabolic genes are upregulated there. The expression in the *patched* domain in the pouch can be lower because of repressors expressed in this region like *Scalloped* (unpublished observation of several other Notch targets in the flies of this phenotype by Alexandre Djian, Cambridge). The *in situ* method is not very sensitive and it may be the reason why we did not see much difference in the expression of our genes using flies with the *ptc>Nicd* phenotype. All our genes are expressed throughout the disc and that is why it would be difficult to spot only a mild upregulation of their mRNA. Also, in genes with more transcriptional variants our probes were design to a common exon. In case more of them were expressed but only one transcriptional variant was upregulated it would be very difficult to spot this upregulation.

All the three above mentioned approaches point to the fact that there is a transcriptional response of our selected genes to the Notch signalling pathway. However, it does not say that the enhancers positively tested in the luciferase assays are responsible for

it. To connect these results together and to prove that our genes are really primary Notch targets we plan to GFP-tag our genes in large genomic clones, see their response to Notch *in vivo* and test if this response decreases when we mutate the appropriate Su(H) sites.

6. 3. Notch activation and the transcriptional response of the notch target genes has functional connection to cell metabolism

From the *in vitro* and *in vivo* studies we had a good evidence that Notch pathway can regulate several genes involved in metabolism. We knew that enhancer regions of some metabolic genes possess functional binding sites for Su(H) and that transcription of these genes was up-regulated by active Notch pathway. But is there a functional connection between the increased expression of metabolic genes and changes in cellular metabolism? To get an answer to this question we performed the measurement of respiration (OCR) and glycolysis (ECAR, PPR) by the XF24 analyzer using three cell lines and imaginal wing discs with overactivated Notch pathway. Only one experiment (with two repeats) was done but there are several interesting points to discuss:

Indeed, it seems that cellular metabolism shifts toward the Warburg effect after the activation of Notch pathway since respiration is decreased in S2N and Kc167 cell lines. Consistently with this result, it appears that maximal glycolysis (ECAR and PPR after the addition of respiration inhibiting drugs) is also increased in S2N cells. However, this increase is always visible only in the first of the three repeats of the measurements (see fig. 42). Perhaps when glycolysis increases there is immediately a compensatory mechanism that is recycling the high lactate instead of secreting it away (by measuring ECAR we measure the acidity of the surrounding media presumably due to the lactate secretion when glycolysis runs fast). It may be that *Impl3* and *CG13334*, two lactate dehydrogenases that we think are regulated by Notch, take this role to recycle the lactate.

What the basal level of ECAR concerns it seems to be quite low. In case of the activated cells it would mean that their respiration is stopped but glycolysis is not upregulated which does not make sense because cells need to gain energy somehow and efficient amount of ATP can be obtained only by oxidative phosphorylation or glycolysis. One possible explanation might be that only a limited amount of lactate is secreted from

cells to the medium in *Drosophila* system (or no lactate at all) and therefore we do not detect changes in pH in ECAR.

Another point to a discussion is the fact that OCR in the S2N and Kc167 cells after the activation of Notch is low since the very beginning of the measurement (which means about 20 minutes from the beginning of the activation of Notch pathway). In our RT-PCR experiments in cell lines the responses of genes involved in promoting glycolysis varied between 15-120 minutes after the activation of Notch. This implies that the mechanism by which Notch switches off respiration is very quick and probably happens even before the glycolysis is increased.

The measurements on wing discs also suggests that there might be lower respiration and higher glycolysis in discs with overactivated Notch pathway but lots of optimization is needed in this system. We need to minimize the time discs spend outside the larvae, we need to measure ECAR for longer time so as the system is in equilibrium and most importantly we need to optimize the concentration of the respiratory drugs, in both the discs and cell line experiments.

To prove the functional connection between the transcriptional regulation of metabolic genes and changes in cellular metabolism we plan to involve other types of tests including metabolite measurement by Dr. Petr Šimek (using HPLC), measurements of the uptake of glucose or using various commercially available metabolic kits (ATP/ADP ratio NAD/NADH ratio, pyruvate kinase activity or lactate ratio).

6. 4. Notch signalling pathway drives expression of metabolic genes directly

We proved that transcriptional response of four metabolic genes (*Hex-A*, *CG13334*, *Glut1* and *hairy*) is influenced by Notch signal *in vitro* and *in vivo*. We believe that these genes are not just influenced by the Notch signalling pathway indirectly but that they are primary Notch pathway target genes. Few months ago Landor et al. published their work showing that both hypo- and hyperactivated Notch signalling pathway induce glycolysis in mammalian cancer cells. They claim that the hyperactivated Notch pathway activates phosphatidylinositol-3-kinase/AKT pathway that upregulates the expression of the hexokinase and glucose transporter genes (83). However, in an experiment where they block PI3K by a drug LY294002 the expression of these two genes still increases. This rather

supports our view that Notch regulates these genes directly. Based on our data and the data of Landor's group it is rather possible that the expression of *Glut1* and *Hex-A* needs cooperation of the two signalling pathways. We want to test this hypothesis further by involving other types of tests such as Q-RT-PCR of cell lines treated with cycloheximide to inhibit protein synthesis or chromatine immunoprecipitation to see if activation complex is assembled in enhancer region of these genes.

7 Bibliography

1. R. Kopan, M. X. G. Ilagan, The canonical Notch signaling pathway: unfolding the activation mechanism., *Cell* **137**, 216-33 (2009).
2. E. J. Allenspach, I. Maillard, J. C. Aster, W. Pear, Notch Signaling in Cancer, *Therapy* **1**, 466-476 (2007).
3. C. F. Brosnan, G. R. John, Revisiting Notch in remyelination of multiple sclerosis lesions., *The Journal of clinical investigation* **119**, 10-3 (2009).
4. N. B. Spinner, CADASIL: Notch Signaling Defect or Protein Accumulation Problem?, *Journal of clinical investigation* **105**, 561-562 (2000).
5. T. Oda et al., Mutations in the human Jagged1 gene are responsible for Alagille syndrome., *Nature genetics* **16**, 235-42 (1997).
6. M. I. Darville, D. L. Eizirik, Notch signaling: a mediator of beta-cell de-differentiation in diabetes?, *Biochemical and biophysical research communications* **339**, 1063-8 (2006).
7. O. Warburg, On the Origin of Cancer Cells, *Science* **123**, 309-314 (1956).
8. <http://www.cancer.org/Treatment/TreatmentsandSideEffects/ComplementaryandAlternativeMedicine/DietandNutrition/metabolic-therapy>.
9. <http://www.worldwithoutcancer.org.uk/metabolictherapy.html>.
10. D. A. Tennant, R. V. Durán, E. Gottlieb, Targeting metabolic transformation for cancer therapy., *Nature reviews. Cancer* **10**, 267-77 (2010).
11. B. Oskouian, J. D. Saba, Cancer treatment strategies targeting sphingolipid metabolism., *Advances in experimental medicine and biology* **688**, 185-205 (2010).
12. <http://scienceblog.cancerresearchuk.org/2009/10/21/ncri-cancer-conference-2009-cell-metabolism/>.
13. R. K. Murray, D. K. Granner, P. A. Mayes, V. W. Rodwell, *Harper's Illustrated Biochemistry* F. Janet, Ed. (ed. 26th, 2003), p. 700.
14. A. R. Fernie, F. Carrari, L. J. Sweetlove, Respiratory metabolism: glycolysis, the TCA cycle and mitochondrial electron transport., *Current opinion in plant biology* **7**, 254-61 (2004).
15. J. T. Brosnan, Glutamate and Glutamine in Metabolism, *American Society for Nutritional Sciences* **130**, 988-990 (2000).
16. M. G. Vander Heiden, L. C. Cantley, C. B. Thompson, Understanding the Warburg effect: the metabolic requirements of cell proliferation., *Science (New York, N.Y.)* **324**, 1029-33 (2009).
17. M. López-Lázaro, The Warburg Effect: Why and How do Cancer Cells Activate Glycolysis in the Presence of Oxygen?, *Science* **8**, 305-312 (2008).
18. H. H. Kim et al., The Mitochondrial Warburg Effect: A Cancer Enigma, *Interdisciplinary Bio Central* **1**, 1-7 (2009).
19. C. J. Sherr, Cancer Cell Cycles, *Science* **274**, 1672-1677 (1996).

20. H. Krebs, C. Dang, Energy Boost: The Warburg Effect Returns in a New Theory of Cancer, *Nature Reviews Cancer* **96**, 1805-1806 (2004).
21. J.-whan Kim, C. V. Dang, Cancer's molecular sweet tooth and the Warburg effect., *Cancer research* **66**, 8927-30 (2006).
22. M.-A. C. Déry, M. D. Michaud, D. E. Richard, Hypoxia-inducible factor 1: regulation by hypoxic and non-hypoxic activators., *The international journal of biochemistry & cell biology* **37**, 535-40 (2005).
23. P. P. Hsu, D. M. Sabatini, Cancer cell metabolism: Warburg and beyond., *Cell* **134**, 703-7 (2008).
24. S. Matoba et al., P53 Regulates Mitochondrial Respiration., *Science (New York, N.Y.)* **312**, 1650-3 (2006).
25. E. Hajdуч, Protein kinase B (PKB/Akt) – a key regulator of glucose transport?, *FEBS Letters* **492**, 199-203 (2001).
26. B. Alberts et al., *Molecular Biology of the Cell* (ed. 5th, 2008), p. 1700.
27. S.-F. Lee et al., Gamma-secretase-regulated proteolysis of the Notch receptor by mitochondrial intermediate peptidase., *The Journal of biological chemistry* **286**, 27447-53 (2011).
28. S. Bray, A. Krejč, Notch activation stimulates transient and selective binding of Su(H)/CSL to target enhancers, *Genes & Development* **21**, 1322-1327 (2007).
29. V. Hartenstein, J. W. Posakony, Development of adult sensilla on the wing and notum of *Drosophila melanogaster*., *Development (Cambridge, England)* **107**, 389-405 (1989).
30. M. Eddison, I. Le Roux, J. Lewis, Notch signaling in the development of the inner ear: lessons from *Drosophila*., *Proceedings of the National Academy of Sciences of the United States of America* **97**, 11692-9 (2000).
31. S. S. Saravanamuthu, C. Y. Gao, P. S. Zelenka, Notch signaling is required for lateral induction of Jagged1 during FGF-induced lens fiber differentiation., *Developmental biology* **332**, 166-76 (2009).
32. L. J. Manderfield et al., Notch activation of Jagged1 contributes to the assembly of the arterial wall., *Circulation* **125**, 314-23 (2012).
33. B. H. Hartman, T. a Reh, O. Bermingham-McDonogh, Notch signaling specifies prosensory domains via lateral induction in the developing mammalian inner ear., *Proceedings of the National Academy of Sciences of the United States of America* **107**, 15792-7 (2010).
34. I. Becam, N. Rafel, X. Hong, S. M. Cohen, M. Milán, Notch-mediated repression of bantam miRNA contributes to boundary formation in the *Drosophila* wing., *Development (Cambridge, England)* **3789**, 3781-3789 (2011).
35. K. Tossell, C. Kiecker, A. Wizenmann, E. Lang, C. Irving, Notch signalling stabilises boundary formation at the midbrain-hindbrain organiser., *Development (Cambridge, England)* **138**, 3745-57 (2011).
36. J. Culi, J. Modolell, Proneural gene self-stimulation in neural precursors: an essential mechanism for sense organ development that is regulated by Notch signaling, *Genes & Development* **12**, 2036-2047 (1998).

37. S. Lin et al., Lineage-specific effects of Notch/Numb signaling in post-embryonic development of the *Drosophila* brain., *Development (Cambridge, England)* **137**, 43-51 (2010).
38. T. Ikawa, H. Kawamoto, A. W. Goldrath, C. Murre, E proteins and Notch signaling cooperate to promote T cell lineage specification and commitment., *The Journal of experimental medicine* **203**, 1329-42 (2006).
39. B. Duvic, J. A. Hoffmann, M. Meister, J. Royet, Notch signaling controls lineage specification during *Drosophila* larval hematopoiesis., *Current biology: CB* **12**, 1923-7 (2002).
40. A. Chitnis, Why is delta endocytosis required for effective activation of notch?, *Developmental dynamics: an official publication of the American Association of Anatomists* **235**, 886-94 (2006).
41. S. Shi, P. Stanley, Protein O-fucosyltransferase 1 is an essential component of Notch signaling pathways., *Proceedings of the National Academy of Sciences of the United States of America* **100**, 5234-9 (2003).
42. S. J. Bray, Notch signalling: a simple pathway becomes complex., *Nature reviews. Molecular cell biology* **7**, 678-89 (2006).
43. K. Mishra-Gorur, M. D. Rand, B. Perez-Villamil, S. Artavanis-Tsakonas, Down-regulation of Delta by proteolytic processing., *The Journal of cell biology* **159**, 313-24 (2002).
44. A. Krejčí, F. Bernard, B. E. Housden, S. Collins, S. J. Bray, Direct response to Notch activation: signaling crosstalk and incoherent logic., *Science signaling* **2**, ra1 (2009).
45. M. Furriols, S. Bray, A model Notch response element detects Suppressor of Hairless-dependent molecular switch., *Current biology: CB* **11**, 60-4 (2001).
46. T. Borggreffe, F. Oswald, The Notch signaling pathway: transcriptional regulation at Notch target genes., *Cellular and molecular life sciences: CMLS* **66**, 1631-46 (2009).
47. C. J. Fryer, J. B. White, K. A. Jones, Mastermind recruits CycC:CDK8 to phosphorylate the Notch ICD and coordinate activation with turnover., *Molecular cell* **16**, 509-20 (2004).
48. R. Vasquez-Del Carpio et al., Assembly of a Notch transcriptional activation complex requires multimerization., *Molecular and cellular biology* **31**, 1396-408 (2011).
49. K. L. Arnett et al., Structural and mechanistic insights into cooperative assembly of dimeric Notch transcription complexes., *Nature structural & molecular biology* **17**, 1312-7 (2010).
50. E. Maniati et al., Crosstalk between the canonical NF- κ B and Notch signaling pathways inhibits Ppar γ expression and promotes pancreatic cancer progression in mice, **121**, 4685-4699 (2011).
51. A. Blokzijl et al., Cross-talk between the Notch and TGF-beta signaling pathways mediated by interaction of the Notch intracellular domain with Smad3., *The Journal of cell biology* **163**, 723-8 (2003).
52. M. Nagao, M. Sugimori, M. Nakafuku, Cross talk between notch and growth factor/cytokine signaling pathways in neural stem cells., *Molecular and cellular biology* **27**, 3982-94 (2007).

53. F. Bernard, A. Krejci, B. Housden, B. Adryan, S. J. Bray, Specificity of Notch pathway activation: Twist controls the transcriptional output in adult muscle progenitors, *Stem Cells* **137**, 2633-2642 (2010).
54. F. Oswald, M. Winkler, Y. Cao, S. Bourteele, RBP-J κ /SHARP Recruits CtIP/CtBP Corepressors To Silence Notch Target Genes, *Molecular and cellular biology* **25**, 10379-10390 (2005).
55. F. Meier-Stiegen et al., Activated Notch1 target genes during embryonic cell differentiation depend on the cellular context and include lineage determinants and inhibitors., *PloS one* **5**, e11481 (2010).
56. K. Kannan et al., DNA microarrays identification of primary and secondary target genes regulated by p53, *Oncogene* **20**, 2225-2234 (2001).
57. J.-C. Wang, Finding Primary Targets of Transcriptional Regulators, *Cell Cycle* **4**, 356-357 (2005).
58. B. J. Nickoloff, B. a Osborne, L. Miele, Notch signaling as a therapeutic target in cancer: a new approach to the development of cell fate modifying agents., *Oncogene* **22**, 6598-608 (2003).
59. V. Bolós, J. Grego-Bessa, J. L. de la Pompa, Notch signaling in development and cancer., *Endocrine reviews* **28**, 339-63 (2007).
60. U. Koch, F. Radtke, Notch and cancer: a double-edged sword., *Cellular and molecular life sciences : CMLS* **64**, 2746-62 (2007).
61. A. Efstratiadis, M. Szabolcs, A. Klinakis, Notch, Myc and breast cancer., *Cell cycle (Georgetown, Tex.)* **6**, 418-29 (2007).
62. L. J. Beverly, D. W. Felsher, A. J. Capobianco, Suppression of p53 by Notch in lymphomagenesis: implications for initiation and regression., *Cancer research* **65**, 7159-68 (2005).
63. K. Lefort et al., Notch1 is a p53 target gene involved in human keratinocyte tumor suppression through negative regulation of ROCK1/2 and MRCKalpha kinases., *Genes & development* **21**, 562-77 (2007).
64. J. T. Whelan, A. Kellogg, B. M. Shewchuk, K. Hewan-Lowe, F. E. Bertrand, Notch-1 signaling is lost in prostate adenocarcinoma and promotes PTEN gene expression., *Journal of cellular biochemistry* **107**, 992-1001 (2009).
65. G. a Helt et al., Genoviz Software Development Kit: Java tool kit for building genomics visualization applications., *BMC bioinformatics* **10**, 266 (2009).
66. P. C. Jayakumar, Y. S. Shouche, M. S. Patole, Cloning of two hexokinase isoenzyme sequences from *Drosophila melanogaster*, *Insect Biochemistry and Molecular Biology* **31**, 1165-1171 (2001).
67. S. P. Mathupala, Y. H. Ko, P. L. Pedersen, Hexokinase II: cancer's double-edged sword acting as both facilitator and gatekeeper of malignancy when bound to mitochondria., *Oncogene* **25**, 4777-86 (2006).
68. D. Palmieri et al., Analyses of resected human brain metastases of breast cancer reveal the association between up-regulation of hexokinase 2 and poor prognosis., *Molecular cancer research : MCR* **7**, 1438-45 (2009).

69. M. Younes, R. W. Brown, D. R. Mody, L. Fernandez, R. Laucirica, GLUT1 expression in human breast carcinoma: correlation with known prognostic markers., *Anticancer research* **15**, 2895-8 (1995).
70. S. A. Escher, A. Rasmuson-Lestander, The Drosophila glucose transporter gene: cDNA sequence, phylogenetic comparisons, analysis of functional sites and secondary structures., *Hereditas* **130**, 95-103 (1999).
71. K. Singer et al., Warburg phenotype in renal cell carcinoma: high expression of glucose-transporter 1 (GLUT-1) correlates with low CD8(+) T-cell infiltration in the tumor., *International journal of cancer. Journal international du cancer* **128**, 2085-95 (2011).
72. R. L. Abu-Shumays, J. W. Fristrom, IMP-L3, A 20-hydroxyecdysone-responsive gene encodes Drosophila lactate dehydrogenase: structural characterization and developmental studies., *Developmental genetics* **20**, 11-22 (1997).
73. B. M. Deichmann et al., S100-Beta, Melanoma-Inhibiting Activity, and Lactate Dehydrogenase Discriminate Progressive From Nonprogressive American Joint Committee on Cancer Stage IV Melanoma, *Society* **17**, 1891-1896 (1999).
74. K. Seibert, C. Little, T. Gee, Prognostic Significance of Serum Lactate Dehydrogenase in Malignant Lymphoma, *Cancer* **46**, 139-143 (1980).
75. I. A. Murray, K. Coupland, J. A. Smith, I. D. Ansell, R. G. Long, Intestinal trehalase activity in a UK population: establishing a normal range and the effect of disease, *Scandinavian Journal of Gastroenterology* **44**, 241-245 (2000).
76. S. Gross et al., Cancer-associated metabolite 2-hydroxyglutarate accumulates in acute myelogenous leukemia with isocitrate dehydrogenase 1 and 2 mutations., *The Journal of experimental medicine* **207**, 339-44 (2010).
77. J. R Prensner, A. M Chinnaiyan, Metabolism unhinged: IDH mutations in cancer., *Nature Medicine* **17**, 291-293 (2011).
78. A. Hogan, S. M. Pinchin, K. M. Howe, M. Lardelli, M. Ish-Horowicz, The Drosophila hairy protein acts in both segmentation and bristle patterning and shows homology to N-myc, *The EMBO Journal* **8**, 3095-3103 (1989).
79. D. Zhou et al., Mechanisms underlying hypoxia tolerance in Drosophila melanogaster: hairy as a metabolic switch., *PLoS genetics* **4**, e1000221 (2008).
80. D. Bianchi-Frias et al., Hairy transcriptional repression targets and cofactor recruitment in Drosophila., *PLoS biology* **2**, E178 (2004).
81. Dual-Luciferase Reporter Assay System, Technical Manual TM040, Promega corporation, .
82. Steve Rozen and Helen J. Skaletsky (2000) Primer3 on the WWW for general users and for biologist programmers. In: Krawetz S, Misener S (eds) Bioinformatics Methods and Protocols: Methods in Molecular Biology. Humana Press, Totowa, pp 365-386 Source co, .
83. A. P. Mutvei et al., Hypo- and hyperactivated Notch signaling induce a glycolytic switch through distinct mechanisms, *Proceedings of the National Academy of Sciences of the USA* **15**, 18814-18819 (2011).

8 Supplement

Supplement1: Sequences of cloned enhancer with marked mutated Su(H) binding sites. Mutated Su(H) binding sites are marked in red (or blue in case of one of the Hex-A (1) construct). Red (blue respectively) brackets bound mutagenesis primer sequences. Mutations in Su(H) binding sites are showed underneath of each of the mutated sequence.

CG13334 (1)

```
CTGCTCCATTTGCTGTTGACCTATTGAAATGCGACAGTTTCACATGTGTTTTCGGG
ATTGCGTGGGATGATCGTGGAGCACGTGTGTGTTGACATACTGACCGCAGAGAGT
GTA CTTGAGCAAGGGACTTCCCCGTGAATCTGCCCGCCTGCTCAAGTGCTACGTA
ATTTGCATGGTCTGGATTTTTTCAAATTACATGACATTTTCCCACACTGATTAGCCC
GCACATGCCATTCTCTATTTTCGATGTGCATCCGAGTGCGACCTTCGAACAGGCAA
ACAGCCAGTGCAGCCTGCATCCGATGCACATCCATTGCATCCAGTGCAACGAAGT
GCAACGCCATCATTTTTTCCCACAGCCGAGGGCTCTGGGTTATATTTAACAAATGC
ATGAGAGATTTGGGTGCGCTACGTTTTTCGTTTTTCGTTTCGGA
```

CG13334 (2)

```
CCCTGGATACAGACGATTGCGCTCCACTGATTTTTCCCATCATCGAGCGATGCTCC
CTGCCTTTGGGCACTTTCTTCATCTCCTGGCTGGCCTCCTGCAATTTGCTGTGAAC
CTGTTCGAAAATTATGCATCGATGCGCATCAGTGGCAATCATGGATGGCAACATAA
TAATGGGATGCTGCTGATGAGTTTGCTCATAAACTGATGAGGGTACCTGGCTGTCT
ACCTAGCTACCTGTACCTGTGATTCATTTTCGATTGCCTAGCTGCTGATTCTGTTTAC
CTGTTTCGTTTGCTACACTTTATGCATGCTTCGGCAGTTTTTCTAATTATGACTTATGAT
CTCTGGGATTAGACAAACAATGGATCGTGGCACGTGGTTCCCAAGATGCTTTCGC
TTGTGCCTGACCTTTTCCCACGATCTGTTTGCGGTTGAGCGCTCGAGGCCCATGAT
CACCGCAAATCCCCTGCAGACAAAACAGCCAAAGG
```

CG13334 (3)

```
TGGACGCAACCATCATATTCTTCTGCGCTCCTGATCCTTTTTCCAATACCTCGATTG
GGAGTTCTCACGCGAGCACATGCCAAAGCGAAAAAAGGGACAGGGAAACAAT
TAACA ACTAATTTAGGCCTCTGCATATAATTTTATGGAGAGTGGTGCGGAGAGTCG
CAGTCCCACAGGGAGATGCCTATCTGCAGGAGCTGTGGGAAAAAATACGTTACAT
TCCTTTCCTTTGCTTTCCTTCTCTCTGCTGCTGCTTTCGCGCATTATTCCCACGC
GATCCTCGACTCTCGTTTTTGTGGTTTTTCGGGGTTTTCGTTTTCGTGGAGTA
```

Hex-A (1)

TGTGCTACAAGCGAAAGCAGACATCGCAAGTATAACAGTTGAAGGTGACACTGG
AGACCCTGGCGATAGGACACGTATAACAGTTCTGTAATCC {CAACATTGGCTGAC
GAAATCATGGGAATGCAAGGCGT {GGTTGGGCGG} GTTAAGCCACTTCTCCAAA
AAGTTATAAAAACCCATC } TGGAACCAGTTGATTTTTTGTATTTATCTGGTTCTGTT
GACATGGTGATTTTACTTCAAAGAACCCGTTTATGAAATTCGAAACCTACAATGTA
AATGGAAATCCCTGAGTCAATTTTTCCAATATGCAACTCCTTTGGA

ATGGGAA → ATTGTIA
TTCTCCC → TAATACC

Hex-A (2)

CAGCACCGAATGGAAATTGCACATGAAATCTAGCTGCAAAAATATGAAACAACAA
AATCCATTGAATGGAGAGCCAGAAAGAGCGAAGTAGAGGGGAAGAGAGTGAG
AGAAGGAGGGGAGCGGAACTTCAAACCTGGGCGGCACGTACACACACAAAAGAGG
GCAGGGCGGGGAGACGAGCCCCACGGACACTGAACAAAAATACATACAAATGCA
AAGATATATGTATTTGAGGATGTTGACGCGTCGCTAGAACTTGAGAATTCCAAGAA
GCGGTAAAACGGGTGAGACGATGATGGTAGGGGAGTTGGGGAGGGGAAGGTA
GCTGTCAACAGCTACGCAAACCTTGCTCTCCATTTTTCTGGGTAAACCTTGCTCTT
TCTCATCTAAAACGGCATTGTTATACTAACCCGATGCCGAG {GGAGAGCGAGATC
GCTGAGAGTGGGAAAGCGGGTGGTGGGGCCCGGC} GCCGAACAGGGGGTTCAA
AGAACGAAGCCAA

GTGGGAA → GTTGTIA

Hex-A (3)

GCGACGCATAAGGGTTTCCGCATAAACACGCGTTTGACTCATTCTCATTATAGCC
ACTCTCTCGCCCCCTCTCTCACGCGCACCCCTATCAATATGCCATTTGTGGACCCCT
CAGCGTCGCACATATACAGCCATATCTCCAACCATGCCG

Glut1

GAAGACGACGACATGACTGCCTTTTTATTGCTCCTACGCCTCTGC {CTAGCCCCTCC
GTTCCCATTTTCCACGCCCCCTCCCTTTTGTTTCAGC} TGTCGTGGCCGTTGAACAA
ATGAACAACATAAATAATTGCAGAGGCACACACACTGACACACACACACACACG
CGTTCTGAGGAACTCGCACGCACTGACAAAGAGTGGGAAAATCGCAGGACT
CCCAAGGAACGTTTGCAGCCTTCGAATTGAGATTAATGAGCAGCAAAAGTGATTC
AAAGTCAGCATCCTCG

TTCCAC → TAACAAC

Treh

CGTAAACGAAAGGAAAAGTGCATAAAAGCGAGCAGAGATAGCGTCAGAATGACT
TATCGCG{TATACGCCCCGTTGAGCCACGTGAAAAATGTTTAGTTCTTATGAAAT}C
GTTCAAAGGCCCAAAGCAAATCAGCTGAAAGCATAAAAATAAACCAATATAAA
CATACTATGTGTGTGTGCCTGACGAGCCCCATACTTATGTACTTCGCTCACGCG
CTAGTGTGCGTGTAAACTTTTGTATGTCTGCGAAATGTTATAAACTGGTTTTTCATG
TACTCTCTCGATCTAAAAACAGGCAAAGGGATAAGATACAAACGTGATTGAGTG
TTTCTTCCGATTGATTTCGACTTCGGAACCCTTTGATATTTAAATATAACTTTTGAAT
AATGCAACTGCCGCTCGATCGACAATGGAGTTGTTCTTCTTTTCGATAAGTAATGCT
TATCTTTTGTCTGGCTCTTGCTCTTTATATGTGTGTGTTACGAGTGGTTGCCAAA
GGTCACCGACGAAGGTCGTTGGTATTTTCGAGATGAAAACGTGCTGTTGTTGGGA
GAAACTTGGCAGTCTCTGTGGATAGAGTCTGTAGACTGGCATAATTTTCGGAACC
GGTTTGTCTGGCAGAAAAAGGAGGCAGAAA

GTGAAAA → GTTATTA

ImpL3

TCAGTTTCGTTTGGGGAGAGCTAAACTCAAGACCAACTGAAGTTCACTTCAGTTT
TCAG
CTCCCGAGCAGCAGCAGCAGCAGCAACTTTCGAGATATACGAGCATTGTCACAT
AAAA
CTGCAACGCCTTTCCCATTTGTCAGCTCGCCACGAAGACTTGGTCGCTGTTTGCTT
TTGCTTTTGGCCATAAAATATATGGCCCCGTATCGCAAAAAGCTGCGAGTGTGAA
ATTTAAGTTTTAATTTAAGCGATATGAAAAAAAAGGGCAAGACGGCAAACGGCG
GTCTGCAGTCGTCGAATCGTGCACGAAATGAAGCCATTTTCATATTTATGAATTTT
GCCCTTATCGAAAAACGCTTCAATTGGCCATCGACTTGGGGCCGGCAAATTTAA
TATGGGCAGTCATAAACGATA
{CTGACAGGTCGGTGGGATCTGTGGGAAAGGGGCAAGATTCCGGGGA}ACTTG
GAGATCCAGAATCCAGAGCGTAACATCCTCGCCGACTTAGCTGAGTTATTAAGGC
ATCTTTATAGCCAATCTCAATGAGGTGTGAAGTGCAATCGTTGTTGGCCTTTTTATT
AATACGCGAAAATATATTTTATTTGTTGTTCCGTCTGCGATCGACTGCGATATTAAG
C

GTGGGAA → GTAGAAA

IDH

GTAATAGCTGGGCGGAATGCGATCGGAAGTGTGGGTGTTTGGCGTGGAGTGTG
AACCGGTTTATATAAGGCTAAACAAATGCTCCACTTACCTTTTAGAATATTTAAAAT
GCCGAATTTAGAATGTTAGAGCACAGACTAATTAATTGCAGACCGAAAGATCTC
GAACCACTCCCAATCAGACGCAGCGAATAACTGAAACTGATTTGGCGACGACAA
CAATAAAGAGCAAGAGGTGGCGCGTGTGGAAGATAATTCCGTAGATAAAAACAT
GTTATTCAA {TCAGCTGCTTGCGAAGAGCT**TTCTCAC**GAACTTTAAGCTTTACTCT
C}GAGTTCTGCAGCACTCAGTATTAGTTCGTCTTGCTGAACCGCCAAACATAAAAT
TTGAATTCTCAATTACCGCAACTTGTGAGAGCAGCGTGC GTTTCGTTTGCTTTAATG
ACGCTAAAAGAAAATCCATAAAATGTGCTCCAAAAGTGAAATGTTAGCCGG

TTCTCAC → TAATAAC

hairy

AGCAACAACACCAACACCACCGCGACCATCACCAACAGCACAGCCAGAAACAC
AGCCTCTTGTAATCCCTCAGTTAGCAGAGCCCAGCAGAGTCAAGCCAAACCGA
TCGCTGATCGACCGACCGACCGACGATCACCAATGGGGGTTTCGCAGTGTGATTT
C{CAAAAAGGAAGAAATGCCCA**TTCCCGC**GAGCCACGGGGGCGTATGAG}TAAC
GCGGTG

TTCCCGC → TAACAGC

Supplement 2: Measured values of luciferase assay. Data are arranged according to the day of measurement. X in some cells means that this construct wasn't measured that day. Last three rows gives average of all measurement, their standard deviation and standard error (used to make error bars)

	MB	1_1	Hex-A (1)	Hex-A (1) mI	Hex-A (1) mII	Hex-A (2)	Hex-A (2) m	Hex-A (3)	Glut1	Glut1 m
8.5.2011	7,23727	4,21946	8,21912	x	x	4,73731	x	3,56419	10,36243	x
20.5.2011	5,63454	1,34803	4,78718	x	x	2,70742	x	2,09714	6,58516	x
7.8.2011	3,92619	1,61726	2,72140	1,80768	0,47360	x	x	x	1,91406	0,81690
17.8.2011	11,56907	2,25387	2,69378	2,23336	2,29697	x	x	x	5,73577	2,28379
24.8.2011	38,33058	5,77835	6,05545	2,18474	3,23476	x	x	x	7,36025	4,78478
29.8.2011	5,63754	1,56080	5,06501	3,34423	2,72433	x	x	x	2,19655	2,72071
19.10.2011	19,77739	1,57035	x	x	x	2,20363	2,42267	x	x	x
26.10.2011	4,73972	1,97452	x	x	x	2,74859	1,86331	x	x	x
21.10.2011	8,67412	1,37893	x	x	x	2,26764	2,57344	x	x	x
average	11,72516	2,41128	4,92366	2,39250	2,18242	2,93292	2,28647	2,83067	5,69237	2,65154
stdev	11,10144	1,54432	2,09771	0,66239	1,20198	1,03864	0,37414	1,03736	3,22138	1,63877
sterr	3,70048	0,51477	0,85621	0,33120	0,60099	0,46451	0,21627	0,73572	1,31485	0,81938

	Treh	Treh m	ImpL3	ImpL3 m	h	hm	CG13334 (1)	CG13334 (2)	CG13334 (3)	IDH	IDH m
8.5.2011	4,81904	x	5,11052	x	8,13066	x	7,15193	5,98560	30,41405	4,84621	x
20.5.2011	3,10298	x	4,89897	x	2,69101	x	3,01132	3,41904	13,79867	3,05990	x
7.8.2011	x	x	x	x	1,40292	3,03000	x	x	x	x	x
17.8.2011	x	x	x	x	6,95111	1,76867	x	x	x	x	x
24.8.2011	x	x	x	x	5,18517	1,75817	x	x	x	x	x
29.8.2011	x	x	3,10954	1,97980	2,81753	1,26116	x	x	x	x	x
19.10.2011	2,84450	2,15910	2,31932	1,76995	x	x	x	x	x	2,41128	3,58835
26.10.2011	2,36106	2,04605	3,10564	1,63683	x	x	x	x	x	1,45392	1,14339
21.10.2011	2,77958	2,65943	3,25398	0,33391	x	x	x	x	x	2,55100	1,50798
average	3,18143	2,28819	3,63299	1,43012	4,52973	1,95450	5,08162	4,70232	22,10636	2,86446	2,07990
stdev	0,95340	0,32643	1,11420	0,74432	2,65890	0,75509	2,92785	1,81483	11,74885	1,25088	1,31901
sterr	0,42639	0,18869	0,45496	0,37216	1,08527	0,37755	2,07649	1,28711	8,33251	0,55943	0,76243

Supplement 3: Measured values of time course analysis. Measurement were performed 3x always in triplicates. Table gives average values of duplicates normalized to rp49.

	Glut1								
	S2N			Kc167			dmD8		
	<i>Exp. 1</i>	<i>Exp. 2</i>	<i>Exp. 3</i>	<i>Exp. 1</i>	<i>Exp. 2</i>	<i>Exp. 3</i>	<i>Exp. 1</i>	<i>Exp. 2</i>	<i>Exp. 3</i>
Ctrl	0,000407	0,00092	0,000474	0,0046	0,0063	0,0019	0,00233367	0,001721979	0,000706351
15	0,000407	0,001003	0,00056	0,0089	0,0066	0,0018	0,00115085	0,001331077	0,000570852
30	0,000353	0,00098	0,000493	0,0035	0,0074	0,0025	0,0012898	0,00167773	0,000489918
45	0,000346	0,001007	0,000985	0,004	0,0075	0,0024	0,00135279	0,002472625	0,000248798
60	0,001062	0,00157	0,001459	0,0037	0,0081	0,0028	0,00230751	0,001939582	0,000584731
120	0,001932	0,002023	0,002025	0,0055	0,0069	0,0022	0,0011918	0,002080941	0,000321154

	CG13334								
	S2N			Kc167			dmD8		
	<i>Exp. 1</i>	<i>Exp. 2</i>	<i>Exp. 3</i>	<i>Exp. 1</i>	<i>Exp. 2</i>	<i>Exp. 3</i>	<i>Exp. 1</i>	<i>Exp. 2</i>	<i>Exp. 3</i>
Ctrl	0,00010171	0,0005475	6,38E-005	0,0002655	0,0005951	7,022E-005	0,00011	0,00037	8E-005
15	0,00011826	0,0005118	5,14E-005	0,0001664	0,0005772	9,914E-005	0,00012	0,00032	5E-005
30	0,0001134	0,0004643	7,44E-005	0,000169	0,0006276	6,416E-005	0,00035	0,00034	5E-005
45	9,097E-005	0,0005289	8,65E-005	0,0002096	0,0005348	8,774E-005	0,00019	0,00058	3E-005
60	0,00013557	0,0005607	0,0002694	0,0001338	0,0006614	9,740E-005	1E-004	0,0003	7E-005
120	0,00019568	0,0005309	0,0002077	0,0002385	0,0005887	6,986E-005	8E-005	0,00027	5E-005

	CG42807								
	S2N			Kc167			dmD8		
	<i>Exp. 1</i>	<i>Exp. 2</i>	<i>Exp. 3</i>	<i>Exp. 1</i>	<i>Exp. 2</i>	<i>Exp. 3</i>	<i>Exp. 1</i>	<i>Exp. 2</i>	<i>Exp. 3</i>
Ctrl	0,0012748	0,001044	0,000189	0,0001634	0,000105	0,000132	0,0048876	0,008549	0,00096
15	0,001741	0,001228	0,000498	0,0001783	0,00013	0,000187	0,0043516	0,00657	0,0023
30	0,0015183	0,000892	0,000768	0,0001377	0,000202	7,00E-005	0,0063929	0,012879	0,0007
45	0,0014435	0,001606	0,001047	0,0006504	0,000344	0,00017	0,0067111	0,020701	0,00012
60	0,0018679	0,001821	0,000992	0,0001698	0,000251	0,000247	0,00639	0,030593	0,0027
120	0,0037097	0,002471	0,00126	0,0002226	0,000471	0,000172	0,0048144	0,022549	0,00313

	CG42808								
	S2N			Kc167			dmD8		
	<i>Exp. 1</i>	<i>Exp. 2</i>	<i>Exp. 3</i>	<i>Exp. 1</i>	<i>Exp. 2</i>	<i>Exp. 3</i>	<i>Exp. 1</i>	<i>Exp. 2</i>	<i>Exp. 3</i>
Ctrl	7,46E-005	0,000277	0,000132	0,0001838	0,000308	0,0001053	5,71E-005	0,0001391	0,0001485
15	7,23E-005	0,000379	0,000113	0,0001724	0,00035	0,0001671	7,19E-005	0,0001274	0,0001055
30	5,67E-005	0,000287	0,000111	0,0001753	0,00033	9,62E-005	6,41E-005	0,0001297	7,77E-005
45	7,28E-005	0,000299	0,000161	0,0001734	0,000408	0,0001217	5,29E-005	0,0003811	6,44E-005
60	9,79E-005	0,000422	0,00016	0,0001646	0,000431	0,0001086	4,78E-005	0,0001499	0,0001193
120	0,0001468	0,000401	0,000158	0,0002544	0,000398	0,0001106	5,31E-005	0,0001044	8,74E-005

	Hex-A								
	S2N			Kc167			dmD8		
	<i>Exp. 1</i>	<i>Exp. 2</i>	<i>Exp. 3</i>	<i>Exp. 1</i>	<i>Exp. 2</i>	<i>Exp. 3</i>	<i>Exp. 1</i>	<i>Exp. 2</i>	<i>Exp. 3</i>
Ctrl	0,58019	1,75381	0,36422	0,4272938	1,1588871	0,742293	0,46731237	0,9543763	0,150405
15	0,63183	2,45678	0,21667	0,639981	1,1694498	0,4453588	0,33541445	0,6995731	0,215686
30	0,44069	1,57922	0,23053	0,5344959	1,5319122	0,3307934	0,57740375	0,7129137	0,111112
45	0,50067	1,47686	0,21066	0,4699081	1,2113164	0,3239041	0,37761017	0,9740281	0,007162
60	0,56336	1,1642	0,13035	0,6244977	0,9607195	0,290518	0,28815249	1,2546381	0,101716
120	0,57713	0,56524	0,06744	0,7787822	1,0599987	0,1391205	0,19468765	0,4928141	0,008737

	Impl3								
	S2N			Kc167			dmD8		
	<i>Exp. 1</i>	<i>Exp. 2</i>	<i>Exp. 3</i>	<i>Exp. 1</i>	<i>Exp. 2</i>	<i>Exp. 3</i>	<i>Exp. 1</i>	<i>Exp. 2</i>	<i>Exp. 3</i>
Ctrl	0,019244	0,023404	0,003559	0,3564	0,42774	0,3566	0,663356561	0,85451889	0,06265652
15	0,026168	0,045296	0,015329	0,5038	0,80706	0,3264	0,609316109	0,70761617	0,04749581
30	0,023429	0,032109	0,002639	0,4076	0,73741	0,174	0,766290677	0,96570785	0,03660722
45	0,02648	0,030674	0,003022	0,294	0,4386	0,2951	0,561325282	0,77889531	0,01239305
60	0,015417	0,019736	0,002107	0,1673	0,42489	0,2299	0,381736507	0,67471234	0,03712742
120	0,027835	0,022114	0,001522	0,3052	0,42011	0,0688	0,416527034	0,44552319	0,01365012

	Treh								
	S2N			Kc167			dmD8		
	<i>Exp. 1</i>	<i>Exp. 2</i>	<i>Exp. 3</i>	<i>Exp. 1</i>	<i>Exp. 2</i>	<i>Exp. 3</i>	<i>Exp. 1</i>	<i>Exp. 2</i>	<i>Exp. 3</i>
Ctrl	0,0215219	0,041764	0,0121852	0,042397	0,07854	0,028245	0,0526951	0,066905	0,01915174
15	0,0171736	0,0456546	0,0098963	0,038804	0,086867	0,023975	0,0437034	0,0544821	0,0224479
30	0,0175074	0,0359854	0,010634	0,033363	0,081025	0,026747	0,0477545	0,0574562	0,0132372
45	0,0193714	0,0338664	0,0125607	0,034283	0,071439	0,02244	0,0465617	0,0662961	0,00147815
60	0,0197406	0,0319789	0,0071012	0,036273	0,079022	0,023466	0,0390434	0,0707713	0,01612485
120	0,0224701	0,0171057	0,0053263	0,047837	0,076101	0,02221	0,0268921	0,0397815	0,00362008

	IDH								
	S2N			Kc167			dmD8		
	<i>Exp. 1</i>	<i>Exp. 2</i>	<i>Exp. 3</i>	<i>Exp. 1</i>	<i>Exp. 2</i>	<i>Exp. 3</i>	<i>Exp. 1</i>	<i>Exp. 2</i>	<i>Exp. 3</i>
Ctrl	0,2710031	0,1729837	0,1331167	0,5477743	0,349119	0,285176	0,497789	0,272386	0,208093
15	0,295953	0,165974	0,1171501	0,5610712	0,364541	0,319372	0,37509	0,214431	0,185037
30	0,2748074	0,1626233	0,1011665	0,4268143	0,371947	0,281009	0,461418	0,255396	0,140724
45	0,2696353	0,1491717	0,1019712	0,4546742	0,390988	0,352888	0,383792	0,262107	0,012273
60	0,3582608	0,1202968	0,0985108	0,3923524	0,41481	0,326388	0,350926	0,260691	0,153551
120	0,3274468	0,1306994	0,09442	0,6509091	0,41952	0,282875	0,358365	0,204482	0,043246

	hairy								
	S2N			Kc167			dmD8		
	Exp. 1	Exp. 2	Exp. 3	Exp. 1	Exp. 2	Exp. 3	Exp. 1	Exp. 2	Exp. 3
Ctrl	0,051628	0,1215689	0,043008	0,16447	0,1898117	0,241826	0,173907	0,1183121	0,037597
15	0,074417	0,1344764	0,034656	0,228788	0,1875874	0,15278	0,13698	0,0819391	0,045318
30	0,12235	0,1076835	0,034783	0,137132	0,1712833	0,046895	0,200367	0,1112894	0,021608
45	0,122803	0,0648337	0,011874	0,082059	0,0911456	0,04218	0,103485	0,0836509	0,001314
60	0,038698	0,0338127	0,004309	0,111334	0,0974398	0,045501	0,080797	0,078792	0,016838
120	0,057423	0,0285724	0,006358	0,128406	0,1397948	0,036889	0,094205	0,0753732	0,003585